ANCHOR SYSTEMS FOR SHEET PILES

by

G. K. Raptis

funded by the State Scholarships Foundation of Greece

A dissertation submitted to the University of Durham in partial fulfilment of the requirements for the degree of MSc by Advanced Course.

September 1997

I believe in the heart of man,
the soil threshing-floor, where day and night
Lord fights with death.

"Help!" You shout, Lord. "Help!"
You shout, Lord and I listen.
Inside me the ancestors and descendants
and all the races, and all the earth, we
listen with fear, with joy, Your shout.

Blessed whoever listens and is rushed
to save You, Lord, and says:
"I and You only exist."

Blessed whoever saved You, is joined
with You, Lord, and says:
"I and You are one."

And blessed three times whoever holds,
and does not bend, on his shoulders,
the great, wonderful, unspeakable secret:

"AND THIS ONE DOES NOT EXIST!"

N. Kazantzakis
Extract from the book "*Asceticism*"

ACKNOWLEDGEMENTS

I would like to thank the State Scholarships Foundation of Greece for the financial support, without which I would not have ever attended this MSc course. It is a honour for me to be considered a scholar of this Foundation. Furthermore, I would like to thank the academic, technical, and secretarial staff of the School of Engineering for their help and co-operation throughout the last year.

Especially, I would like to express my gratitude to my supervisor Dr Alan Selby for his guidance, and the technicians Bernard McEleavy and Steve Richardson, without whose untiring assistance the laboratory experiments could not have been carried out. Besides, I would like to thank my fellow student and friend Christini Rizou for her precious help for the preparation of some of the most important graphics in this dissertation.

I would like also to thank my family for the financial and sentimental support they gave me through years. Last but by no means least, I would like to thank Despina Aggelopoulou for the translating of the articles written in French language, and particularly for the help, support, and patience she has shown to me for the last whole year.

ABSTRACT

When designing an anchored sheet pile wall the choice of the anchorage, that means the type and location of the anchor with respect to the sheet pile wall, is very significant to the behaviour and the dimensions of the system as a whole. Usually, the anchor is located well away from the sheet pile wall in order the active and passive soil zones not to intersect. However, this may not be possible in cases where land use is restricted. This M.Sc. dissertation examines the effect of the tie–rod length on the anchor resistance and the kinematics of failure of anchor sheet pile wall in granular soil. Laboratory experiments were performed with a model sheet pile wall and anchor. A plane technique was used to measure the soil displacements at failure and subsequently the cumulative shear strain in soil. Furthermore, the finite difference method was employed to contribute to the laboratory experiments. It is shown that the soil deformations at failure are strongly related to the length of tie–rod. The anchor resistance is also influenced by the tie–rod length and the depth of anchorage.

LIST OF SYMBOLS

A	cross–sectional area (m^2)
A_p	anchor resistance (N)
b	width of sheet pile wall (m)
b_a	width of anchor (m)
C_u	coefficient of uniformity
c	cohesion (Pa)
d	depth of embedment of wall (m)
d_a	depth to bottom of anchorage (m)
d_i	depth of intersection of active and passive planes of potential failure (m)
E	Young's modulus of elasticity (Pa)
F	factor of safety
F_p	factor of safety with respect to gross passive resistance
F_s	factor of safety with respect to mobilised shear strength
G	shear modulus of elasticity (Pa)
H	height of wall (m)
h	retained height of soil (m)
h_a	height of anchor (m)
I	moment of inertia of cross–sectional area (m^4)
K	bulk modulus of elasticity (Pa)
K_0	coefficient of earth pressure at rest
K_a	active pressure coefficient
K_p	passive pressure coefficient
l_r	length of tie–rod (m)
M	bending moment on sheet pile wall (Nm)
P_a	total active thrust (N)
P_p	total passive resistance (N)
P_s	total shearing resistance from both ends of anchor (N)
p_a	active pressure (Pa)
p_p	passive pressure (Pa)
T	tie–rod force (N)
t	depth of tie–rod (m); thickness of sheet pile wall (m)
v	Poisson's ratio

y	depth below excavation level of zero bending moments in fixed earth support method (m)
Z	section modulus of cross section (m^3)
z	depth co-ordinate (m)
γ	unit weight (N/m^3); shear strain
δ	wall friction (degrees)
$\varepsilon_1, \varepsilon_2, \varepsilon_3$	principal strains ($\varepsilon_1 > \varepsilon_2 > \varepsilon_3$)
ε_v	volumetric strain
ρ	flexibility number (Pa^{-1})
$\sigma_1, \sigma_2, \sigma_3$	principal stresses ($\sigma_1 > \sigma_2 > \sigma_3$) (Pa)
σ_h	horizontal stress (Pa)
σ_v	vertical stress (Pa)
φ	angle of shearing resistance (degrees)
φ_{cv}	angle of shearing resistance at critical state (degrees)
φ_p	peak angle of shearing resistance (degrees)
ψ	angle of dilation (degrees)

CONTENTS

	ACKNOWLEDGEMENTS	iii
	ABSTRACT	iv
	LIST OF SYMBOLS	v
	CONTENTS	vii
	LIST OF FIGURES	ix
1	INTRODUCTION	1
	1.1 General	1
	1.2 Previous Work	5
2	THEORY IMPLEMENTATIONS	11
	2.1 Idealised Stress–Strain Relations for Soil. Theory of Plasticity	11
	2.2 Theories of Earth Pressure	14
	2.2.1 Rankine's theory of earth pressure	14
	2.2.2 Coulomb's theory of earth pressure	19
	2.3 Application of Earth Pressure Theory to Retaining Walls	21
	2.3.1 Mode of wall movement	23
	2.3.2 Wall flexibility	23
	2.3.3 Soil stress and strain properties	26
	2.3.4 Initial stress in the soil and construction technique	28
	2.4 Design of Anchored Sheet Pile Walls	29
	2.4.1 Modes of failure for anchored sheet pile walls	30
	2.4.2 Free earth support method	32
	2.4.3 Fixed earth support method	33
	2.5 Design of Balanced Anchorages	35
3	LABORATORY EXPERIMENTS	38
	3.1 Soil Classification	39
	3.1.1 Particle size distribution	39
	3.1.2 Shear strength parameters	40
	3.1.3 Density	41
	3.2 Design of Equipment	41
	3.2.1 Tank	41
	3.2.2 Sheet pile wall	43

3.2.3 Anchorage 44
3.3 Measurement Techniques 46
3.3.1 Measurement of the tie–rod force 46
3.3.2 Measurement of the soil displacements 47
3.4 Experimental Procedure 48
3.4.1. Initial stage 48
3.4.2 Final stage 49
3.4.3 Comments on the procedure 50
3.5 Results and Discussion 51
4 FINITE DIFFERENCE ANALYSIS 62
4.1 The *FLAC* programme 63
4.1.1 General features and fields of application 63
4.1.2 Background 64
4.2 Design of Analysis 67
4.2.1 Dimension and properties of materials 67
4.2.2 Analyses 69
4.3 Results and Discussion 70
5 CONCLUSIONS 76
6 REFERENCES 80

– APPENDIX A 84
– APPENDIX B 91

LIST OF FIGURES

1	Cross–sections of British Steel patented piles	2
2	Types of sheet pile walls	3
3	Various types of anchorages	4
4	Soil idealisations	12
5	State of plastic equilibrium in a two–dimensional soil element	15
6	Rankine's considerations	16
7	Curvature due to wall friction	20
8	Development of active and passive wedges in a retaining wall	21
9	Relationship between earth pressure and wall rotation for normally consolidated sand (after Terzaghi)	22
10	Active and passive pressure distributions for a smooth wall (after Potts and Fourie)	24
11	Arching effects (after Craig)	25
12	Limit states for anchored sheet pile walls (after BS 8004)	31
13	Free earth support method	32
14	Fixed earth support method	33
15	Conventional design of anchorages (after British Steel Co.)	37
16	Details of tank	42
17	Design of anchorages for the laboratory experiments	46
18	Test 2. Vectors of total soil displacement	53
19	Test 2. Contours of horizontal, vertical displacement, and cumulative shear strain in the soil	54
20	Test 3. Vectors of total soil displacement	55
21	Test 3. Contours of horizontal, vertical displacement, and cumulative shear strain in the soil	56
22	Test 4. Vectors of total soil displacement	58
23	Test 4. Contours of horizontal, vertical displacement, and cumulative shear strain in the soil	59
24	Test 5. Vectors of total soil displacement	60

25	Test 5. Contours of horizontal, vertical displacement, and cumulative shear strain in the soil	61
26	Basic explicit calculation cycle of *FLAC* programme (after *FLAC* User's Manual)	65
27	Grid and geometry of models for *FLAC* analysis	68
28	Anchor resistance and tie–rod relation with respect to depth of anchorage d_a and angle of shearing resistance of soil φ'	71
29	Collapse conditions with respect to the tie–rod length for depth of anchorage $d_a = 0.18$ m	73
30	Collapse conditions with respect to the tie–rod length for depth of anchorage $d_a = 0.24$ m	73
31	Collapse conditions with respect to the tie–rod length for depth of anchorage $d_a = 0.42$ m	74

1 INTRODUCTION

1.1 General

The sheet piling is a method of retaining wall construction widely used to provide support to soil surfaces and defence against the ingress of water. In contrast to the other types of retaining wall, a sheet pile wall consists of a row of interlocking light piles—made of timber, reinforced concrete but mostly of steel—of which their lower end is driven into the ground.

Sheet pile walls are extensively used as a form of permanent construction for river frontages, quay walls, wharves, dock and harbour works, and other waterfront structures. They are also used in land reclamation and cofferdam structures. Although sheet pile walls are used as temporary constructions for support, it is only recently that they have been considered as an economical alternative for the permanent support of basements and deep foundations in building works, provided that some increase in ground movements around the excavation can be permitted.

In the United Kingdom steel sheet piles are produced by the British Steel Corporation which rolls two types of patented pile, the Frodingham and the Larsen. Cross-sections of each are shown in Figure 1 on page 2:

Each type has a wide range of properties (weight, moment of inertia, section modulus), along with varying section dimensions and is facilitate with corner, junction,

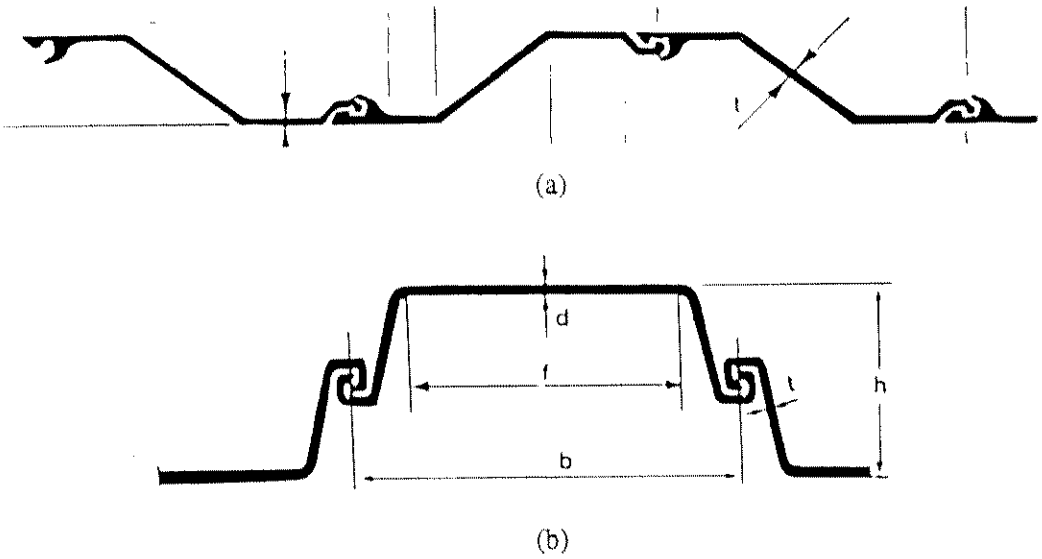

Figure 1 Cross-sections of British Steel Co. patented piles: (a) Frodingham, and (b) Larssen.

and special piles so as to cover the design demands of any construction work. The quality of steel used is in accordance with the British Standard BS 4360: 1986; Grades 43A (mild steel) or Grades 50A (high yield steel) which their ultimate and minimum yield stresses are well defined. The effective life of unpainted, or otherwise unprotected, steel sheet piling depends upon the combined effects of the imposed stresses and corrosion. Whenever corrosion is thought to be a particular problem it is possible to coat the sheet piles with organic coatings.

Sheet pile retaining walls are classified into either cantilever or anchored types, as shown in Figure 2 on page 3. Cantilever walls are dependent for stability exclusively on the penetration of the sheet piling into the soil. Thus, long and therefore heavy sections of pile are required making cantilever walls economical only for small to medium retained heights. It is usual the maximum height of these walls to be limited to five metres. Furthermore, as minor changes in conditions such as variations in height,

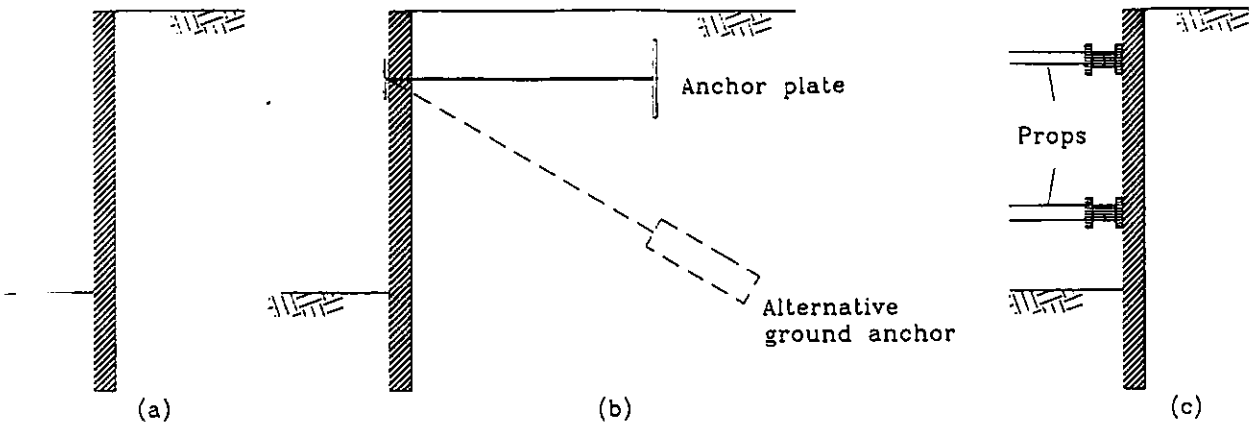

Figure 2 Types of sheet pile walls: (a) cantilever, (b) anchored, and (c) propped.

loading, soil properties, and yield of the soil can have considerable effect on the alignment of cantilever walls, these are usually used in temporary works.

The stability of anchored wall is derived partly from the penetration of the sheet piling into the soil and partly from a horizontal support near the top of the wall provided either by a prop or anchorage.

The anchorage is usually a high tensile cable (tie–rod) anchored to a sheet pile or concrete anchor walls (continuous) or plates (a series of separate units) which are buried in the ground at some distance behind the main wall. It is maintained in its position by the resistance of the adjoining soil against lateral displacement. If the ground conditions are unsuitable for any of the above-mentioned types of anchorage, then anchorages which develop frictional resistance, by means of raking (batter) piles, can be used. Sheet pile anchorages are of balanced or cantilever type. Figure 3 shows various types of anchorage:

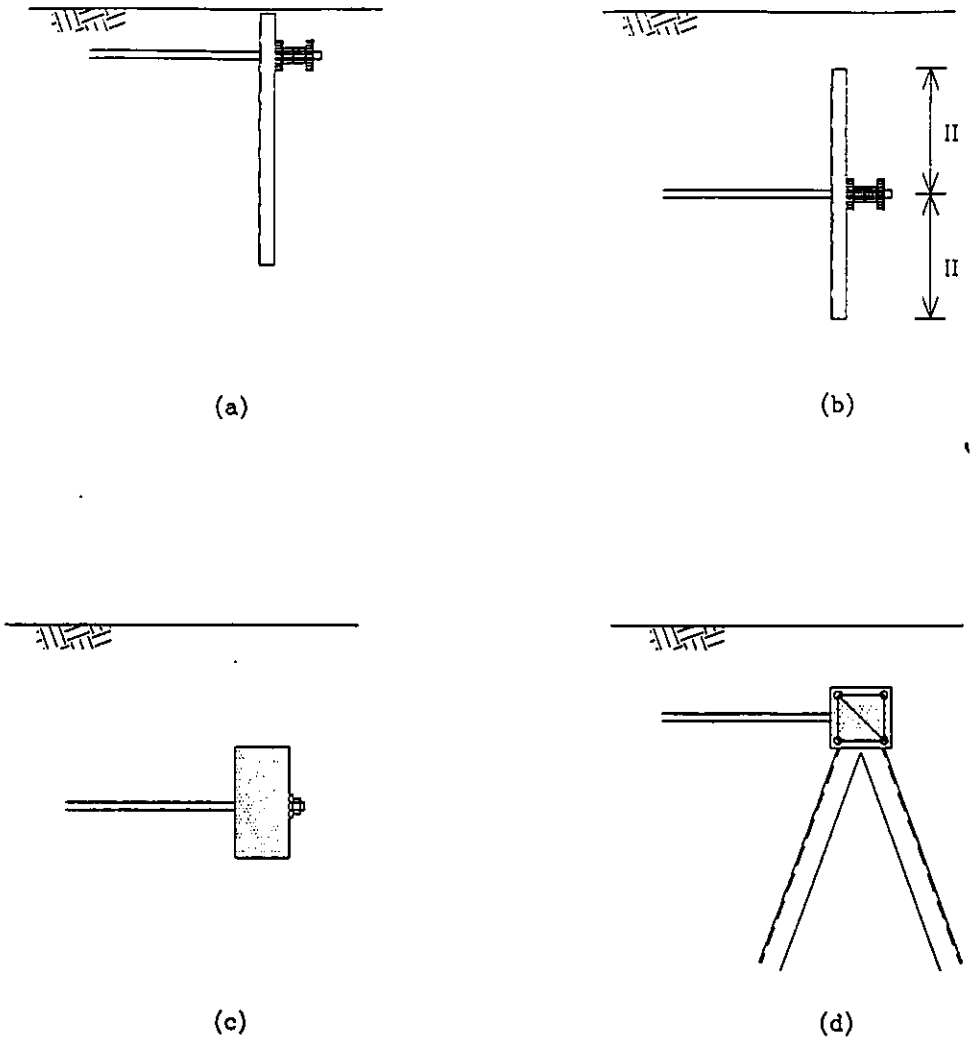

Figure 3 Types of anchorages: (a) cantilever sheet pile anchorage, (b) balanced sheet pile anchorage, (c) mass concrete anchorage, and (d) anchorage with raking piles.

It is crucial in the simple anchorages to provide them with such dimensions that the tie–rod forces do not exceed the external force required to produce failure. The ratio between the tie–rod force and the maximum force the anchorage can stand is called the factor of safety of the anchorage.

Anchored sheet pile walls are widely used as permanent structures in waterfront construction, land reclamation, and deep–foundation construction. They

can give a sufficient support with effectively light structural characteristics, especially in cases where land use is restricted. However, viewing the previous work on anchored sheet pile walls it is obvious that the design of minimum tie-rod lengths has received little attention. Therefore, this thesis was set out to consider the performance of the tie–rod and the effect of various tie–rod lengths on the behaviour of the adjoining soil and consequently the wall. For this purpose a single anchored sheet pile wall with an anchor plate, retaining a granular material, has been considered. The main aim was to study the tie–rod forces and the geometry of soil deformation behind the wall for varying lengths of tie–rod. This was accomplished by undertaking a series of laboratory tests using a model tank. Although, due to practical difficulties it was not possible to take measurements of the tie-rod forces the deformations in the soil were measured using a plain technique. In addition to the tests, a finite difference analysis was employed contributing to the laboratory results.

1.2 Previous Work

In order to adopt the appropriate pile section, it is vital to have a detailed knowledge of the characteristics and the behaviour of anchored sheet pile walls, in relation with the physical and mechanical parameters (earth pressures, soil type, wall movement, etc.) of any particular problem. This necessity has led to a considerable body of literature determined from model tests, theoretical analyses, and measurements taken on full–scale walls.

The theoretical analyses involved the consideration of stability by investigating the earth pressures and their distribution upon the wall, in relation with a philosophy of limit state at which failure occurs. The earlier analyses were based on Coulomb's and Rankine's theories. Coulomb with his work, now known as "The Classical Theory of Earth Pressures" (1776), established the important concept of limiting equilibrium to a continuum and postulate the basic concepts of the active and passive earth pressures giving the well known expressions for these cases. In a paper entitled "Stability of Loose Earth", Rankine (1857) criticised Coulomb's theory and proposed a theory of his own which yielded simple expressions for the active and passive conditions.

In later theoretical analyses, when the soil–structure interaction had been observed, it was attempted to approach the case by treating the soil as an elastoplastic material or by replacing it by springs of varying and non–linear stiffness (Turabi & Balla 1968, Arslan, Breth & Wanninger 1981). However, the theories of Coulomb and Rankine are still used in design due to their simplicity and the ease with which they could be applied in practical applications. Therefore, they are discussed in detail in the following chapter.

Rowe (1952) studied the influence of surcharge, anchor depth, anchor displacement, excavation level, soil type and density, pile flexibility, and distribution of soil pressure by performing a comprehensive series of tests on anchored flexible walls which retained cohesionless soils. He found agreement with earlier work of Stroyer and Tschebotarioff, when the same conditions applied. Besides he indicated the conditions under which Coulomb theory was appropriate and proposed modifications

: Coulomb pressure distributions as a result of the wall deformation and soil arching. The flexibility of the wall was recognised as an important parameter, particularly for :he decrease in bending moment, making Rowe to recommend his moment reduction :actors. Rowe's work had serious implications for the design of anchored sheet pile walls.

Later model tests were performed by a lot of researchers giving interesting results for earth pressure distribution, maximum anchorage loads, and wall and soil deformation. Terzaghi (1954), using a small model wall retaining a bed of sand, recorded the amount of rotation needed to reach the active and passive states. He found that the active state was reached with very little movement; in contrast much more movement was needed to reach the passive state. This has led to the concept that only a small proportion of the passive pressure should be used in design.

Das (1975), performing model tests on individual anchor plates in cohesionless soil proposed two equations for the ultimate pullout resistance of square and circular anchors respectively, based on Meyerhoff's concept of equivalent free surface.

A more detailed investigation on the behaviour of anchor plates, with either vertical or horizontal axis, in granular soils was done by Rowe and Davis (1982) where model tests were done to confirm the theoretical approach of the authors. Consideration was given to the effects of anchor embedment, friction angle, dilatancy, initial stress state, and anchor roughness. The results were presented in influence

graphs of the anchor capacity factor F_γ, allowing an estimate of anchor capacity to be made for a wide range of geometric and soil types.

A year later (1983) Milligan studied the deformations behind an anchor sheet pile wall using model walls and a radiographic method for measuring displacements. His approach was interesting as he considered the sheet pile wall and the anchorage as an integrated system and he tried to predict the soil deformations using a simple velocity field. However, the results showed that the pattern of soil displacement, related to the deformation of the wall, are quite complex but could be divided into a number of relatively simple zones.

More recently the use of finite element methods have allowed attempts to be made at the complete solution of the problem, determining stresses and deformations in both the wall and adjoining soil. Pitilakis (1981) investigated the interaction between an anchored sheet pile wall and a granular soil in relation with the flexibility of the whole system. He concluded that the relative displacement of the anchorage with the wall could modify the tie–rod force. He pointed out that the flexibility of the system was dependent on the distance between the anchorage level and the excavation level. In addition, he showed the distribution of soil pressure upon the anchor plates. Finally, the kinematics of soil deformation were concerned, been geometrically influenced by the length of the tie–rod.

Potts and Fourie (1986) employed a finite element method to investigate the influence of the wall movement on the generation of earth pressure. It was shown that

:ne distribution of earth pressure was highly dependent on the mode of wall deformation. The magnitude of the displacement necessary to mobilise limiting conditions was also effected by the mode of wall movement. Considerably large displacements were necessary for a wall rotating about its base. Furthermore, it was shown that the relative displacements necessary to mobilise active and passive condition depended on the wall roughness, the value of earth coefficient at rest, and the distribution of Young's modulus. Although the effect of the soil dilation, the initial horizontal stress, and the distribution of soil stiffness with depth were also examined there was not any investigation of the performance of a tie–rod in the case of an anchored wall.

Simpson (1992) studied the importance of displacement and strain incorporating into the design methods being used for earth retaining walls. Based on the concept that most soils exhibit much higher stiffness at very small strains than were measured in traditional laboratory tests he introduced a new constitutive model of soil behaviour. Despite its simplicity the model led to predictions of a wide range of soil properties for both normally consolidated and overconsolidated states. Furthermore, the model was incorporated into a finite element programme and reproduced fairly well the ground movements for two full-scale cases.

Selby (1997) employed a large displacement finite difference method to investigate the kinematics of failure and the tie-rod tensions of a sheet pile wall and anchor system in granular soils. In addition, the effects of soil properties, wall stiffness, surcharge, and excavation depth were studied. He indicated an alternative pattern of

soil movements at failure and proposed that shorter tie-rod lengths may be used than the traditional design.

2 THEORY IMPLEMENTATIONS

2.1 Idealised Stress–Strain Relations for Soils. Theory of Plasticity

Since the actual behaviour of a soil is very complicated, showing a great variety when subject to different conditions, drastic idealisations are essential in order to develop simple mathematical stress–strain, or in other words constitutive, models for practical applications.

One such idealisation is shown by the dotted lines in Figure 4(a) on page 12. A linearly elastic behaviour is assumed between O and Y followed by unrestricted plastic flow (strain) YP at constant stress. The point Y is the assumed yield point. This idealisation is known as the "elastic–perfectly plastic" model of material behaviour. An another idealisation is the "elastic–strain hardening plastic" model, shown in Figure 4(b), in which plastic flow beyond the yield point necessitates further stress increase. A significant characteristic of strain hardening is the increase in the yield stress when unloading and reloading takes place subsequent to yielding.

The characteristics of yielding, hardening, and flow are described by a yield function, a hardening law, and a flow rule respectively. The yield function is written in terms of stress components and represents the yield point (or yield surface in space). For instance the Mohr–Coulomb criterion is one possible yield function, if perfectly plastic behaviour is assumed. The hardening law represents the relationship between the increase in yield stress and the corresponding plastic strain components. The flow

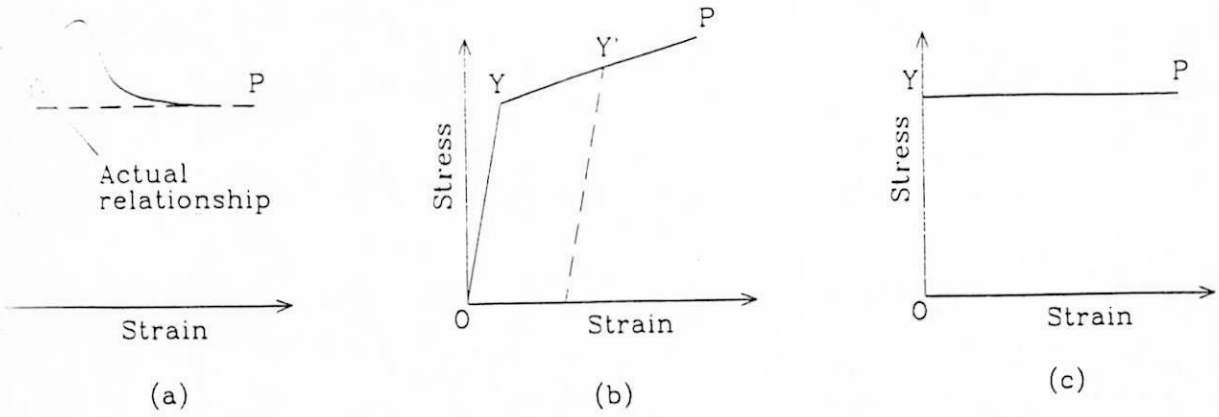

Figure 4 (a) Elastic–perfectly plastic, (b) elastic–strain hardening plastic, and (c) rigid–perfectly plastic models of material behaviour.

rule specifies the plastic strain rate components during yielding under a particular state of stress.

The problem of the behaviour of a soil mass supported by a retaining structure is a problem where both stress and displacements are considered. It involves the knowledge of appropriate equations defining a constitutive relation of the soil, and the solution of the equilibrium and compatibility equations for the given boundary conditions. The rigorous analysis of such problem is rarely possible. However, provided that a consideration of displacements is not required, it is usually the condition of the ultimate failure of the retained soil mass and the determination of the load system at that condition which is of primary interest. This defines the problem as a stability problem in plasticity.

Thus, the soil can be idealised as a "rigid–perfectly plastic" model, shown in Figure 4(c), in which yielding and unrestricted plastic flow, in the form of shear failure, take place at a constant stress level. The soil mass is then said to be in a state of plastic

equilibrium. The load computed on the basis of this ideal situation is called plastic limit load.

In real conditions plastic collapse occurs after the state of plastic equilibrium has been reached in part of a soil mass, resulting in the formation of an unstable mechanism in which this part of the soil mass slips relative to the rest of the mass. The load system corresponding to this condition is defined as plastic collapse load.

By means of limit analysis and the lower and upper bound theorems the plastic limit load usually gives a good approximation to the collapse load. The theorems of limit analysis can be stated as follows:

Lower bound theorem. If a state of stress can be found which balances the applied loads and at no point exceeds the failure criterion for the soil, then collapse will not occur; the applied loads constitute a lower bound plastic limit load.

Upper bound theorem. If a compatible mechanism of plastic deformation is assumed and if, in an increment of displacement, the work done by the applied forces is equal to the dissipation of energy by the internal stress, then collapse must occur; the applied loads will be higher or equal to the plastic collapse load (upper bound limit load).

Over the past few years sophisticated finite element and finite difference programmes have been developed. They have incorporated complex elastoplastic soil

models and they have been able to yield information on the details of stress distribution (at loads smaller than the ultimate) and strain characteristics. However, these are research tools mostly, not available to designers.

The conventional methods of design do not explicitly require a consideration of plasticity. Still, the idealisation of plasticity is implicitly used in the methods of Coulomb and Rankine for determining earth pressures. As was noted before (section 1.2) the basis for any retaining wall design is the determination of the earth pressure likely to occur. Therefore, the Rankine's and Coulomb's theory of earth pressure are going to de discussed in the following section.

2.2 Theories of Earth Pressure

2.2.1 Rankine's theory of earth pressure

Rankine considered the distribution of stress in a soil mass when the condition of plastic equilibrium has been reached, i.e. when shear failure is on the point of occurring throughout the mass. His original work was orientated in cohesionless soils, but later his theory was expanded to include soils with cohesion greater than zero. His theory satisfies the conditions of lower bound limit analysis solution since it considers only stresses and failure and gives no consideration to soil kinematics.

The Mohr circle is used to represent the state of stress at failure, as shown in Figure 5. The state of plastic equilibrium can be developed only if a sufficient deformation of the soil mass take place in two distinct ways, either a lateral expansion or a lateral compression.

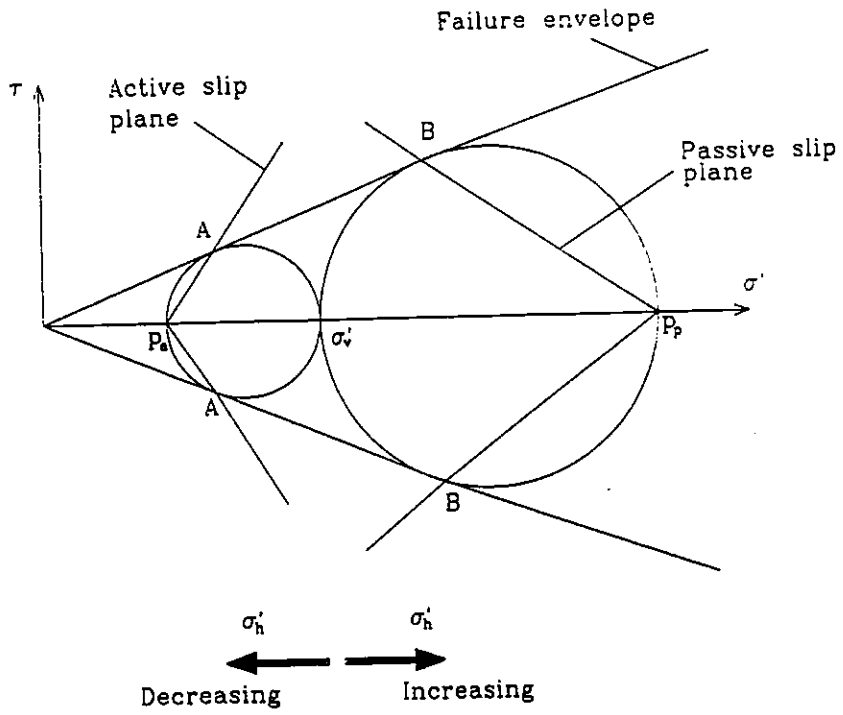

Figure 5 State of plastic equilibrium in a two–dimensional soil element.

A semi–infinite mass of cohesionless soil with a horizontal surface is considered, having in addition a vertical boundary formed by a smooth wall surface extending to semi–infinite depth, as represented in Figure 6. The unit weight of the mass is γ and φ is the angle of shearing resistance. A soil element at any depth z is subjected to a vertical stress σ_v and to a horizontal stress σ_h (assumed plain strain conditions). Since the surface is horizontal, there is no lateral transfer of weight and thus no shear stresses exist on horizontal or vertical planes. Consequently, the vertical and horizontal stresses are principal stresses.

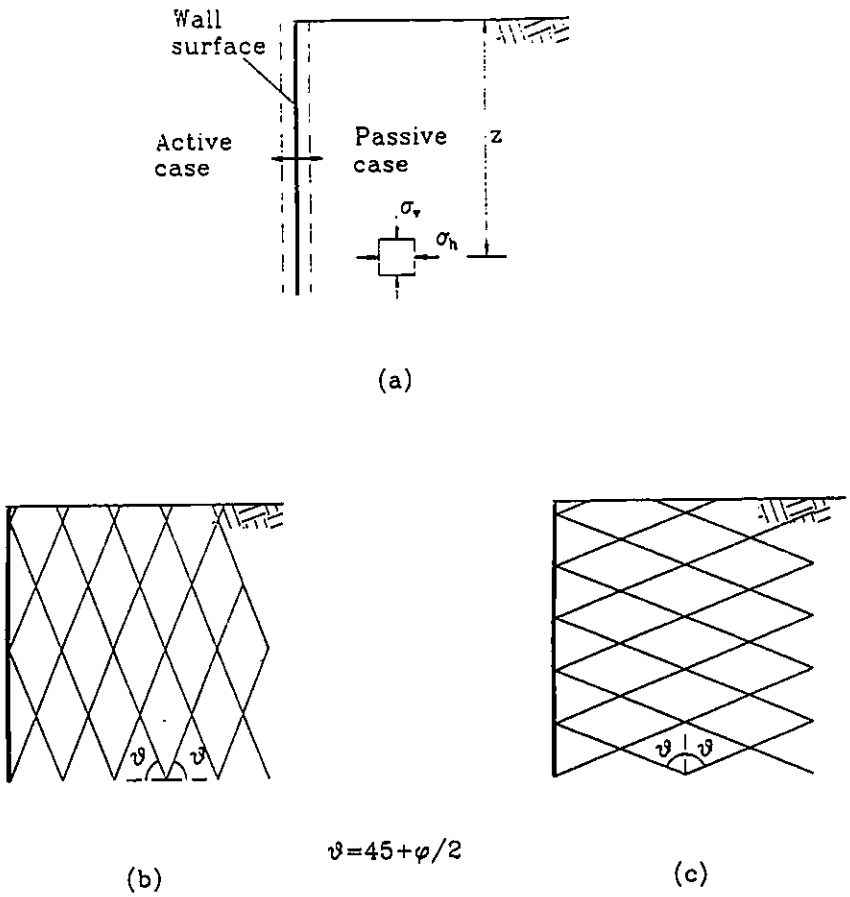

Figure 6 Rankine's considerations.

If there is now a movement of the wall away from the soil, the horizontal stress σ_h decreases as the soil expands outwards. Hence, the horizontal stress must be the minor principal stress σ_3 and eventually the vertical stress is the major principal stress σ_1. The value of σ_1 is the overburden pressure at depth z, i.e. $\sigma_1 = \gamma z$. If the expansion is large enough the value of σ_h decreases to a limiting (minimum) value at which a state of plastic equilibrium is developed. The plastic state which is produced by this lateral expansion of the soil mass is called active Rankine state, since the weight of the soil assists in producing the expansion.

The limiting horizontal stress for the above condition is defined as the active pressure (p_a). It can be determined form the Mohr circle passing through the point representing $\sigma_v = \sigma_1$, when touches the failure envelope of the soil. Referring to Figure 5 and that $\sigma_{h\,min} = p_a = \sigma_3$, $\sigma_v = \gamma z = \sigma_1$,

$$p_a = \sigma_v\left(\frac{1-\sin\varphi}{1+\sin\varphi}\right), \\ = K_a \gamma z \qquad (2.1)$$

where $K_a = \dfrac{1-\sin\varphi}{1+\sin\varphi}$ is defined as the active pressure coefficient.

There are two sets of shear failure planes each inclined at $\left(45^\circ + \varphi/2\right)$ to the horizontal, the direction of the major principal plane, as shown in Figure 6(b).

If the wall is moved against the soil mass, there will be lateral compression of the soil and the value of σ_h will increase until a state of plastic equilibrium is reached. For this condition σ_h becomes a limiting (maximum) value and is the major principal stress (σ_1) while the vertical stress becomes the minor principal stress, $\sigma_v = \sigma_3 = \gamma z$. The plastic state produced by the lateral compression is called passive Rankine state, since this compression is resisted by the weight of the soil.

The maximum horizontal value is defined as passive pressure (p_p). Similar to active pressure, passive pressure can de derived when the Mohr circle through the point representing the value of σ_v (= σ_3) touches the failure envelope of the soil. Referring again to Figure 6,

$$p_p = \sigma_v\left(\frac{1+\sin\varphi}{1-\sin\varphi}\right),$$
$$= K_p\gamma z \qquad (2.2)$$

where $K_p = \frac{1+\sin\varphi}{1-\sin\varphi}$ is defined as the passive pressure coefficient.

In the passive Rankine state there are again two sets of failure planes; however, each one is inclined at $\left(45^\circ + \varphi/2\right)$ to the vertical, since is the direction of the major principal plane. See Figure 6(c).

When the failure envelope of the soil includes a cohesion intercept (c), the active pressure is smaller than if there were no cohesion, by an amount

$$\delta_{p_a} = 2c\sqrt{\frac{1-\sin\varphi}{1+\sin\varphi}} = 2c\sqrt{K_a}.$$

Conversely, in the case of passive state the passive pressure is greater by an a amount

$$\delta_{p_p} = 2c\sqrt{\frac{1+\sin\varphi}{1-\sin\varphi}} = 2c\sqrt{K_p}.$$

The force per unit length of a wall due to active distribution is called the total active thrust (P_a) while the force due to passive pressure distribution is referred to as the total passive resistance (P_p). Equations 2.1 and 2.2 show that both active and passive pressures increased linearly with depth forming triangular distributions for

cohesionless soils. Thus, both active thrust and passive resistance act at a distance $\frac{1}{3}H$ above the bottom of a wall with height H.

The main drawback of Rankine's theory is the assumption that the wall surface is smooth; thus, the wall does not affect the stresses. In practice considerable friction may be developed between the wall and the adjacent soil, depending on the wall material. Due to this assumption, Rankine's theory overestimates the active pressure and underestimates the passive pressure.

2.2.2 Coulomb's theory of earth pressures

Coulomb considered the stability of a soil wedge between a retaining wall and a trial failure plane when the wedge is on the point of sliding either up or down the failure plane. In other words, he considered the stability of the wedge when it was in a condition of limiting equilibrium. The force between the wedge and the wall surface was then determined by the equilibrium of forces acting on the wedge, been at this limiting state.

A significant parameter to Coulomb's theory is that the friction between the wall and the adjacent soil is taken into account. The angle of friction between the soil and the wall material is referred to as wall friction (δ) and can be determined by direct shear tests. Due to wall friction a shearing resistance per unit area, $p_n \tan\delta$, is developed on the wall surface, where p_n is the normal pressure at any point on the wall. Thus, the

shape of the failure surface is curved near the bottom of the wall in both the active and passive cases, as represented in Figure 7.

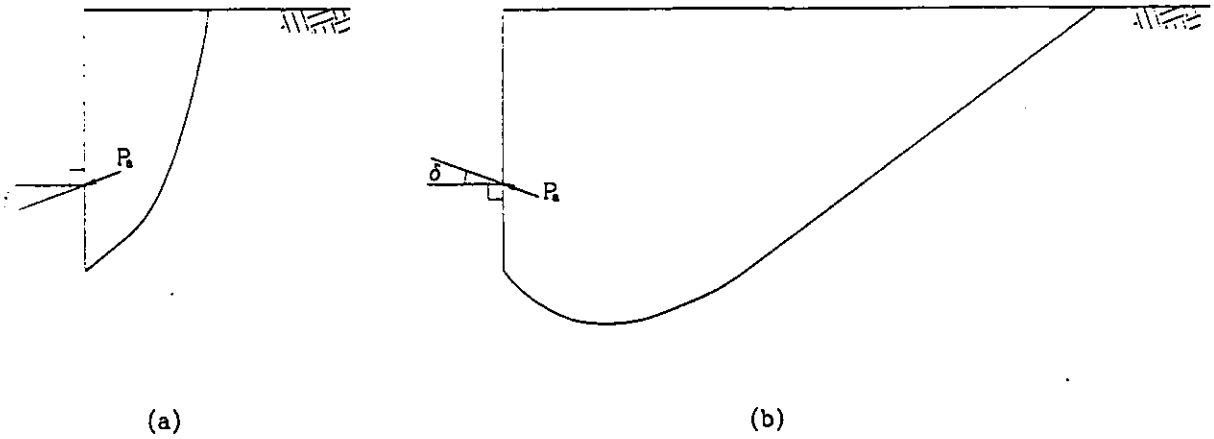

Figure 7 Curvature due to wall friction.

Although the wall friction is taken into account, the failure surfaces are assumed to be plane in Coulomb's theory. This impose an error which in the active case is relatively small, since the curvature is slight. In the passive case the error may be small for values of wall friction less than $\varphi/3$, but for higher value the error becomes relatively large. When $\delta = 0$, the Coulomb's theory gives results identical to those obtained from the Rankine's theory, for the case of a vertical wall and a horizontal soil surface.

The Coulomb's theory is now interpreted as an upper bound limit analysis solution, for the collapse of the soil mass above a chosen failure plane which occurs as the wall moves away form or into the soil. In general, the theory underestimates the total active thrust and overestimates the total passive resistance.

2.3 Application of Earth Pressure Theory to Retaining Walls

It has been stated that the transition of a semi–infinite soil mass from a state of elastic into a state of plastic equilibrium can only be accomplished by an imaginary lateral expansion or compression of the soil as a whole. However, this is without any parallel in the physical world. The movement of a retaining wall of finite dimensions can develop active or passive states in a soil mass which are never extended beyond the boundaries of very narrow zones. Thus, the active state, for example, would be developed only within a wedge of soil between the wall and a failure plane passing through the lower end of the wall and at angle of $\left(45^\circ + \varphi/2\right)$ to the horizontal. Similar the passive state can be developed within a wedge of soil between the wall and a failure plane at an angle of $\left(45^\circ - \varphi/2\right)$ to the horizontal. Figure 8 represents the development of the active and passive states.

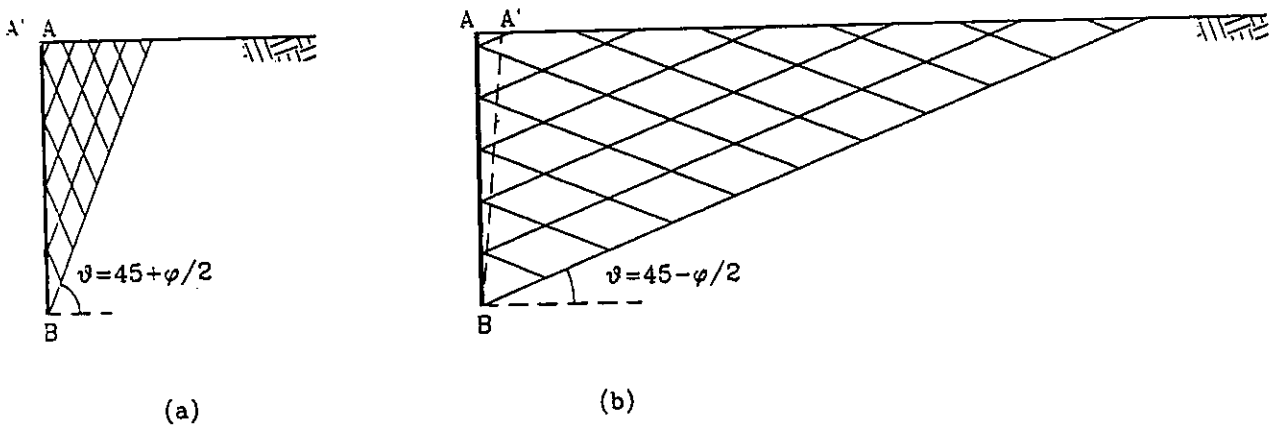

Figure 8 Development of active and passive states in a retaining wall.

In order an active or passive state to be developed, a specific value of lateral strain is necessary. This strain can be produced by a movement of the wall. It has been shown by Terzaghi that in the case of normally consolidated sands the active case can be reached with very little movement. On the contrary, much more displacement is needed for the mobilisation of passive state, as shown in Figure 9.

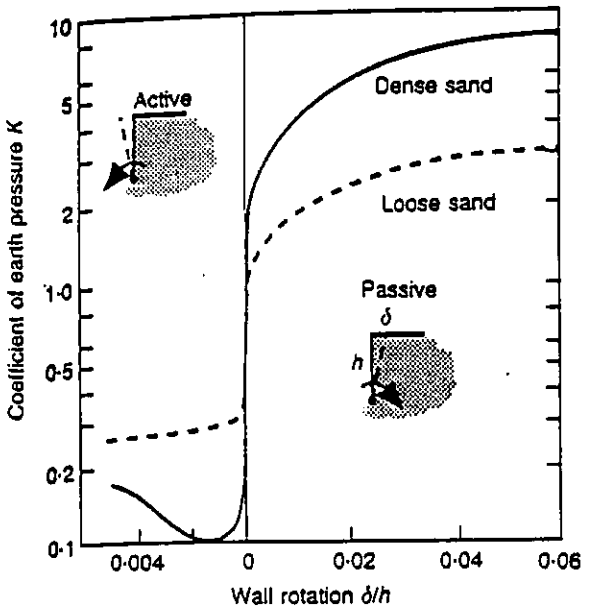

Figure 9 Relationship between earth pressure and wall rotation for normally consolidated sand (after Terzaghi).

Furthermore, Potts and Fourie showed that the magnitude of the displacement necessary to mobilise limiting conditions depends on the mode of wall movement (rotation, translation). Thus, considerably large displacements are necessary for a wall rotating about its base.

One additional concept that differs from theory to actual condition is the distribution of earth pressures. The simple linear assumptions about active and passive

pressures are a considerable simplification of some very complex processes. which depend on the following factors:

- the mode of wall movement
- the wall flexibility
- the soil stress and strain properties
- the in situ stress in the soil and the construction techniques.

2.3.1 Mode of wall movement

The distributions of earth pressures are greatly dependent on the way the wall moves. For a wall rotating about its top or bottom the distributions are far from linearity, as shown in Figure 10 on page 24. For example, for a wall rotating about its top the soil on the active side at failure is in a passive condition near the top attaining to the active condition with the depth. Similarly for a wall rotating about its bottom the soil on the active side at failure exceeds the classical value lower down. In consequence, although the values of both active and passive pressures do not appear to differ greatly from their theoretical values, the points of action of the resultant forces, particularly the total active thrust, are high dependent on the mode of wall movement, having a direct effect upon the resultant wall bending moments.

2.3.2 Wall flexibility

It forms a particular factor for flexible anchored sheet pile walls, since they are relatively light structures and impose a deformation condition on the soil which, in turn, affects the soil pressure distribution.

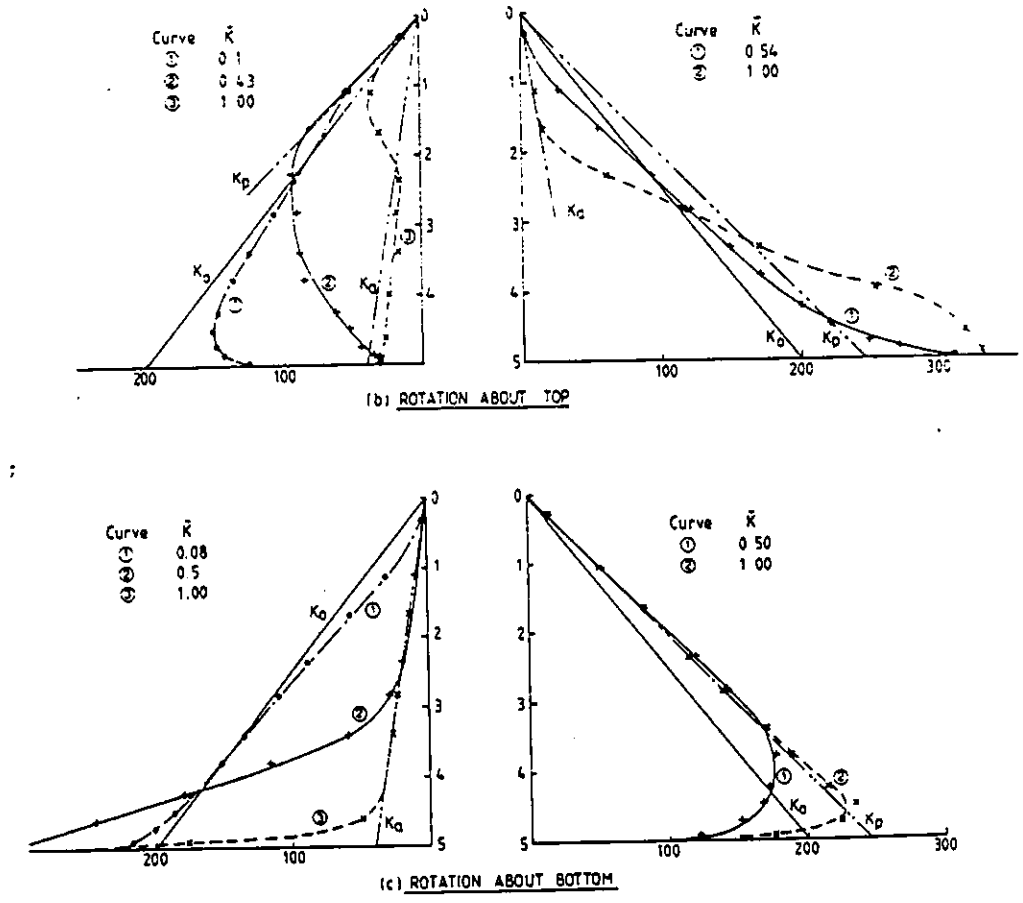

Figure 10 Active and passive pressure distributions for a smooth wall (after Potts and Fourie)

In the case of flexible anchored sheet pile walls, the part between the anchorage and excavation level is able to deflect outwards. Subsequently the pressures at this part are reduced at the expense of higher pressures at the vicinity of the anchorage and below excavation level. These redistributions of earth pressure, represented in Figure 11, are the result of the phenomenon known as arching.

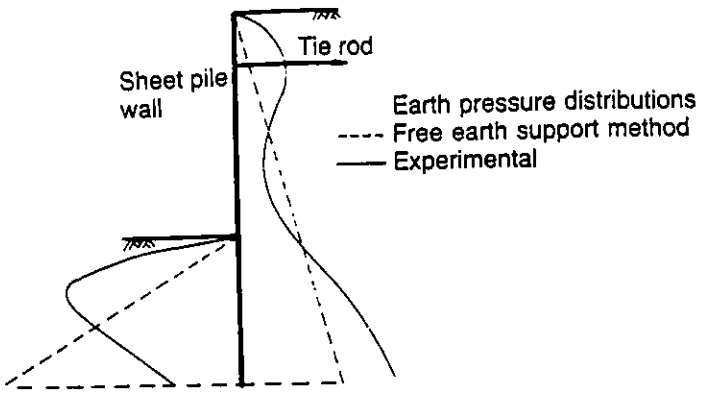

Figure 11 Arching effects (after Craig)

Arching was defined by Terzaghi in the following way:

> If one part of the support of a soil mass yields while the remainder stays in place the soil adjoining the yielding part moves out of its original position between adjacent stationary masses of soil. The relative movement within the soil is opposed by a shearing resistance within the zone of contact between the yielding and the stationary masses. Since the shearing resistance tends to keep the yielding mass in its original position, it reduces the pressure on the yielding part of the support and increases the pressure on the adjoining stationary part. This transfer of pressure from a yielding mass of soil onto adjoining stationary parts is commonly called the *arching effect*, and the soil is said to *arch* over the yielding part of the support. Arching also takes place if one part of a yielding support moves out more than the adjoining parts. [Theoretical Soil Mechanics, 8th edition, p. 66]

In the situation of the flexible sheet pile wall described above, the arching is reduced to an extend, if yield of the anchorage also takes place. The reduce is depended on the amount of yielding. On the passive side of the wall the pressure is increased just below excavation level as a result of larger deflections into the soil.

Wall flexibility depends on the material of construction and the shape of section. It is represented by the flexibility number $\rho = H^4/EI$, where H is the overall height of the wall, E the modulus of elasticity of the wall material, and I the moment of inertia of the cross–sectional area of the wall. The product EI is called flexural rigidity of the wall. The redistributions of the wall flexibility and arching result in lower bending moments than those obtained from design methods. The same applies in the tie–rod forces. In particular, maximum bending moment and tie–rod force are increased as the wall flexibility is decreased. There are moment reduction factors proposed by Rowe (1952) which are applied to the results of "free earth support" analyses (described in section 2.4.2) in order to adjust the maximum bending moment in a more realistic value.

2.3.3 Soil stress and strain properties

Such as these consider the angle of shearing resistance (φ) and the angle of dilation (ψ) of the soil. (The discussion is limited to the cohesionless soils.) In earth pressure theories a constant value of φ is assumed throughout the soil above the failure surface. However, approaching a limiting state the stresses (and consequently the strains) vary significantly throughout the soil mass and in particular along the failure surface. This results in a respective variation of the mobilised angle of shearing resistance.

In the case of dense sands the average value of φ along the failure surface corresponds to a point beyond the peak value φ_p, where the overriding of the

interlocking particles has occurred, that of the critical state φ_{cv}. In the case of loose sands there is no significant interlocking to be overcome and the principal stress difference increases gradually to an ultimate value without a prior peak. Hence, in the limiting conditions the angle of shearing resistance along the failure surface will be again the φ_{cv}. So, by using the peak value φ_p there would be an underestimation of total active trust and an overestimation of passive resistance. Therefore, the angle of shearing resistance used in design is either the peak value φ_p divided by a factor F_s = 1.2, or the critical state value φ_{cv}.

The term dilatancy is used to describe the increase in volume of dense sand during shearing. (In the case of loose sands shearing takes place at constant volume.) Rowe developed a stress–dilatancy theory relating the ratio of principal stresses, the geometry of ideal particle arrangements, and the relative rates of change of volumetric and major principal stains. The angle of dilation was defined either in terms of the maximum and the minimum principal strain increments $d\varepsilon_1$ and $d\varepsilon_3$ or in terms of increments of volumetric stain ($d\varepsilon_v$) and shear strain ($d\gamma$) as follows:

$$\sin \psi = \frac{d\varepsilon_1 + d\varepsilon_3}{d\varepsilon_1 - d\varepsilon_3} = -\frac{d\varepsilon_v}{d\gamma}$$

According to Bolton, the effect of increasing ψ at a constant φ may either be neutral or beneficial to the overall stability, depending on the particular geometry of the problem. The angle of shearing resistance will be $\varphi = \varphi_{cv} + 0.8\psi$. On the other hand, as Potts and Fourie show, the angle of dilation has very little influence on the overall stability of a retaining wall, increasing the passive and reducing the active

pressure approximately 3–4 per cent. It must however be noted that their work was on cohesion soil conditions.

2.3.4 Initial stress in the soil and construction technique

The value of K_0 (coefficient of earth pressure at–rest), which represents the initial state of stress in the soil, does not effect the final (limiting) values of earth pressure. Yet, the values of lateral strain required to mobilise active and passive pressure in a particular case depend on the value of K_0. Thus, and in contrast to normally consolidated soils, for soils having a high K_0 value (in the range of 1–2), such as overconsolidated clays, active and passive conditions can be mobilised at similar displacements. In addition, the initial stress has an effect on the behaviour of the wall, imposing bending moments and tie–rod forces, in the case of high values of K_0, which greatly exceed the theoretical values.

The construction technique, backfilling or excavation, represents the subsequent stress path the soil undergoes from the initial state and is associated with the value of K_0, having an effect both to soil limiting conditions and wall behaviour. For backfilled walls the value of K_0 has only a small influence on wall behaviour. In contrast, for excavated walls the value of K_0 dominates the behaviour.

In high K_0 soils, the behaviour of excavated walls is dominated by the vertical unloading caused by excavation, resulting in large vertical displacements and greater bending moments and tie–rod forces than those calculated using the theory. Passive

conditions in front of the wall are completely mobilised at small excavation depths and before active conditions are approached down the back of the wall. In general, the required deformation in the excavated walls is less than that in the backfilled walls for a particular soil. It should be noted that for backfilled walls the lateral stain at a given point is interpreted as that occurring after backfilling has been placed and compacted to the level of that point.

2.4 Design of Anchored Sheet Pile Walls

From the discussion in the previous section, it is obvious that the design of earth retaining structures requires a detailed consideration of the soil–structure interaction. According to British "Code of practice for earth retaining structures" it requires the performance of two sets of calculations:

1) a set of equilibrium calculations to determine the overall proportions and the geometry of the structure necessary to achieve equilibrium under the relevant earth pressures and forces;
2) structural design calculations to determine the size and properties of the structural sections necessary to resist the bending moments and shear forces determined from the equilibrium calculations. [BS 8002: 1994]

Both sets of calculations are carried out for specific design calculations in accordance with the principal of limit state design. Usually the codes of practice are concentrated on the ultimate limit states, where failure of a structure occurred, and drawing attention on balancing forces, by means of factors of safety. Any soil deformation is assumed to be a secondary problem in the working state. However, the displacements

may be larger than normally expected and cause severe damages to structures or services adjacent to the retaining structure, and to the retaining structure itself. In the revised British code consideration is given to serviceability limit states, in which serviceability is assumed by limiting the proportion of the soil's strength which is mobilised in the working state, hence by limiting displacement.

Although there are various types of factors of safety, either "lumped" or partial, the design of anchored sheet pile walls is based on two methods of analysis, depending on the fixity of the bottom of the wall: The free earth support and the fixed earth support method. These are described in the sections 2.4.2 and 2.4.3 respectively.

2.4.1 Modes of failure for anchored sheet pile walls

The following ultimate limit states should be considered in the case of anchored sheet pile walls, represented in Figure 12.

Slip failure. It is associated with the analyses for stability of slopes considering the soil, wall, and anchorage as a whole.

Failure by rotation of the wall about the anchorage. It is associated with insufficient passive resistance due to small embedment depth and it is incorporated into the "free earth support" method of analysis.

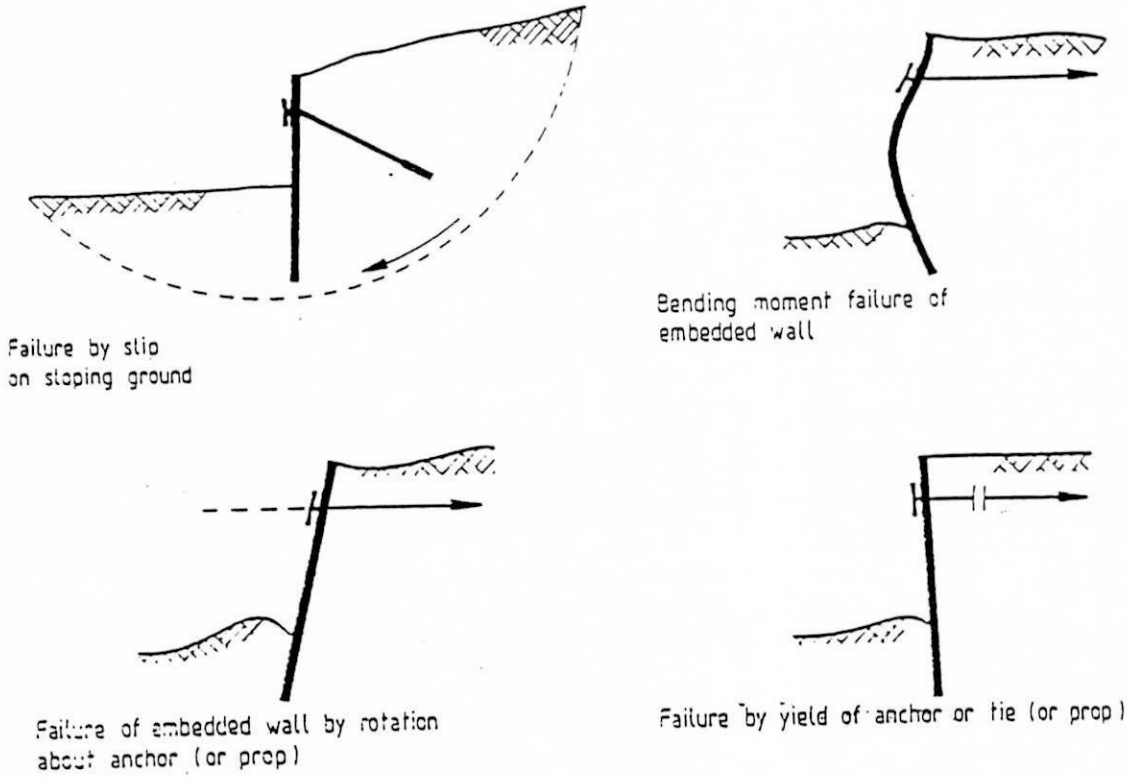

Figure 12 Limit states for anchored sheet pile walls (after British Standard 8004).

Failure by bending of the wall. It is a result of a flexible wall in relation with a relatively rigid anchorage and a deeply embedded bottom of wall, imposing fixity to these parts. It is incorporated into the "fixed earth support" method of analysis.

Failure by breaking of the tie–rod or by yield of anchorage. In the former case failure is caused by insufficient tensile strength of the tie–rod and it can be prevented by designing this particular structural element to have an adequate strength with respect to the acting forces of the system. In the latter case failure of the wall is due to insufficient passive resistance of the soil in front of the anchorage to the movement imposed by the tie–rod force. It is actually this kind of ultimate limit state

which was considered in this thesis. Both cases fail in a cantilever way by rotating about the base of the wall.

2.4.2 Free earth support method

This method of analysis assumes that the embedment is such that the passive resistance in front of the wall is sufficient to resist the forward movement of the bottom of the wall, but not sufficient to prevent rotation. In the limiting equilibrium condition the anchored sheet pile wall is analogous to a simply supported beam. Figure 13 illustrates the cross–section, idealised earth pressure distributions, bending moment diagram, and deflection curve of the wall assumed to occur.

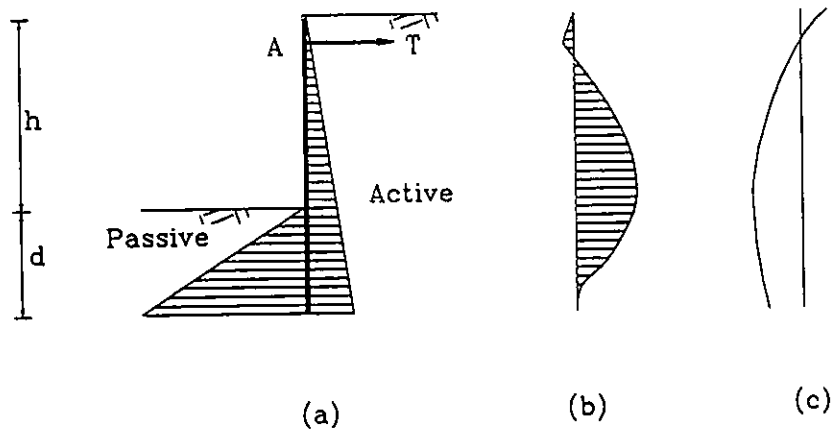

Figure 13 Free earth support method: (a) cross–section and idealised earth pressure distributions, (b) bending moment diagram, and (c) deflection curve.

The mode of failure, as noted before, is rotation about the point of application of the anchorage (A). By taking moments about A, where the algebraic sum of them must be zero, the required depth of embedment (d) can be determined. Subsequently, the tie–rod force (T), per unit length of wall, can be determined by considering the

equilibrium of forces in the horizontal direction. It is important that a factor of safety should be incorporated, usually in respect of gross passive resistance (F_p). Finally, the maximum bending moment can be calculated and thus, the structural dimensions of the wall can be defined.

2.4.3 Fixed earth support method

In this method the embedment of the wall is assumed to be such that the passive resistance in front of the wall is sufficient to prevent both forward movement and rotation of the bottom. In the state of limiting equilibrium the wall is analogous to a cantilever beam, fixed at the bottom, with a simple support at the point of application of the anchorage. Figure 14 illustrates the cross–section, idealised distributions of earth pressure, bending moment diagram, and deflection curve of the wall assumed to occur.

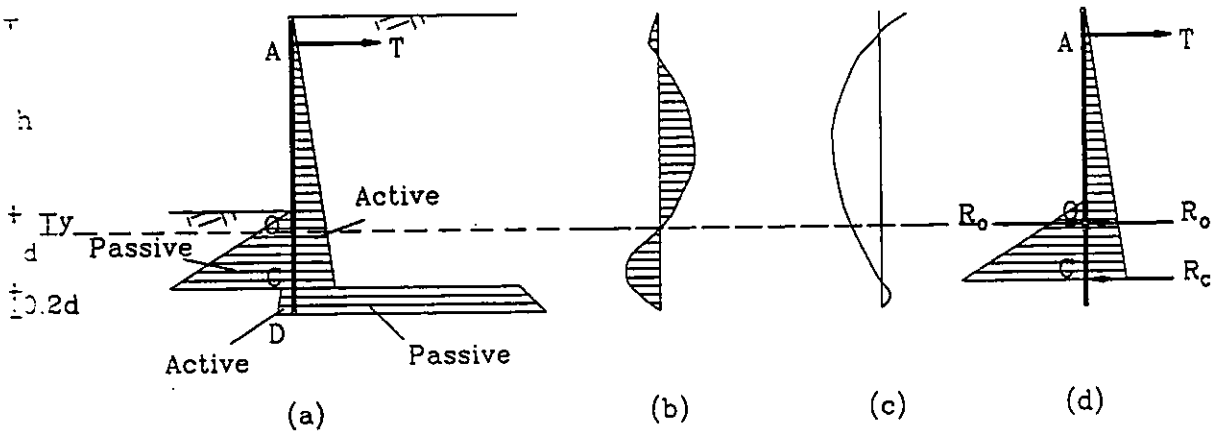

Figure 14 Fixed earth support method: (a) cross–section and idealised earth pressure distributions, (b) bending moment diagram, (c)deflection curve, and (d) equivalent beam.

The failure is only due to bending. The point C in Figure 14(a) is the point of fixity. Passive resistance acts in front of the wall above C and behind the wall below C, thus providing a fixing moment. For the design purposes the net passive resistance is replaced arbitrarily by a concentrated force R_c, which is assumed to act at a distance 0.2d above the bottom of the wall. The depth of embedment is thus 1.2d. No factor of safety is applied to the passive resistance due to the fixity of the base of the wall.

At the point O, in Figure 14(b), the bending moment is zero. Therefore, a hinge may be considered at this point and the problem is analysed as two separate beams by the "equivalent beam" method. For the upper beam, assumed simple supported, the unknowns are the forces T and R_o and the distance y. Terzaghi, for the case of granular soil, determined the following values of y in terms of the retained height of soil h:

φ =	20°	30°	40°
y =	0.25h	0.08h	- 0.007h

The forces T and R_o can be determined by the equilibrium of moment about A or O and by the equilibrium of forces in the horizontal direction. For the lower beam, assumed fixed at the bottom and simply supported at the other end, the unknowns are the force R_c and the distance (d - y). This distance can be determined by taking moments about C (where $R_c = 0$). The maximum bending moment is obtain by again considering the upper beam.

Although the fixed earth support method results in longer walls, the values of the bending moments are lower than those calculated by the free earth support method. This means that lighter pile sections can be used.

2.5 Design of Balanced Anchorages

There are three basic design requirements to be satisfied by the anchorage:

a) The anchorage should not yield by moving forward a significant distance.

b) The anchorage should not undergo excessive settlement or rotation in relation to the tie–rods.

c) The anchor element (wall or plate) should be design to resist the bending moments and shear forces resulting from the tie–rod forces and earth pressures acting upon it.

The resistance to forward movement of an anchorage is directly related to the net passive resistance of the soil and the shearing resistance, developed on both ends of an anchor plate due to the shear, from the adjacent soil, of the wedge of the soil in front the anchor plate. The requirement for settlements is rarely significant for undisturbed granular soils, but where uncompacted backfill or weak soils are incorporated into the design it may be necessary to provide a foundation to the anchorages.

If the height of the anchorage (h_a) is equal or greater than half the depth (d_a) from the surface to the bottom of the anchorage, it can be assumed that limiting conditions are developed over the depth d_a. The net passive resistance of the soil is the

difference between the passive resistance (P_p) in front of the anchorage and the active trust (P_a) developed behind the anchorage. For an individual anchor plate of width b_a the resistance of the anchor must be equal to the tie–rod force. Thus,

$$T = \frac{1}{F}\left(P_p - P_a\right)b_a + P_s,$$
$$= \frac{\gamma d_a{}^2 b_a}{2F}\left(K_p - K_a\right) + P_s.$$

where $P_s = \frac{1}{3}\gamma d_a{}^3 K_a \tan\left(45° + \varphi/2\right)\tan\varphi$ is the total shearing resistance from both ends of the plate,

F is the factor of safety, usually of two, to ensure the design requirement.

If the height of the anchorage is small compared with the depth, the anchorage should be expected to yield by ploughing through the ground without producing shear failure extending to the surface. The resistance of such an anchor with height h_a is approximately equal to the bearing capacity of a continuous footing with a width h_a whose base is located at a depth $d_a - h_a/2$ below the ground surface.

The above, traditional, design of anchorages requires the location of the anchorage in a distance behind the main wall such that the passive wedge of the anchor does not intersect the active wedge of the wall. Figure 15 on page 37, illustrates the correct position of the anchorage and the planes of potential failure. Where the active and passive wedges of the sheet pile wall and the anchor necessarily interfere, the

anchor will should be assumed not to develop full passive resistance due to lateral stress relief of a zone inside the passive wedge, which follows the active movement of the main wall. Hence, the inadequate distance between the main wall and the anchorage reduces the anchor resistance approximately by the amount

$$\frac{1}{2}\gamma d_i^{\,2}\left(K_p - K_a\right),$$

where d_i is the depth from the surface to the point of intersection of wedges.

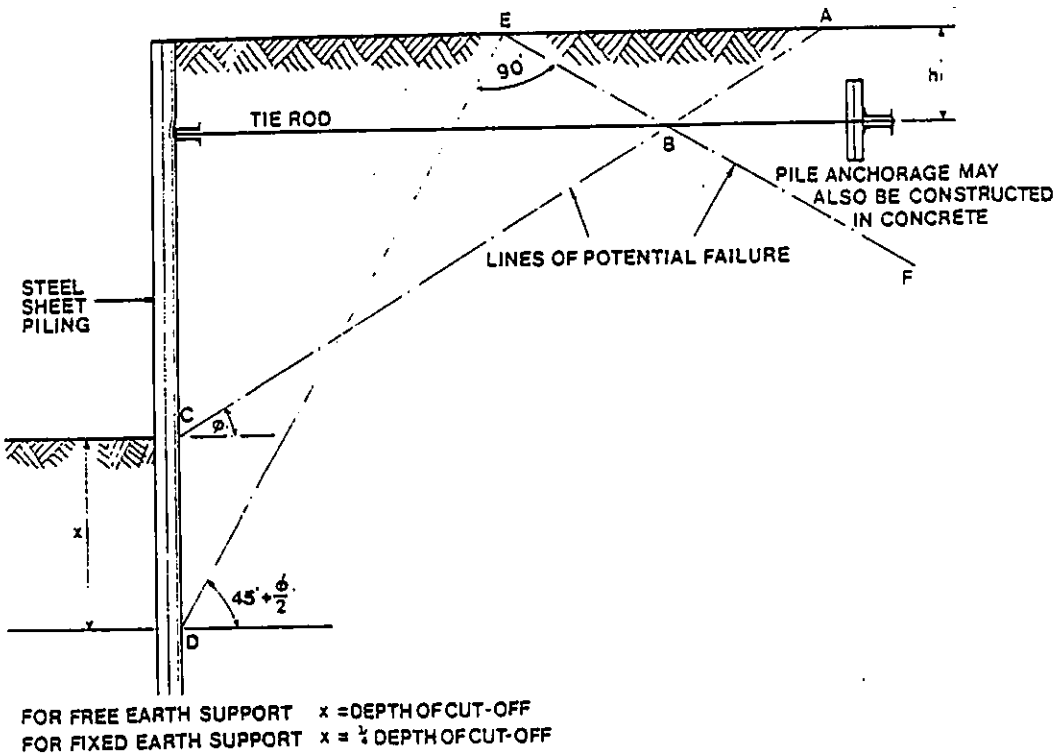

Figure 15 Conventional design of anchorages (after British Steel Co.).

3 LABORATORY EXPERIMENTS

As previously discussed, especially in the review of the research literature (see section 1.2), there is a lack of interest in the effects of the tie–rod on the sheet pile wall–anchorage system. This effect should be considered not only on the anchorage resistance, but also in the ground movements around an anchored sheet pile wall in the state of plastic equilibrium. The latter is of great importance because of the possible effects on adjacent buildings and services.

The laboratory experiments were carried out to investigate the geometry of soil deformation, and the resistance of the anchorage with respect to varying lengths of tie–rod. The traditional design of simple sheet pile anchorages is based on the appropriate location of the anchorage so as to achieve non–intersction of the active wedge behind the sheet pile wall and the passive wedge in front of the anchor. However, this is quite arbitrary, offering nothing but a simplicity in the design calculations. The soil wedges are considered almost "closed" to their limiting conditions, being unaffected by the rest of the soil and in general the behaviour of the system as a whole. Biarez and Hicher (1993) using plane stress laboratory simulation models demonstrated that the ground movements around a wall with a short tie–rod are of the type of a single modified zone of large movements of the soil. This concept is considerable different to the conventional assumption of discrete active and passive wedges.

3.1 Soil Classification

In order to avoid problems of soil–tightness between the front and the back of the model wall, a sub–angular gravel material was decided to be used. A cohesionless soil was chosen avoiding any complications caused by cohesion. In addition, dry and loose states were incorporated in order to avoid problems of pore–water pressure and to establish critical state conditions at failure. Particle size analysis, direct shear tests, and angle of repose and density measurements were performed to define the properties of the soil.

3.1.1 Particle size distribution

The dry sieving method was employed for the determination of the particle size distribution of the gravel. Two tests were performed under the British Standard Institution procedure BS 1377: Part 2.9: 1990, using approximately 3 kg of gravel for each test. The 14 mm, 10 mm, 6.35 mm, and 4.76 mm test sieves were used. For both tests the loss of material was of 0.01%.

From the results of the tests it was easy to be deduced that the material was a poorly graded (uniform) medium–coarsed gravel of average particle size of 7 mm. The coefficient of uniformity of the material was $C_u = 1.5$.

3.1.2 Shear strength parameters

Since the material was gravel, the angle of shearing resistance of the material was the only parameter to be measured. The dry and loose state, in which the model tests were performed, led to the determination of the effective angle of shearing resistance in the critical state respectively.

Three direct shear tests were carried out in a large shearbox apparatus according to BS 1377: Part 7.5: 1990 for cohesionless soils to a loose state, under 5.3 kPa, 50.5 kPa, and 100.6 kPa normal stress respectively. The rate of displacement was 1 mm/min. The angle of shearing resistance was determined to be $\varphi'_{cv} = 43°$ which corresponded well with the angle of repose measured in simples piles of the gravel.

Furthermore, a series of another three tests were carried out to determine the wall friction and the side friction. A square piece of plywood was used to fill the lower half of the large shearbox while the upper half was filled with gravel. The tests were carried out under 5.3 kPa, 50.5 kPa, and 75.4 kPa normal stress. The rate of the displacement, which was parallel to the wood orientation, was again 1 mm/min. Finally, tests carried out to determine the side friction between the gravel and glass. The method was similar to the previous tests. The wall friction was measured to be $\delta = 33°$ while the friction between the gravel and the glass was 19°.

3.1.3 Density

The density of the material for the laboratory experiments was measured directly during the experiments by weighing the gravel prior to use. In each test the net volume of the tank was known and so the density was easily defined by the equation $d = M/V$. From the density measurements the unit weight of the soil was measured to be $\gamma = 14.4$ kN/m^3 with a standard deviation of 0.1 kN/m^3.

3.2 Design of Equipment

3.2.1 Tank

The tank used in the experiments was design by Wells (1984) for the performance of model tests on sheet pile walls in sand. One side was transparent, made of a 6 mm rectangular plate glass, while the other was made of 12 mm plywood. The frame around the glass was designed in timber of 50 mm × 50 mm cross–sectional area. The bottom and ends of the tank were also designed in 12 mm plywood. The two faces of the tank were held together by lengths of 12 mm diameter threaded bar spaced around the frame. Extra stiffening was added at two levels across the glass side of the tank, taken the form of timber stiffened with 25 mm × 25 mm steel angle sections.

Wells performed tests in Leighton Buzzard sand. Since in the series of tests performed in this thesis, the soil material had greater particle size (see section 3.1), the need for a higher sheet pile wall came up. So, the tank was turn over such that the internal dimensions became 1.16 m × 0.21 m × 1.58 m height. Figure 16 illustrates the details of the model tank.

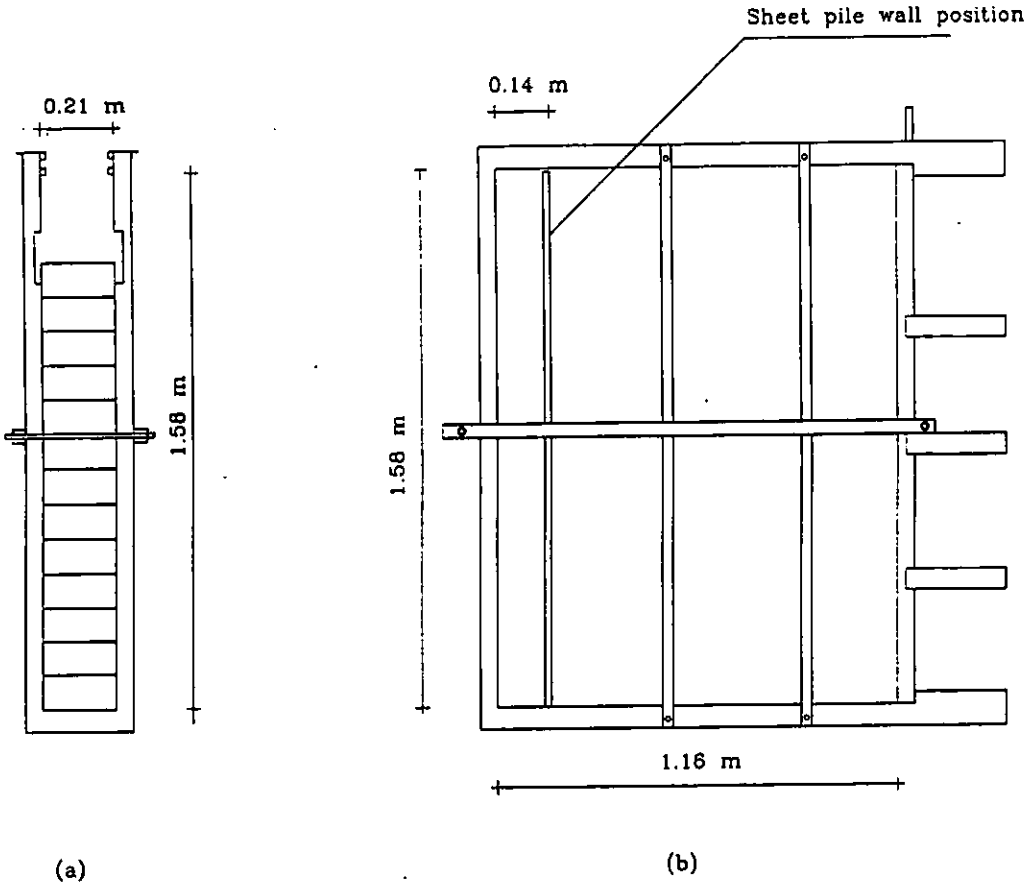

Figure 16 Details of tank: (a) front view, (b) side view.

Due to the limited length of the tank and in order to avoid influence on the ground movements on the active side a clearance of only 140 mm was allowed between the pile and the front of the tank providing a length of soil on the active side of 1.02 m. During the tests there was space in the tank which had no effect on the

general behaviour of the system. This was at the bottom far corner from the wall. The space was eliminated by polystyrene blocks with appropriate dimensions for each test.

The width of the 0.21 m was considered adequate for establishing plain strain condition against edge effects. According to Arthur and Roscoe (1965) the side friction is not a large factor in determining the strain and hence the stress field in model tests. On the contrary, the intermediate principal stress, being directly influenced by the rigidity of the tank, is a significant parameter which strongly affects both the shear strength and the strain distribution within the tested soil. Therefore, to ensure the rigidity of the tank and the plain strain condition in the model, an additional stiffening was designed by means of two hollow steel bars, embracing the tank at approximately mid–height. The steel bars had a rectangular 40 mm × 40 mm cross sectional area and were held together by two 12 mm threaded bars, one at each end.

3.2.2 Sheet pile wall

The experiments were performed with a single pile across the width of the tank. To ensure rotational failure of the top of the wall a wooden block of 100 mm height and thickness 40 mm was used as a prop in front of the wall base, preventing both forward movement of the bottom and rotation about the top. Free earth support conditions were assumed to occur and the tie–rod force on the wall was calculating using this method.

Since the primary concern of the dissertation was the anchor resistance, the model wall had to be rigid enough to withstand bending deflections, which would have caused earth pressure redistributions, arching and consequently reduction on the tie–rod force. A sheet pile wall made of plywood with dimensions 1.57 m × 0.21 m × 18 mm thickness was considered to be adequate for the purpose. Moreover two steel bars of 3 mm × 3 mm × 0.5 mm angular cross–section were attached along the front face to reduce wall flexibility.

As the particle size of the soil material was great enough any particular seal between the wall and the sides of the tank was not necessary. However, the sheet pile was designed with knife–edges to reduce the contact friction with the sides. The approximation of a rectangular instead of a trapezoidal cross–section was not so significant and simplified the calculations for the structural properties of the pile. Finally, it should be noted that although the wall friction the sheet pile was considered smooth in the theoretical calculations. All calculations for the design of the wall can be found in Appendix A.

3.2.3 Anchorage

The anchorage used in the tests was provided by means of a balanced anchor plate, made of mild steel and with dimensions 0.12 m height × 0.20 m width × 1.15 mm thickness. The tie–rods were mild steel thread bars of 5.85 mm diameter and was attached to a small steel bar in front of the wall for measuring the tie–rod force by means of strain gauges.

The laboratory tests were performed at two different anchorage depths. The first depth $d_a = 0.22$ m satisfied the traditional design regulations, due to $h_a = 0.12$ m > $d_a/2 = 0.11$ m, giving a ratio with the height of the anchorage $d_a/h_a = 1.8$. The second depth $d_a = 0.38$ m did not satisfy the above design regulation and had a ratio of $d_a/h_a = 3.2$. Using the conventional design, the location of the anchorage in which the active and the passive wedge of the soil would not have been interfered was at 1.14 m behind the sheet pile wall. However, due to the limited length of the tank this position was not able to be achieved, since it extended beyond the back of the tank for 120 mm.

After two preliminary tests three tests where performed at 0.22 m anchorage depth, having short tie–rod lengths of 0.40 m, 0.60 m, and 0.90 m respectively. In the first test the anchorage was well located into the active wedge, in the second test the anchorage was just at the edge of the active wedge, and in the third it was in front of the theoretical location of the passive wedge of the soil for non–intersection conditions. Although in the third test there was a 120 mm space behind the anchor plate, it was left as a clearance space such that there would be no influence on the displacements of the soil. Finally, a single test was performed with depth of anchorage at 0.38 m where the anchor was situated at 0.60 m distance behind the sheet pile wall. The planes of potential failure and the position of the anchorage in each experiment are shown in Figure 17 in page 46.

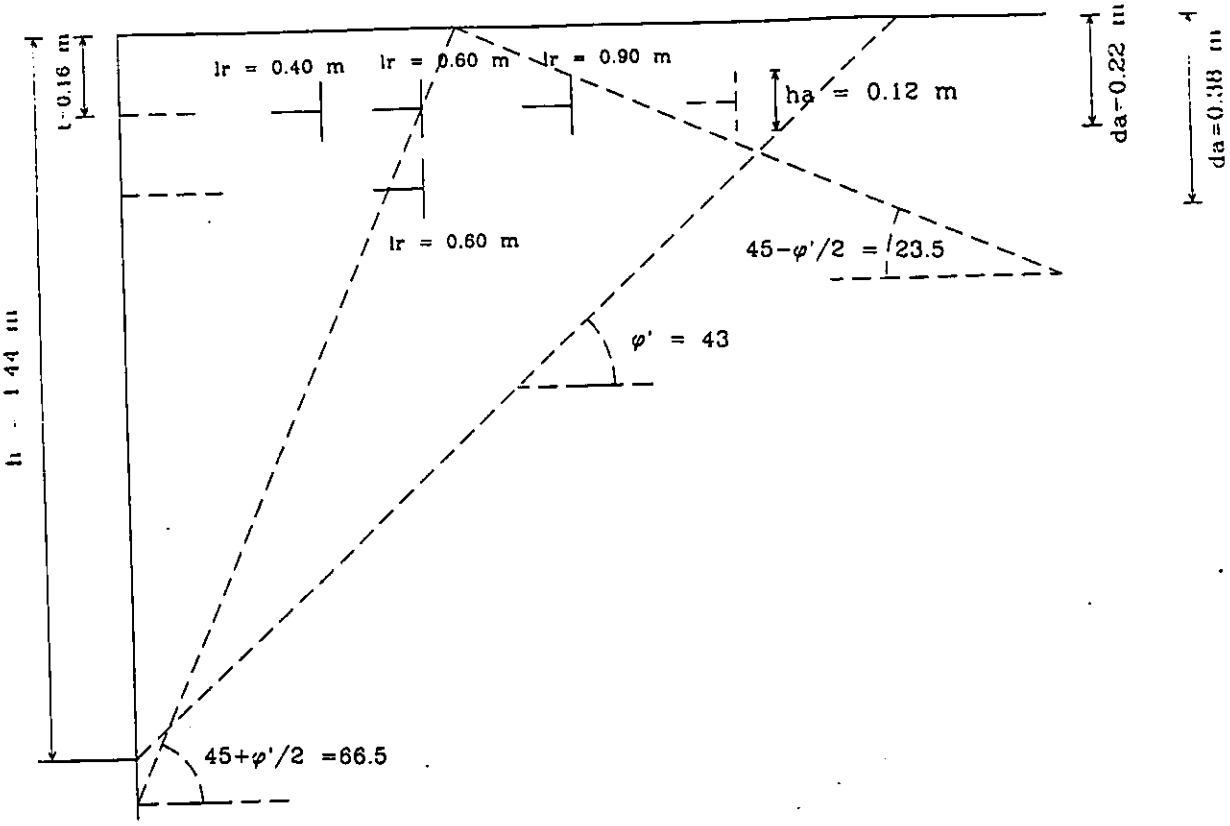

Figure 17 Design of anchorages for the laboratory experiments.

3.3 Measurement Techniques

3.3.1 Measurement of the tie–rod force

The force in the tie–rod was determined by means of a beam attached to the tie–rod and placed on the outside of the wall. The strain caused by bending moments was then measured with the help of four 3 mm strain gauges, placed on the bar in a full–bridge formation. A full–bridge formation was chosen so as to measure both compression and tension of the bar. The bar was calibrated with the measuring device so that any strain readings could be easily translated into tie–rod force. This was

accomplished by attaching the wall bar, tie–rod, and anchor plate together as if in an experiment. Subsequently the wall was balanced across some supports so that the tie–rod and anchor plate were in a vertical position below the bar. Strain readings were then taken, as known weights were added to the anchor. From plotting the results it was determined that the calibration constant of the system was 0.141 N/με.

3.3.2 Measurement of the soil displacements

A plane technique was adopted to measure the soil deformation. The measurements were concentrated on the failure state of the soil, demonstrating thus the geometry of the failure surface. The technique involved a network of wooden cylindrical markers placed in the soil with their flat surfaces against the glass side of the tank. Their diameter was 8 mm, which was compatible with the particle size of the gravel, and their mean length was 190 mm. These dimensions were considered not influence the soil displacements, but rather to leave the markers to move freely with the ground movements. The mesh of the network was approximately 100 × 100 mm starting from 130 mm from the bottom of the tank. The flat surfaces of the markers where additionally coloured white in order to be more distinct from the gravel.

When the tank was full the position of the markers was measured, relatively to a standard point (the front bottom corner of the tank), and assumed to be the initial. At the end of each experiment the final position of the markers were observed and measured. Consequently, the displacement of the markers and hence the soil was able

to be determined. Furthermore, once the displacements of the markers were known, the strains within each mesh of the network could be calculated, on the assumption that each triangle of soil formed by three neighbouring markers was straining uniformly. Roscoe et al (1963) defined a method for computing strains from displacements obtained from radiographs of lead shots buried in a soil. In the experiments the calculation of strains was done by a simpler method which involved the relative displacements and the rotation of three adjacent markers forming a triangle of soil. Although the method was crude it gave acceptable results in the determination of shear strain patterns within the soil. An description of the method is given in Appendix A.

3.4 Experimental Procedure

The experimental procedure can be divided into two stages. The initial stage where a test was set up and the final stage during which measurements were taken.

3.4.1 Initial stage

The wall was placed into the tank and held fixed by wooden wedges smoothly stuck between the top of the wall and the sides of the tank. Caution was shown for the wall to be both vertical and perpendicular to the sides. The tank was then started to be filled with gravel. The weight of the gravel prior to use was measured for the calculation of the density. It was important to ensure that the gravel was at a loose state inside the tank. Therefore, the material was poured, with the help of a laboratory scoop, steadily

from a height of about 0.5 m into the tank, taking about 2 sec for each pouring. This was in accordance with the British Standards preparation of gravely soils for the determination of their minimum dry density (BS 1377: Part 4.4: 1990). Another consideration was given on the even distribution of gravel on both active and passive sides of tank such that no excess material on one side would force the wall to move.

Wooden markers were placed in the tank every 100 mm, starting from 130 mm from the bottom of the tank. They were placed in horizontal lines at approximately 100 mm distance. In this stage the pouring of the material went more slowly in order to carefully cover the markers with gravel, trying not to change their position or buried them totally into the soil. The tank was then filled in the normal manner until the next line of markers was required, allowing so the formation of a network.

At the level of the anchorage of each test the anchor, tie–rod, and the bar were positioned with the strain gauges attached to the bar but the measuring device switched off. The tank was then filled with the remaining gravel and markers.

3.4.2 Final stage

Once the tank was filled, the gravel on the active side was levelled off horizontally with the top of the pile. The position of the markers were drawn on the glass side and measured relatively with the front bottom corner of the tank. The instrumentation of the strain gauges was switched on and the initial readings were taken as zero load. Next, the excavation of the material in front of the wall was started

by removing 100 mm of gravel each time with the help of removable plates, which formed the outer front of the tank. In every excavation level the tie–rod force was measured. At the end of the experiment, and after failure occurred, the new positions of the markers were measured.

It should be noted that the experimental procedure was quite time–consuming, taking at least three days without the analysis of the results.

3.4.3 Comments on the experimental procedure

One drawback of the test procedure was that it did not allow the pile to be hammered into position which would have simulated the industrial method of constructing sheet pile walls. This was not possible as the hammering could have possibly damaged the pile and the tank, due to the lateral and vertical displacement of the soil during the driving.

It should be noted here that unfortunately in all tests the wall did not fail even when the front side was completely excavated. The side friction between the gravel and the wooden back side of the tank was $\delta = 33°$, measured by direct shear tests (see section 3.1.2). Since it was only 9° less than the angle of shearing resistance of the gravel, it was considered to assist in the stability of the system. Hence, a plate of steel of 2 mm thickness had been attached at the whole back side of the tank so that the side friction and the edge effects would be reduced. However, the main explanation of the phenomenon should be laid on the physical properties of the tank with respect to the

specific design of the wall, anchorage and wooden prop in front of the wall. The resistance of the anchor was found to be underestimated while the prop, by transmitting the forces to the frame of the tank, played a significant role preventing not only the rotation of the bottom, but also contributing to the stability of the whole structure.

Under this conditions the failure of the wall in each test was achieved by pulling uniformly the top of the wall. That made the readings of the tie–rod force to be of no use. Still, it was considered that the soil displacements and the geometry of the failure surface were not greatly affected. Therefore, the analysis of the experiments was concentrated only on the ground movements with respect to the various tie–rod lengths.

3.5 Results and Discussion

Four experiments are going to be discussed. Three of them were performed at 0.22 m depth of anchorage while the one was performed at 0.38 m depth. The characteristics of each test are summarised in the following Table:

Test	Unit weight of gravel (kN/m^3)	Depth of anchorage (m)	Length of tie–rod (m)
2	14.5	0.22	0.40
3	14.3	0.22	0.60
4	14.5	0.22	0.90
5	14.3	0.38	0.60

The results are presented in the form of vectors of total soil displacement, contours of horizontal and vertical displacement, and contours of cumulative shear strain in the soil, shown in Figures 18–25. The contours were drawn with the help of Surfer 5.02 software programme, which enables the creation of three–dimensional surfaces, and contours, under various method of analysis of co-ordinates. In these analyses the Krigging method was used. It should be mentioned that in the contours of shear strain smoothing occurred and so they represent a qualitative rather than quantitative estimation.

Test 2 was performed having a tie–rod length of 0.40 m. The deformations of the soil behind the wall were confined to a clearly defined wedge bounded by a line at 69° to the horizontal. The vectors of total soil displacement (Figure 18) were increased in magnitude from zero at the edge of the area to a maximum at the top of the wall and were inclined at angles to the horizontal varying from 50° to 61°. The angles tended to be greater near the bottom of the wall and smaller in the area of the anchorage.

From the contours of horizontal and vertical displacement, shown in Figure 19, it was evident that the vertical movement of the gravel was predominant. Only at the top in an area near the wall the horizontal movement was greater. The shear strains in the soil are shown in the same Figure 19. These were the total shear strains from the beginning of the test. Near the wall, over about the upper half of the retained height of soil, there was a region in which strains were small in contrast of displacements. In this region the soil had been moving as almost rigid body. A narrow zone of high strains

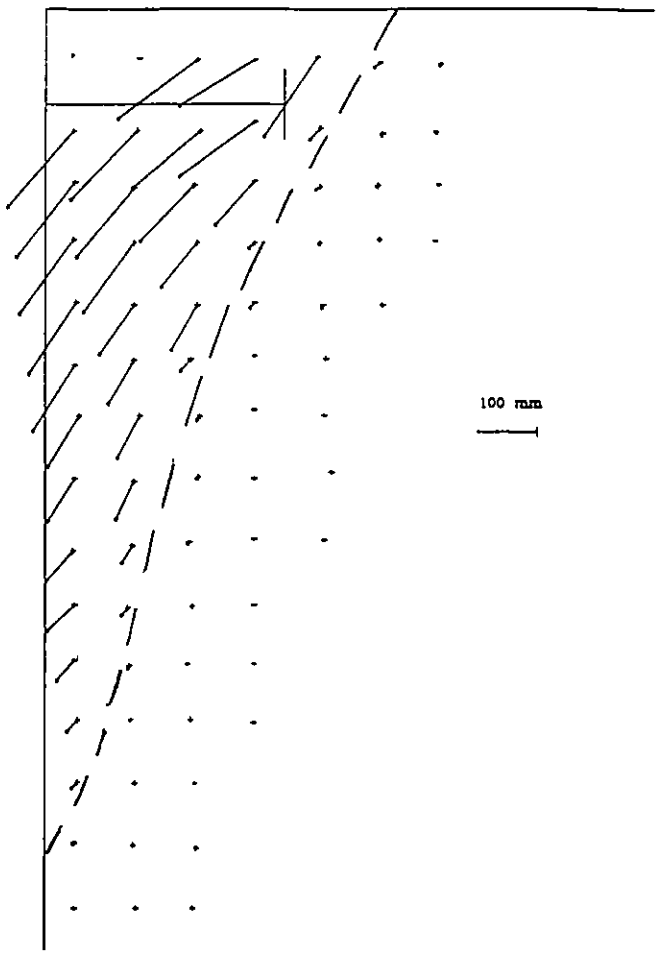

Figure 18 Test 2. Vectors of total soil displacement.

had been formed, inclined at about 70° to the horizontal and coincided with the boundary of the deforming wedge of soil at most parts. Here, the strains had become sufficiently large for the gravel to have reached its plastic state. Thus, a failure surface was developed, along the boundary of soil displacements. The inclination of the failure surface was very near to the theoretical angle for the active wedge of the gravel, that was $45° + \varphi'/2 = 66.5°$ to the horizontal. So, for the case of the anchorage well–situated into the theoretical active wedge, this had no effect on the soil deformation and the failure surface was developed according to theory.

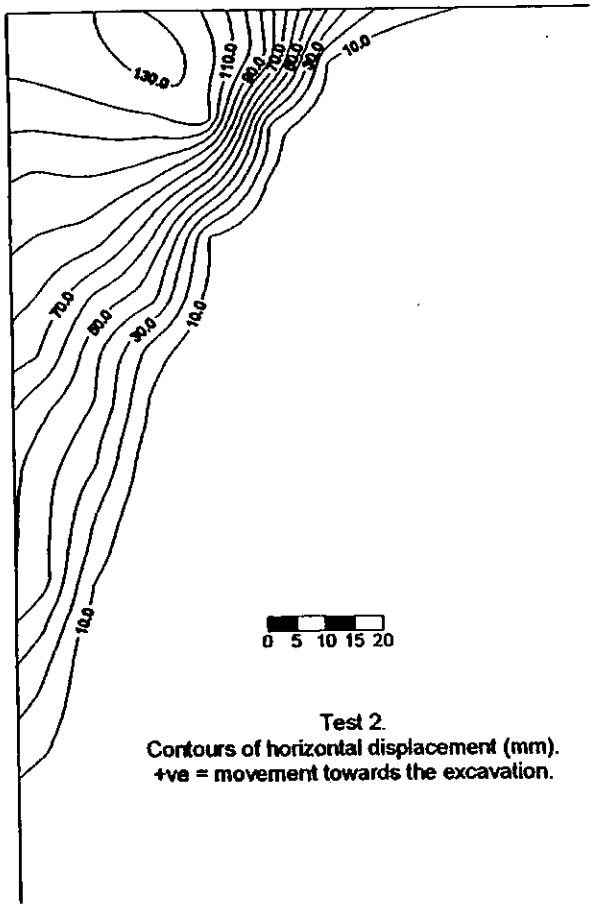

Test 2.
Contours of horizontal displacement (mm).
+ve = movement towards the excavation.

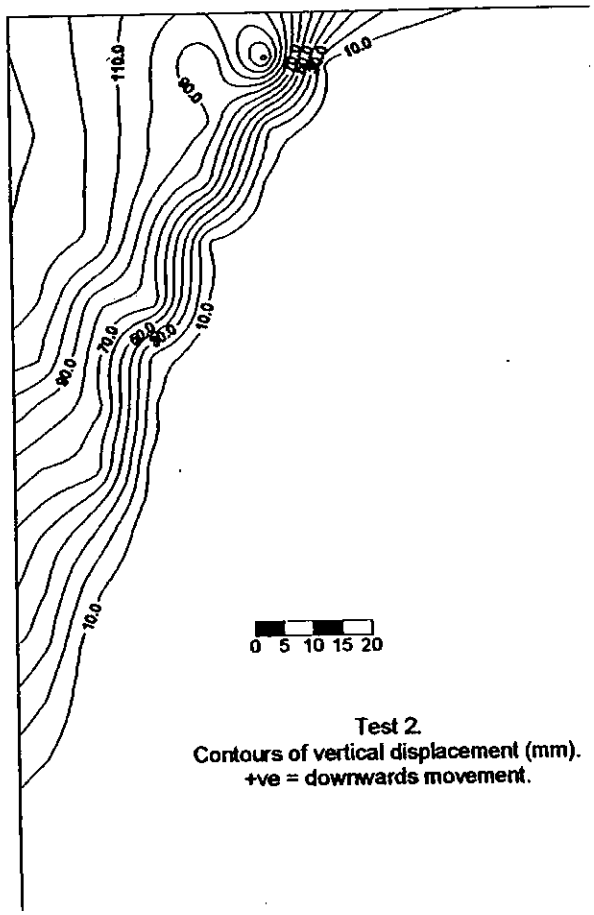

Test 2.
Contours of vertical displacement (mm).
+ve = downwards movement.

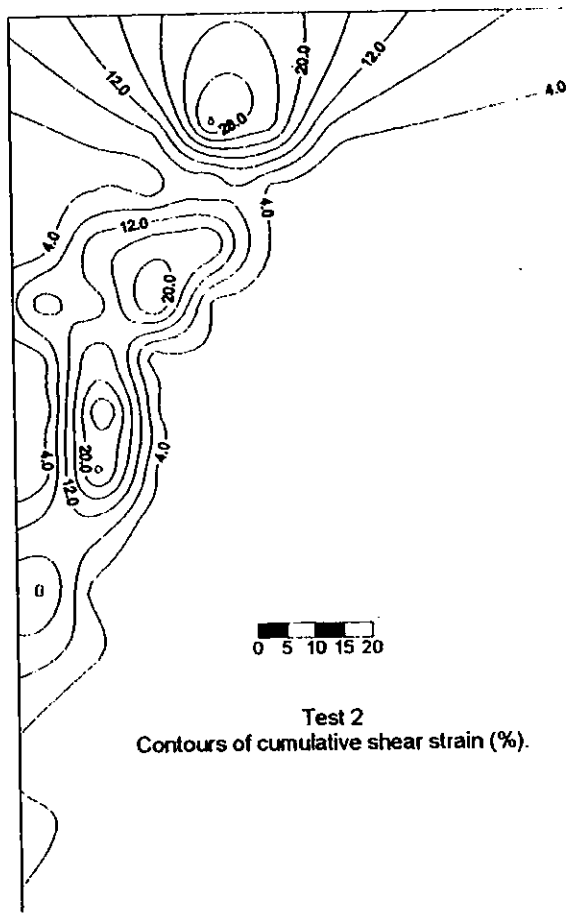

Test 2
Contours of cumulative shear strain (%).

In test 3, performed with 0.60 m tie–rod length, the vectors of soil displacement (Figure 20) were limited by a line inclined with various angles. From the bottom to over the mid–height of the retained soil the boundary was inclined at about 70° to the horizontal, then was curved to approximately 32°, to obtain next its prior angle, at about the initial depth of the anchor plate until the surface of the soil. The displacement vectors again were increased in magnitude from the edge of the boundary tot the top corner of the wall. Their inclinations varied from 45°–55° at the bottom to middle, to 25° at the top.

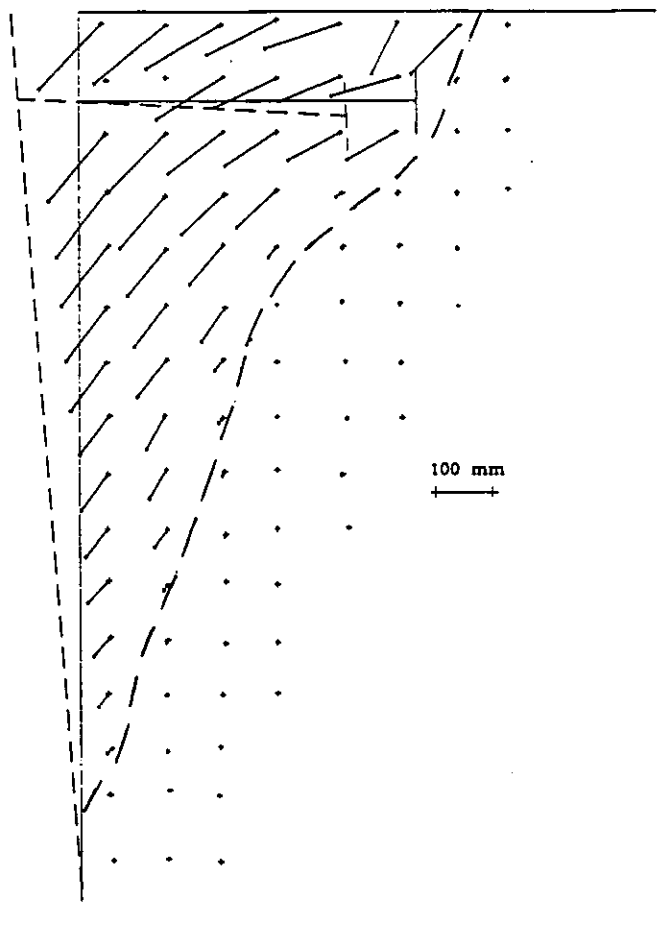

Figure 20 Test 3. Vectors of total soil displacement

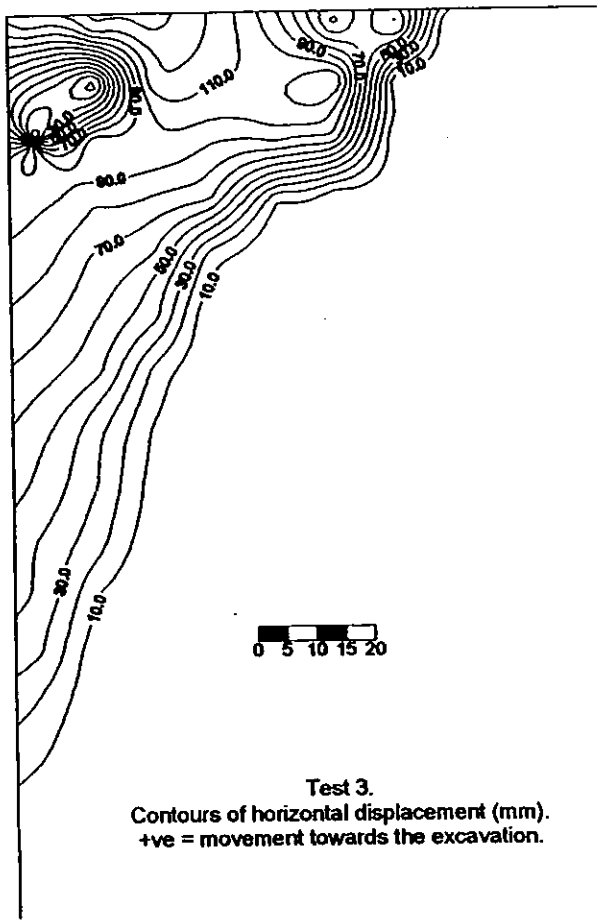

Test 3.
Contours of horizontal displacement (mm).
+ve = movement towards the excavation.

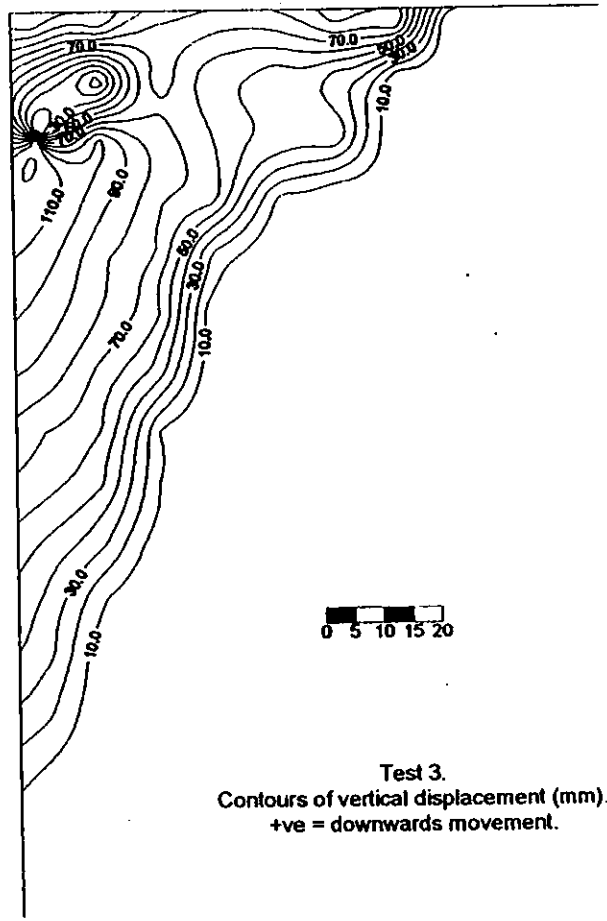

Test 3.
Contours of vertical displacement (mm).
+ve = downwards movement.

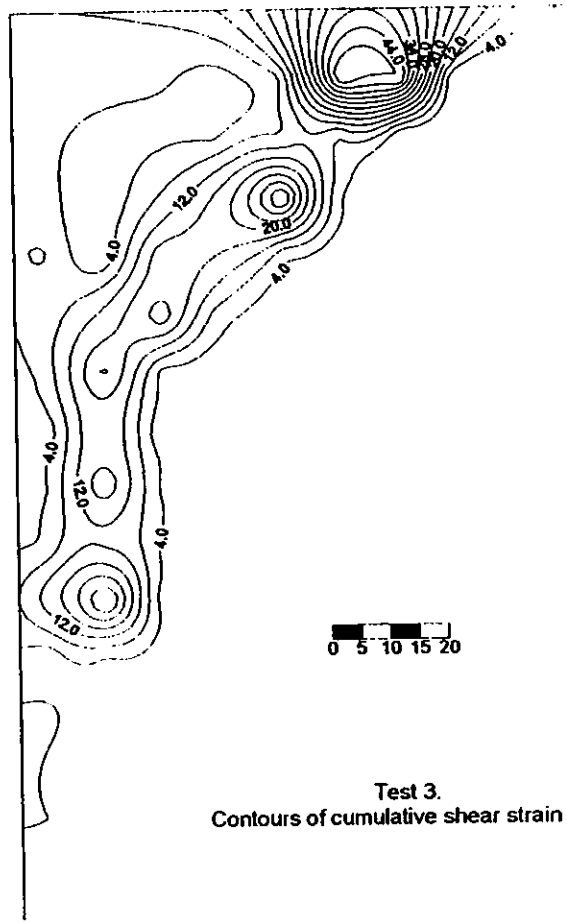

Test 3.
Contours of cumulative shear strain (%

From the contours of horizontal and vertical displacements, it was clear that the lateral movement at the vicinity of the anchorage was greater than the vertical. The high shear strains again were in a narrow zone, defining thus the failure surface in agreement with the boundary of the soil displacements. The region of the soil moving as a rigid body was now more noticeable. Consequently, from the analysis of this experiment it was observed a tendency of the soil to fail not along the theoretical active and passive wedges, but along a modified wedge which included the sheet pile wall and the anchor plate.

In test 4 this single modified zone of large movements of soil was clearly distinguishable, as shown in Figure 22. Its edge was inclined at 70° to the horizontal at the bottom, gradually changed at 53° up to about mid–height, where almost became horizontal until the initial depth of the anchor plate. Then, it attained its first value of about 70°, which was very close to the theoretical active one. As a consequence, the vectors of soil displacement were inclined at 53°–58° to the horizontal from the bottom to mid–heigth of the retained soil, while at the upper part and particularly at the area of the anchor plate were inclined at only about 10° to the horizontal.

The horizontal movement was significant in the area of the anchor, as shown by the displacement contours in Figure 23. Furthermore, upward movement was distinct in front of the plate, together with a downward movement of the soil behind the anchor. As the anchor had moved forward the soil near the front was forced to follow while the soil behind the anchor collapsed into the gap which had been created. This resulted in a heave at the surface of the gravel with a subsidence trough adjacent to it.

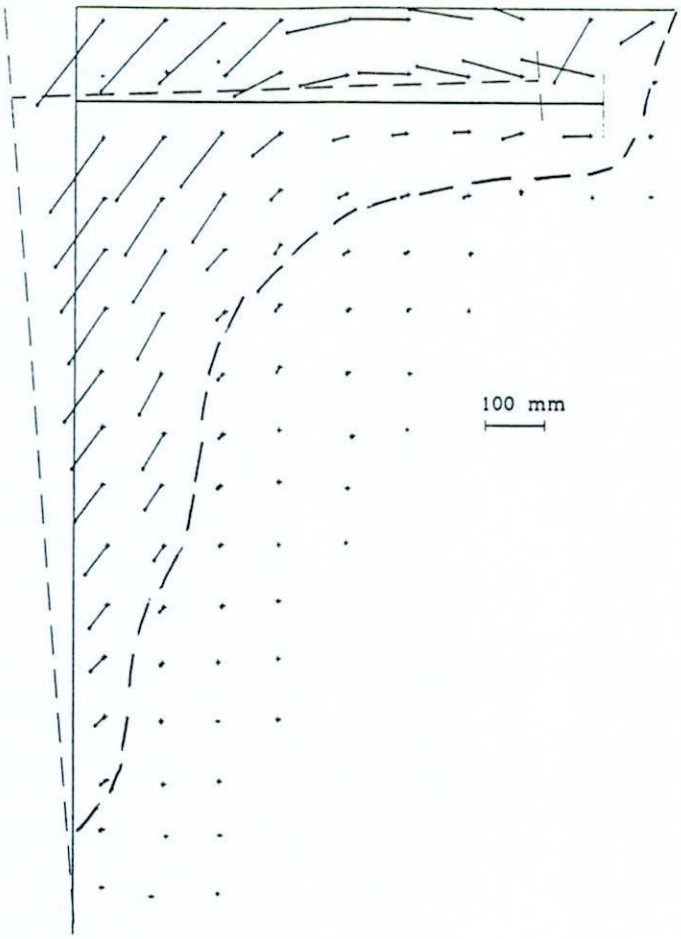

Figure 22 Test 4. Vectors of total soil displacement.

The whole phenomenon is very representative of the formation of the passive and active state in front and behind the anchor plate respectively and is believed to have been developed at the start of the wall movement. However, the failure took place along the boundary of the modified zone of the deforming soil which was a line similar to a logarithmic spiral, passing along the back of the anchor. The shear strain pattern confirmed the above, as the high strained band was limited at the same position as the edge of the modified zone. Finally, as a general observation is should be noted that as the tie–rod was increased, the area influenced by the failure of the system was also increased.

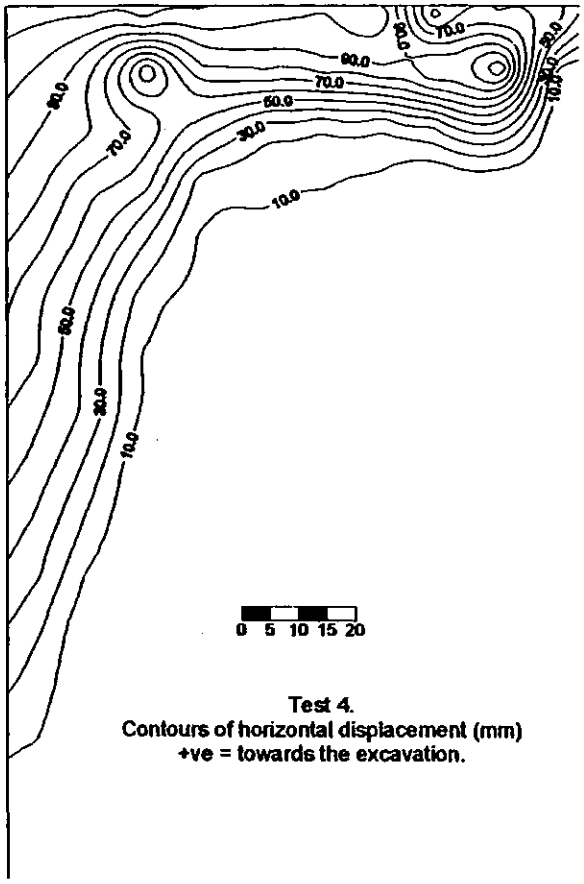

Test 4.
Contours of horizontal displacement (mm)
+ve = towards the excavation.

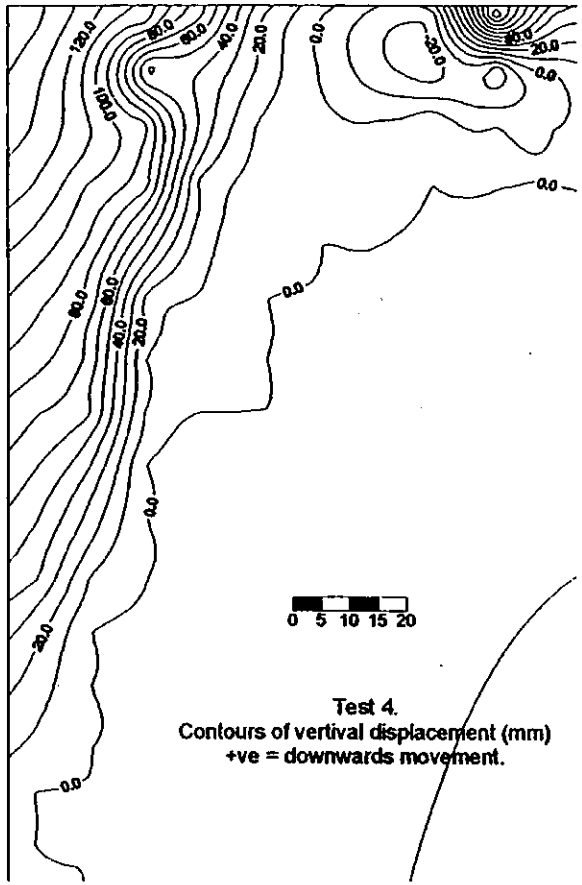

Test 4.
Contours of vertival displacement (mm)
+ve = downwards movement.

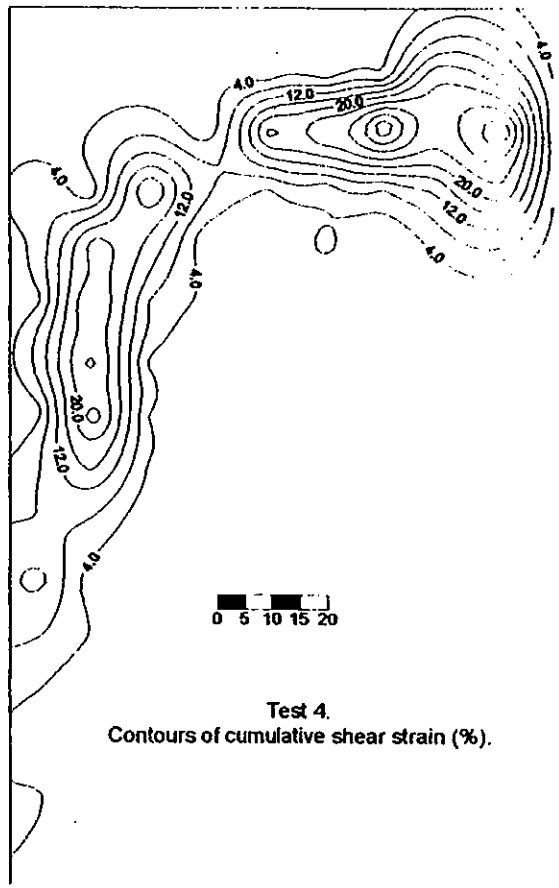

Test 4.
Contours of cumulative shear strain (%).

In test 5, with the anchorage at depth of 0.38 m, the zone of soil displacements had again a tendency to be modified from the theoretical active wedge, as in test 3 with the same tie–rod length but at smaller depth. Here however, the influence of the anchorage was greater and hence the soil was affected into a wider area, creating a deep trough on the surface of the gravel due to downward movement of the gravel in the vicinity above the initial position of the anchor. In Figures 24 and 25 the characteristics of failure surface are represented.

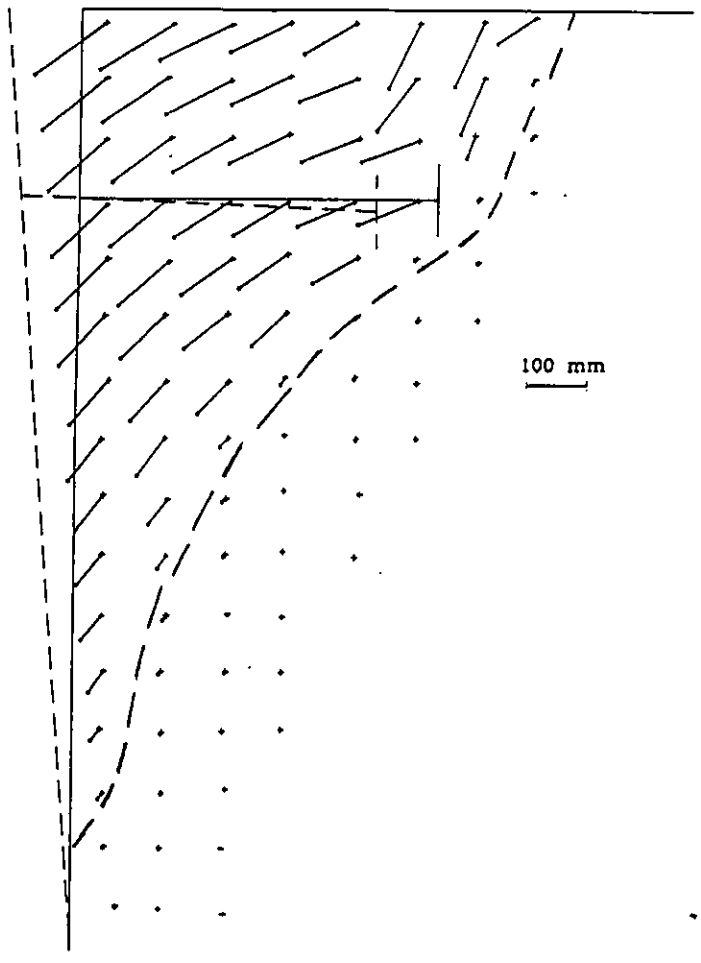

Figure 24 Test 5. Vectors of total soil displacement.

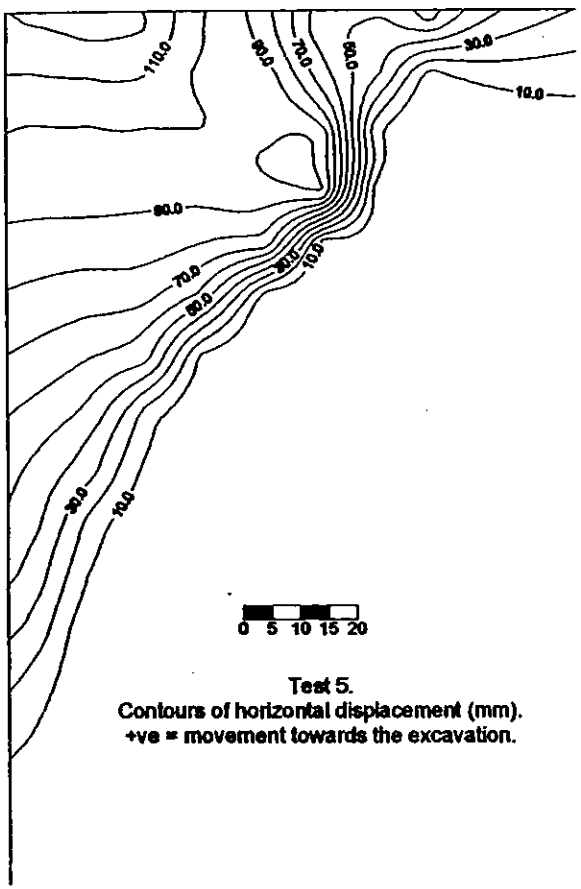

Test 5.
Contours of horizontal displacement (mm).
+ve = movement towards the excavation.

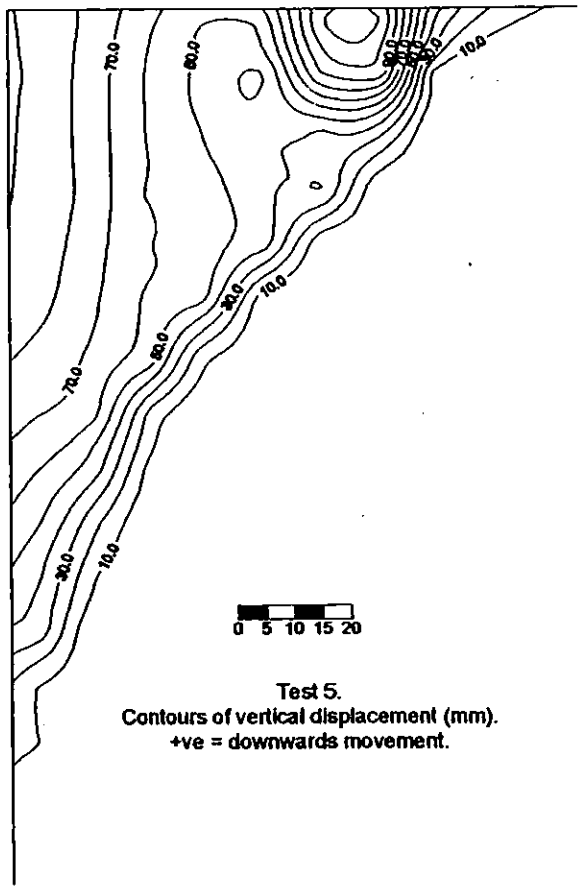

Test 5.
Contours of vertical displacement (mm).
+ve = downwards movement.

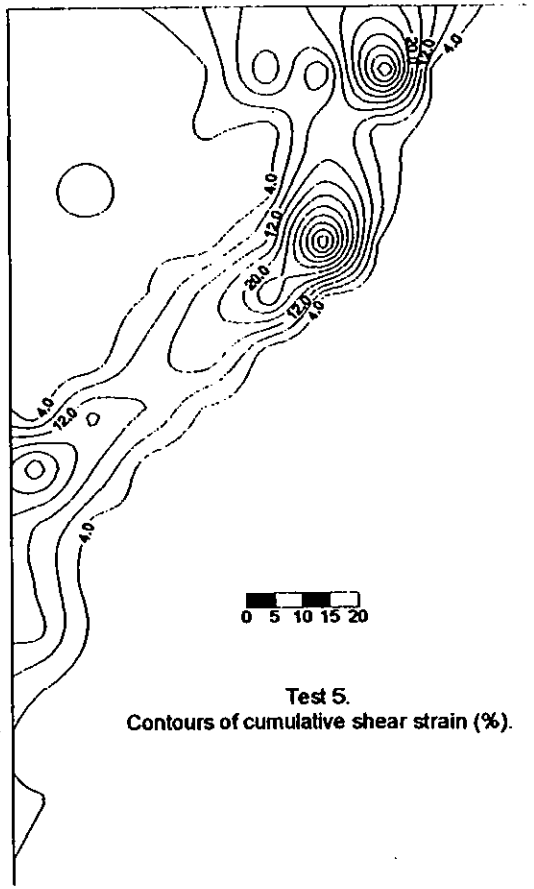

Test 5.
Contours of cumulative shear strain (%).

4 FINITE DIFFERENCE ANALYSIS

Until some years ago in most geotechnical engineering problems, except for the simplest ones, an exact solution could not be found using complicated, but realistic constitutive models of soil. There simply was not enough time available to solve the various differential equations for practical applications. The abilities of modern day computers mean that the same type of engineering problems can now be analysed by sophisticated numerical methods. In recent years, especially since the 1970s, finite element and finite difference programmes have been developed, allowing complex elastoplastic soil models to be incorporated into the analyses, and thus yielding an exact solution for stress and strain characteristics of a particular problem.

The finite difference method is used to solve ordinary or partial differential equations which govern problems involving fluid flow, seepage, torsion and plasticity in a continuous body. In this method the body to be analysed is assumed to be split into a number of elements which form the finite difference grid, and the differential equations are approximated by finite difference equations formed at each point or node in the grid. These equations are usually solved without being combined into a large stiffness matrix, in contrast to finite element method, because it is relative efficient to regenerate the equations at each step of analysis.

4.1 The *FLAC* programme

4.1.1 General features and fields of application

FLAC stands for "Fast Lagrangian Analysis of Continua". In the User's Manual *FLAC* is defined as

> a two–dimensional explicit finite difference programme which simulates the behaviour of structures built of soil, rock, or other materials, which may undergo plastic flow when their yield limit is reached.

The explicit calculation scheme upon which *FLAC* is based, makes the programme well suited for modelling large deformations. Furthermore, *FLAC* has several built–in constitutive models, ranging from the "null" model which represents excavations, to the shear and volumetric yielding models which include strain hardening/softening behaviour, and thus permits the simulation of the highly non–linear mechanic response of geologic, or similar, materials. Though the basic formulation assumes a two–dimensional plain strain state *FLAC* also offers a plane stress option for elastic analyses, and an axisymmetric geometry option for problems involving cylindrical co-ordinates. Another feature of the programme is the incorporation of the fluid flow logic, coupled or not with the mechanical logic, which enables the simulation of steady or non–steady, confined or unconfined flow. Finally, the structural element logic in *FLAC* provides structures, such as tunnel liners, rock or soil anchorages, and sheet pile walls, which interact with the surrounding rock or soil to be easily modelled.

All these features open a wide field of applications to be analysed and design with *FLAC*. Originally, *FLAC* was developed for analysis and design in mining engineering and underground construction. The analysis of progressive failure and collapse, the generation of fault systems and their influence to the surroundings, the simulation of various reinforcement systems, and the performance of deep underground repositories are tasks which can easily be worked with the programme. Moreover, with the incorporation of groundwater flow logic and coupled mechanical–fluid flow analysis, *FLAC* offers a capability for application in soil engineering. Potential applications include analyses of earth retaining structures and slopes under drained and undrained conditions, calculations of bearing capacity and settlement of foundations, as well as tunnelling design in soils. Finally, the dynamic analysis option in *FLAC* allows various engineering dynamic problems, especially in earthquake engineering, to be analysed with the programme.

4.1.2 Background

Material are represented in *FLAC* by elements, or in other words zones, which form the grid which can be adjusted by the user to fit the shape of the body to be modelled. Each zone behaves according a prescribed linear or non–linear stress–strain relationship with respect to the applied forces or boundary restrains.

According to User's Manual *FLAC* incorporates an "explicit", time–marching method, to solve the finite difference equations which are applied at the nodes of the grid. That means that for even a static solution to a problem the dynamic equations of

motion are included in the system. This ensures that the numerical system is correct and stable even when the physical system being modelled is unstable.

The general explicit calculation sequence embodied in *FLAC* is represented in Figure 26. First, new velocities and displacements are derived from stresses by means of equations of motion. Then, strain rates are derived from velocities, and by constitutive laws stresses from strain rates. Every cycle around the loop is one timestep.

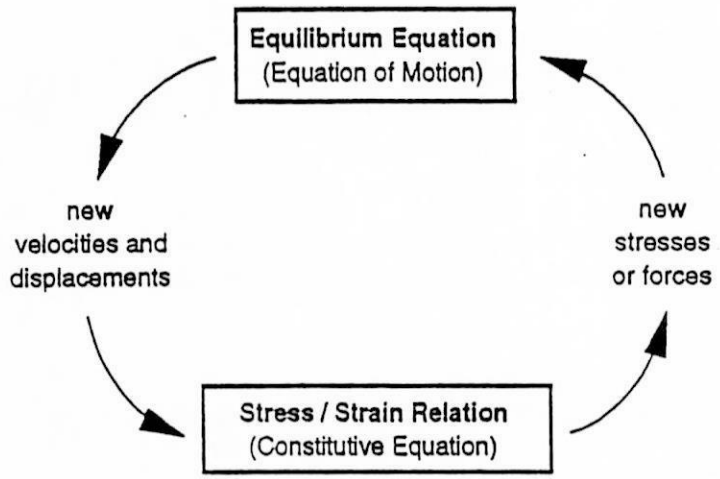

Figure 26 Basic explicit calculation cycle of *FLAC* (after User's Manual).

The important thing is that each set of equations, either of motion or of stress–strain relation, updates all of its grid variables from known values that remain fixed during the calculation process. For example, the lower box in Figure 28 takes the set of velocities already calculated, and for each element, computes new stresses. The velocities are assumed to be frozen for the operation of the box, that means the new calculated stresses do not affect the velocities. This may seen unreasonable, because it is known that if stress changes somewhere within the body, it will influence its adjacent

elements and change their velocity. However, all materials have a maximum speed at which information can propagate. Therefore, a particular small timestep is chosen in which information can not physically pass from one element to another, and thus the assumption of fixed known values is justified. In each timestep, the computed incremental displacements are added to the co-ordinates so that the grid moves and deforms with the material it represents ("Lagrangian" formulation). Hence, after several timesteps, and so several cycles of the loop, disturbances can propagate across zones, just as they would propagate physically.

The structural elements used in *FLAC* are assumed to behave elastically until they reach yielding. They are incorporated into the models by defining the start and end of the structural elements in the form of co-ordinates or gridpoints or by defining the nodes of the structural elements directly into the model. Though the cable elements interact with the body wherever inside the grid, the beam elements need to coincide with the grid elements. A number of facilities, fix, free, rotate nodes, is offered to represent exactly the realistic conditions of a problem. For beam elements the following input parameters are required:

- cross–sectional area
- elastic modulus
- moment of inertia of the area

For cable elements the input parameters that required are the following:

- cross–sectional area
- elastic modulus
- tensile yield strength
- compressive yield strength
- bond stiffness of grout (if any)
- bond strength of grout (if any)

The solution to a problem can either be achieved by iteration to prescribed number of timesteps or assessed by several indicators, such as the maximum unbalance force of the whole grid, gridpoint velocities, or plastic indicators, which define whether the system is stable, unstable, or in unrestricted plastic flow.

4.2 Design of Analysis

4.2.1 Dimensions and properties of materials

The design of finite difference analysis was kept as simple as possible. The laboratory experiments were modelled and again the effects of the tie–rod length were study. The dimensions and properties of the materials were approximated that of the experiments with the assumption of plane strain condition at 1 m width. A grid of 17 × 28 elements was considered having dimensions 2.38 m length × 1.68 m height respectively. The boundaries of the grid were fixed to simulate the sides of the tank. The grid and the geometry of the models are illustrated in Figure 27.

Initially, the soil in the models involved, was considered as an elastic material on which the gravitational force was applied and the models were then run for 1000

steps. Thus, the in–situ stress on the gravel was applied. Subsequently, and for the rest of the analyses the soil was modelled to have an elastoplastic behaviour with the Mohr–Coulomb failure criterion adopted as the yield surface.

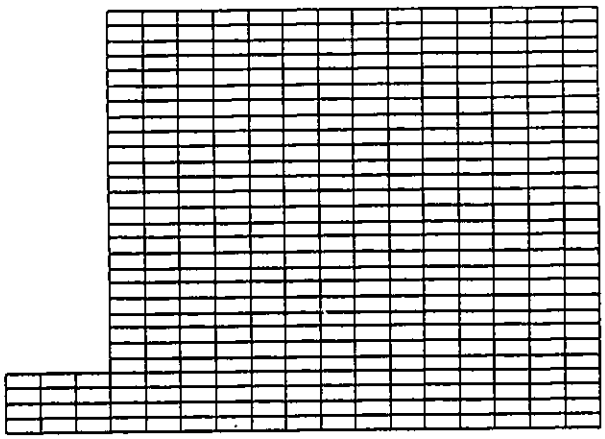

Figure 27 Grid and geometry of models incorporated into *FLAC* analysis.

The properties of the gravel, required for the analyses, included the bulk and shear moduli of elasticity. These were derived considering the gravel as a cohesionless soil at loose state with Poisson's ratio v = 0.33. Thus, the values $K = 40 \times 10^6$ Pa and $G = 15 \times 10^6$ Pa were used as bulk and shear moduli respectively. The soil was assumed to be fully drained, so as to simulate the laboratory conditions, having a bulk unit weight $\gamma = 14.5$ kN/m^3 and hence a density of 1480 kg/m^3. The strength parameters employed was c = 0 Pa and $\varphi_{cv}' = 43°$. The angle of dilation for the post yield behaviour was set to zero, since it was assumed that the gravel is at a loose state.

Next, the sheet pile wall and the anchorage were installed by simulating the wall and anchor plate as beam, and the tie–rod as cable elements. For the beam elements the moment of inertia of the respective cross–sectional areas were calculated

while for the cable element the tensile and compressive yield strengths were derived from recommended values proposed by British Steel Corporation. These values were used in terms of forces for the particular cross–sectional area of the tie–rod. The structural properties of the sheet pile wall, anchor, and tie–rod are summarised in the following Table. The detailed calculations can be found in Appendix B.

Properties			Sheet pile wall	Anchor	Tie–rod
Cross–sectional area	A	(m^2)	1.03×10^{-1}	5.75×10^{-3}	6.40×10^{-4}
Moment of inertia	I	(m^4)	1.90×10^{-4}	1.58×10^{-8}	
Young's modulus	E	(Pa)	200×10^{9}	200×10^{9}	200×10^{9}
Tensile yield strength	y	(N)			2.75×10^{5}
Compressive yield strength	y_c	(N)			1.53×10^{5}

4.2.2 Analyses

A series of models were created and investigated. All of them were excavated to give a retained height h = 1.44 m. The wall was fixed to x–direction at the excavation level so that a simulation with the laboratory experiments to occur.

Initially, an approach to the actual condition of the experiments was made. With the depth of anchorage at 0.24 m, four models were analysed having tie–rod lengths of 1.40 m, 1.12 m, 0.84 m, and 0.28 m respectively and corresponding to various locations with respect to the potential failure planes. These models run until a steady condition were achieved. Then, a different analysis was performed. Various lengths of tie–rods were considered every 0.14 m, from 0.28 m to 1.54 m away from

the sheet pile wall, for depths of anchorage d_a = 0.24 m and d_a = 0.42 m and angles of shearing resistance $\varphi_{cv}' = 43°$ and $\varphi_{cv}' = 32°$. In this analysis a horizontal velocity was applied to the wall, distributed in a triangular manner from zero at the excavation level to 2×10^{-6} m/step at the top of the wall. The models were run 10000 steps so that the horizontal displacement at the top of the wall to be 2 cm. The influence of the depth of anchorage and the angle of shearing resistance were investigated.

Finally, a number of models were analysed in which seven different horizontal velocities were applied for 10000 timesteps, giving the following horizontal displacements at the top of the wall: 0.5 cm, 1 cm, 2 cm, 5 cm, 7.5 cm, 10 cm, and 15 cm. The models involved tie–rod lengths of 1.68 m, 1.54 m, 1.40 m, 1.12 m, 0.84 m, and 0.28 m for depths of anchorage 0.18 m, 0.24 m, 0.42 m with $\varphi_{cv}' = 43°$. The effect of the anchorage yield on the anchor resistance was examined and the collapse anchor resistance was defined for each model. At the collapse condition the lateral pressures on wall and anchor plate, and the soil deformation were investigated. The data used for the analysis of the model with 1.54 m tie–rod length and 2×10^{-6} m/step applied velocity at the wall can be found in Appendix B as an example of the programme style.

4.3 Results and Discussion

The set of models without applied velocity on the sheet pile wall gave results that confirmed the underestimation in the calculations for the anchor resistance in the laboratory experiments. The computed anchor resistance values were greater than the

respective ones used for the design of the experiments. Hence, the soil, sheet pile wall, and anchor system retained its stability, resulting only in small deformations inside its elastic range.

Figure 28 illustrates the relationship between anchor resistance and tie–rod length with respect to the depth of anchorage and the angle of shearing resistance of the soil. This is for the case of 2 cm applied displacement the top of the wall. The anchor resistance increased almost linearly on the increase of tie–rod length. In addition, as both the depth of anchorage and angle of shearing resistance of the soil were increased, the anchor resistance was increased.

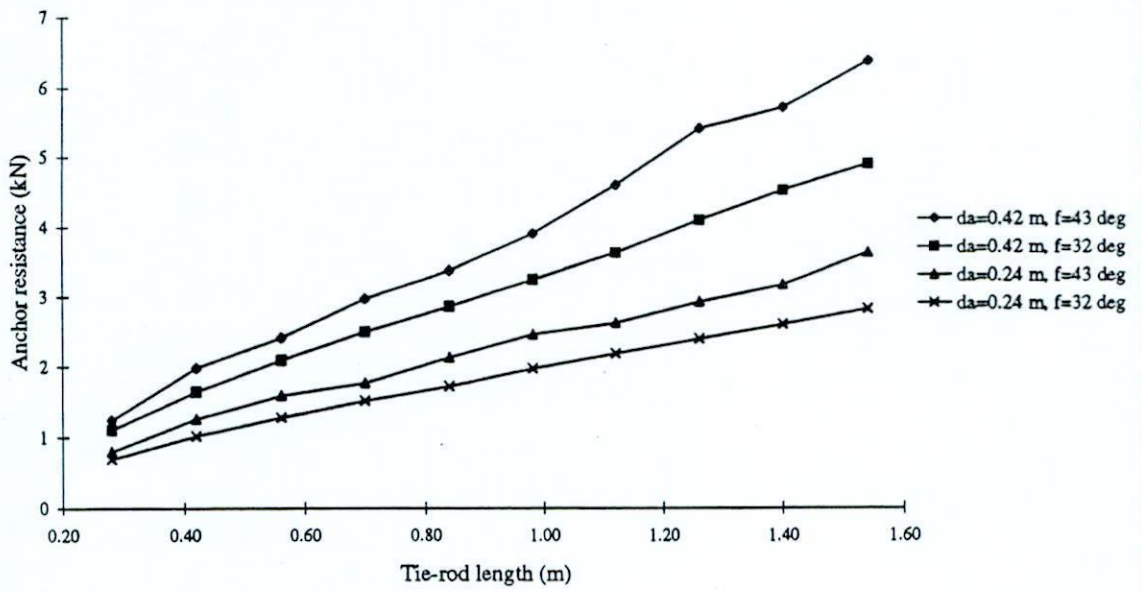

Figure 28 Anchor resistance and tie-rod length relationship with respect to depth of anchorage d_a and angle of shearing resistance of soil φ'.

The variation of the anchor resistance with the anchorage displacement for different lengths of tie–rod and depths of anchorage is illustrated in Figures B–2 to B–

4 in Appendix B on page ... Generally, as the yield was increased the anchor resistance reached a peak value and then started to decrease. This occurred for every tie–rod length and depth of anchorage. The peak value of each curve was considered to be the collapse anchor resistance at which failure occurred, for every particular tie–rod length and anchorage depth.

As the tie–rod length increased, the collapse anchor resistance was increased in approximately linear way, as shown in Figures 31–33. The depth of anchorage had also an additional incremental effect on the anchor resistance. For depth of anchorage 0.24 m and for over the 1.12 m tie–rod length (minimum conventional tie–rod) the anchorage displacement necessary to mobilised collapse conditions was 0.56 % of the overall height of the sheet pile wall (H). However, for tie–rod lengths smaller than 1.12 m the yield was greater reaching the 2.8 %H. So, although the anchor resistance increased with increase in tie–rod length, the deformation of the system prior to failure was greater for short tie–rods. The same applied for the other two depths of anchorage, with the yield to be greater for greater depths. However, at 0.42 m depth the differences, caused by the tie–rod, of the deformation of the system prior to failure had a tendency to equilibrate. This influence of the tie–rod length on the deformation prior to ultimate limit state could have been a significant parameter affected the serviceability of the structure, been worse with anchorages shorter than the minimum conventional designed one.

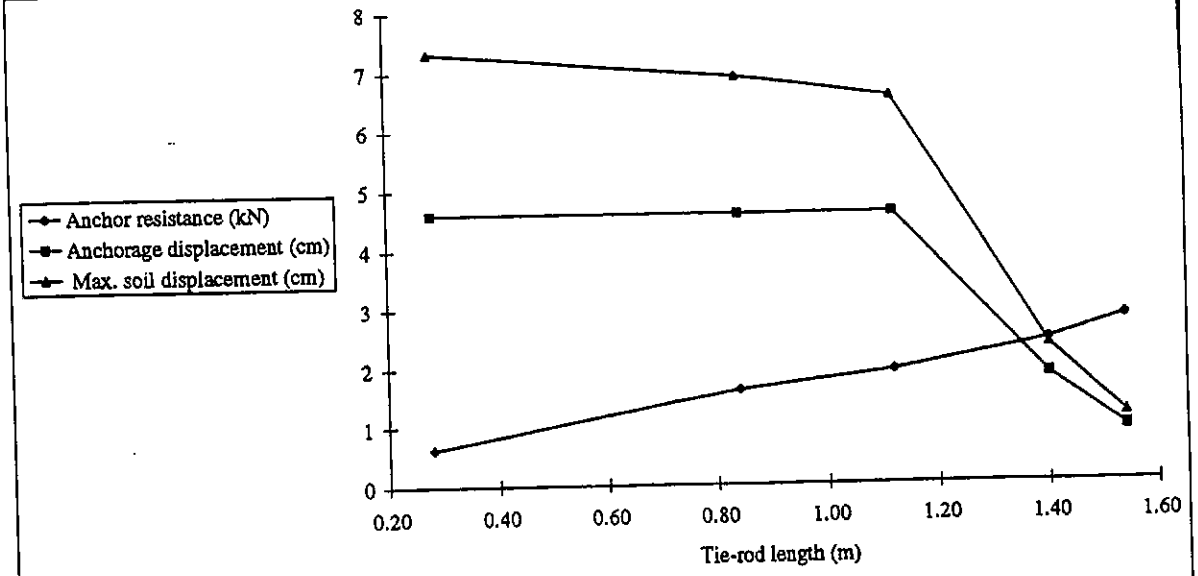

Figure 29 Collapse conditions with respect to tie-rod length for depth of anchorage $d_a = 0.18$ m

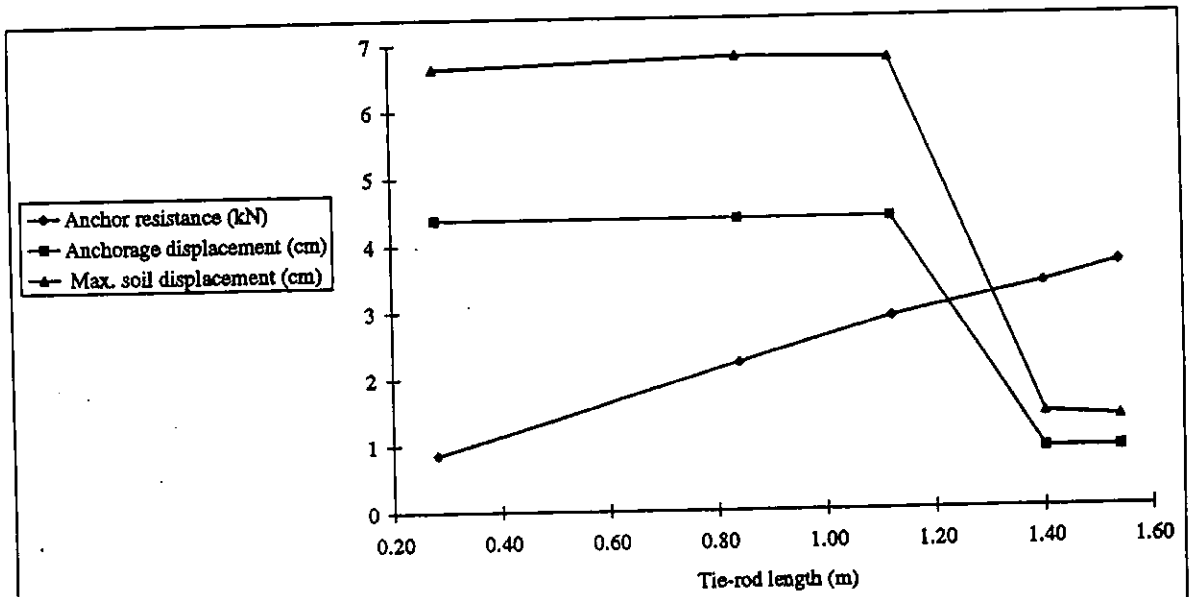

Figure 30 Collapse conditions with respect to tie-rod length for depth of anchorage $d_a = 0.24$ m

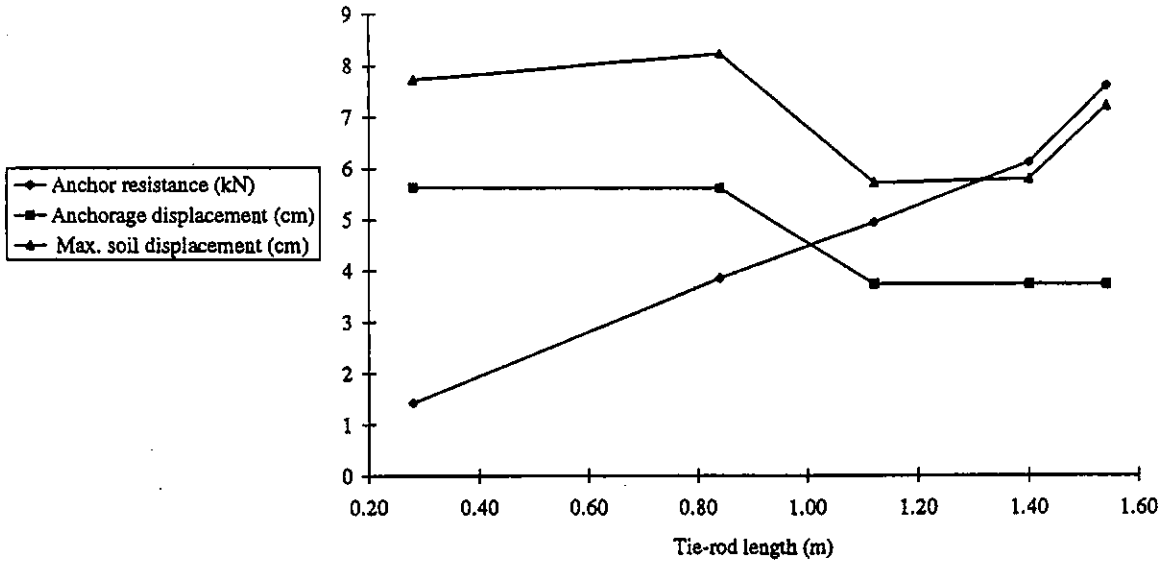

Figure 31 Collapse conditions with respect to tie-rod length for depth of anchorage $d_a = 0.42$ m

For the models involved in the analyses, the vectors of soil displacement at failure shown that for tie–rod lengths situated beyond the theoretical active wedge of the soil adjacent to the wall, there was a single zone of movement which its edge passed behind the back of the anchor. However, and in contrast to laboratory results, failure occurred as a sliding at a uniform angle to the horizontal of approximately the angle of shearing resistance of the soil. When the anchorage was situated inside this active wedge, it had no influence on the geometry of the failure surface which was inclined at approximately the theoretical $\left(45^\circ + \varphi'/2\right)$ angle to the horizontal. Examples of vectors of soil displacement for various models can be found in Appendix B.

For the tie–rod lengths of 1.40 m, 1.12 m, 0.84 m, and 0.28 m the earth pressure distributions behind the sheet pile wall and adjacent to anchor plate were investigated for all the three depths of anchorage. The results are represented in

Appendix B. At the sheet pile wall although the earth pressure distributions were affected by the depth of the anchorage, the length of the tie–rod did not have any significant effect. There were not observed any considerable differences from the theoretically calculated active pressure distribution except at the bottom of the wall due to fixity. Besides, the arching, due to anchorage, was minimal, since the anchorage was not fixed even if the anchor plate was located well away from the wall, at a distance determined by traditional design rules. Along the anchor plate and on its passive side, the earth pressures were increased with reduce in tie–rod length, for anchorages located beyond the active wedge of the wall. Their pressure distribution was the result of the excessive deformation at the back of the anchor, as the soil had moved into the gap left by the displacement of the anchorage. Furthermore, an increase was observed relatively to the increase of the anchorage depth. For the case of the anchor plate located into the active wedge, the distributions of earth pressure on the passive side confirmed that the anchorage had little influence on the kinematics of the system at failure. The soil in front of the anchor plate moved out more than the adjacent masses causing arching effects and pressure redistributions of the kind as shown in Figure B–18.

5 CONCLUSIONS

A series of model tests representing an anchored sheet pile wall retained loose gravel was conducted with various tie–rod lengths, using a simple beam formation to measure the tie–rod force and a network of wooden markers to investigate the deformations in the soil behind the wall. The development of the experimental procedure required a substantial length of time and considerably limited the amount of testing which was completed.

Due to an underestimation in the calculations for the anchor resistance the tie–rod force was not possible to be measured. However, the soil displacements were not considered to be affected. It was observed that as the tie–rod length increased, the area, in which ground movements occurred at failure, was also increased. When the anchorage was located inside the theoretical active wedge of the soil adjacent to the sheet pile, it had very little effect on the kinematics of soil deformation. The ground movements were confined in a triangular area with its boundary inclined to the horizontal at an angle very close to the theoretical one. When the tie–rod length exceeded the theoretical active plane of potential failure, a single modified zone of large movement of soil occurred at failure in contrast to the traditional proposals of two distinct soil zones of movement. This zone was limited by a surface which had a form similar to a logarithmic spiral, passing behind the anchor.

The cumulative shear strains at failure within the soil confirmed the geometry of ground movements. Relatively high strains had been limited within narrow bands

coincided each time with the boundary of the respective soil displacements. In these bands the strain had become sufficient large for the soil to have reached its limit state and thus for a failure surface to have been developed. Adjacent to these bands small strains occurred although the soil displacements were relatively large. There the soil moved as almost rigid body. Finally, the zone of the deforming soil was increased with increase in the depth of anchorage, as a result of the fact that more soil was affected by the anchorage.

A finite difference analysis was undertaken with *FLAC* programme. Various models were incorporated giving interesting results. With the simulation of the laboratory experiments, *FLAC* confirmed the underestimation of the anchor resistance. Furthermore, it was possible with *FLAC* to investigate the interaction between the anchored sheet pile wall and the soil, by applying certain velocities upon the wall.

The effects of the tie–rod length and depth of anchorage were investigated in detail. The anchor resistance show a linear variation with the tie–rod length and a considerable increase with respect to depth of anchorage. A significant influence of the tie–rod length on the yield of the anchorage was observed. In cases shorter than the minimum conventional–designed anchorage, the yielding of the system prior to failure was greater than in cases involving longer anchorages. Consequently, this has to be added in the considerations of the design for minimum length anchorages as a factor not only involving the ultimate limit condition, but also the serviceability of the retaining structure and the relative deformations in this state.

In addition, the soil displacements at failure and the earth pressure distributions behind the sheet pile wall and adjacent to the anchor plate were examined. Ground movements in *FLAC* were in the form of sliding, in contrast to the experiments. Arching was minimal since the anchorage did not stay fixed at failure. Along the passive side of the anchor the earth pressures were increased with reduce in tie–rod length, due to excessive deformation behind the anchor. Exception to that was the shortest anchorage where relatively large soil displacements occurred on the front side.

Further experiments would be interesting and productive. However, they should be performed with more detailed considerations, involving the geometry and the plain strain assumption of the problem with regard to the physical properties of the tank and the strength parameters of the soil which are to be used. The height of the anchor and the depth of anchorage should be such that the anchor–sheet pile wall system will be allowed to fail freely. This will give clear results on the variation of the anchor resistance in respect of the tie–rod length. Besides, the prop at the bottom of the wall, if any, should be short enough to lower the point of rotation, increasing so the active pressures on the free length of the wall. If problems occur with the free mobilisation of the soil, a mechanical pull should be involved by means of a hydraulic ram connected at the top of the wall. This will allow measurement of the tie–rod force and interpretation of the results with the known pulling force of the ram.

Since the strains within the soil play a significant role not only in the determination of the failure, but also in the working state and the serviceability of an earth retaining structure a more accurate examination of the strains should be

incorporated into the model tests, relating strains to stresses developed at any stage of excavation.

Further analyses should be also undertaken by *FLAC*. Since this finite difference programme can provide various options and complex models of material behaviour, more realistic and complicated conditions can be simulated with less effort than by a respective laboratory test. Parameters such as the wall friction, undrained conditions, dilatancy of soil, initial soil state, and construction techniques should be analysed and examined with respect to the behaviour of anchorages.

Finally, it would be also interesting to undertake similar studies for the investigation of anchorages in sheet pile walls retaining cohesive soils.

REFERENCES

Arslan, U., Breth, H., & Wanninger, R. (1981), An elastoplastic analysis of anchored walls, *Proc. 10th Int. Conf. Soil Mech. Found. Engg*, Vol. 2, 21–28.

Arthur, J. R. F., & Roscoe, K. H. (1965), An examination of the edge effects in plain–strain model earth pressure tests, *Proc. 6th Int. Conf. Soil Mech. Found. Engg*, Vol. 2, 363–367.

Bettess, P. (1997), Numerical Methods in Linear Elasticity, Notes for the M.Sc. Advanced Course of Engineering Geology, University of Durham.

Bolton, M. D. (1986), The strength and dilatancy of sands, *Geotechnique*, 36, No. 1, 65–78.

Brasnby, P. L., & Milligan, G. W. E. (1975), Soil deformation near cantilever sheet pile walls, *Geotechnique*, 25, No. 2, 175–195.

British Standard 1377 (1990), *British Standard Methods of tests for soils for civil engineering purposes, Part 2: Classification tests, Part 4: Compaction–related tests, Part 7: Shear strength tests (total stress)*, London: British Standard Institution.

British Standard 6349 (1988), *Code of Practice for Maritime structures, Part 2: Design of quay walls, jetties and dolphins*, London: British Standards Institution.

British Standard 8002 (1994), *Code of Practice for Earth Retaining structures*, London: British Standards Institution.

British Steel (1988), *Piling handbook, sixth edition*, London: British Steel.

Chen, W. F., & Liu, X. L. (1990), *Developments in Geotechnical Engineering Vol. 52, Limit Analysis in Soil Mechanics*, Amsterdam: Elsevier Science Publishers.

Craig, R. F. (1992), *Soil Mechanics, Fifth edition*, London: Chapman & Hall.

Das, B. M. (1975), Pullout resistance of vertical anchors, *J. Geotech. Engng Div. Am. Soc. Civ. Engrs*, 101, No. GT1, 87–91.

Gere, J., & Timoshenko, S. (1991), *Mechanics of Materials, Third SI Edition*, London: Chapman & Hall.

Harper, L. M. (1993), The effects of different tie–rod lengths on the stability of anchored sheet pile walls, M.Sc. dissertation, University of Durham.

Itasca Consulting Group (1993), *FLAC v 3.22, Fast Lagrangian Analysis of Continua*, London: Mott McDonald.

Milligan, G. W. E. (1983), Soil deformations near anchored sheet-pile wall, *Geotechnique*, 33, No. 1, 41–55.

Padfield, C. J., & Mair, R. J. (1984), *CIRIA Report 104, Design of retaining walls embedded in stiff clay*, London: CIRIA.

Pitilakis, K. D. (1981), Interaction Sol — Diaphragme de Soutenement Anre [Interaction Anchored Sheet–Pile Wall — Soil], *Proc. 10th Inter. Conf. Soil Mech. Found. Engg*, Vol. 2, 231–234.

Potts, D. M., & Day, R. A. (1990), Use of sheet pile retaining walls for deep excavations in stiff clay, *Proc. Instn Civ. Engrs*, 88, Part 1, 899–927.

Potts, D. M., & Fourie, A. B. (1986), A numerical study of the effects of wall deformation on earth pressures, *Int. J. Numer. Analyt. Meth. Geomech.*, 10, 383–405.

Potts, D. M., & Fourie, A. B. (1985), The effect of wall stiffness on the behaviour of a propped retaining wall, *Geotechnique*, 35, 347–352.

Potts, D. M., & Fourie, A. B. (1984), The behaviour of a propped retaining wall: results of numerical experiment, *Geotechnique*, 34, No. 3, 383–404.

Roscoe, K. H. (1970), The influence of strains in soil mechanics, Tenth Rankine Lecture, *Geotechnique*, 20, No. 2, 129–170.

Roscoe, K. H., Arthur J. R. F., & James R. G. (1963), The determination of strains in soils by an X–ray method, *Civil Engineering and Public Works Rev.*, Vol. 58 (684) 873–876 and Vol. 58 (685) 1009–1012.

Rowe, P. W. (1952), Anchored sheet–pile walls, *Proc. Instn Civ. Engrs*, 1, 27–70.

Rowe, R. K., & Davis, E. H. (1982), The behaviour of anchor plates in sand, *Geotechnique*, 32, No. 1, 25–41.

Schanz, T., & Vermeer, P. A. (1996), Angles of friction and dilatancy of sand, *Geotechnique*, 46, No. 1, 145–151.

Selby, A. R. (1997), Ground movements around anchored retaining walls, University of Durham.

Simpson, B. (1992), Retaining structures: displacement and design, *Geotechnique*, 42, No. 4, 541–576.

Smith, G. N., & Pole, E. L. (1980), *Elements of Foundation Design*, London: Granada Publishing Limited.

Symons, I. F., & Murray, R. T. (1988), Conventional retaining walls: pilot and full–scale studies, *Proc. Instn Civ. Engrs*, 84, Part 1, 519–538.

Terzaghi, K. (1943), *Theoretical Soil Mechanics*, New York: John Wiley and Sons.

Terzaghi, K. (1954), Anchored bulkheads, *Transactions of Am. Soc. Civ. Engrs*, 119, p.1243.

Tomlinson, M. J. (1995), *Foundation Design and Construction, Sixth Edition*, London: Longman Scientific & Technical.

Turabi, D. A., & Balla, A. (1968), Sheet–pile analysis by distribution theory, *J. Geotech. Engng Div. Am. Soc. Civ. Engrs*, 94, No. SM1, 291–322.

Turabi, D. A., & Balla, A. (1968), Distribution of earth pressure on sheet–pile walls, *J. Geotech. Engng Div. Am. Soc. Civ. Engrs*, 94, No. SM6, 1271–1301.

Verdeyen, J., & Nuyens, J. (1965), Calcul des rideaux d'ancrage de palplances [Analysis of Anchored Sheet Pile Walls], *Proc. 6th Int. Conf. Soil Mech. Found. Engg*, Vol. 2, 417–421.

Ward, E. J. (1991), The effects of excavation in front of a laboratory modelled anchored sheet pile retaining wall, M.Sc. dissertation, University of Durham.

Wells, J. D. (1984), Model sheet pile walls in sand, Final year project, University of Durham.

APPENDIX A

- **Theoretical Calculations For The Design Of The Model Wall**
- **Description Of The Method Used For The Determination Of The Shear Strains In The Soil**

– Theoretical Calculations For The Design Of The Model Wall

Consider

1. Horizontal surface of soil—Smooth wall
2. Linear earth pressure distributions
3. Free earth support conditions
4. Point of rotation at excavation level
5. Full retained height of soil, h = 1.54 m
6. Depth of tie–rod t = 0.16 m
7. No applied factors of safety for limiting equilibrium
8. $K_a = \frac{1-\sin\varphi}{1+\sin\varphi} = 0.19$, $K_p = 1/K_a = 5.29$

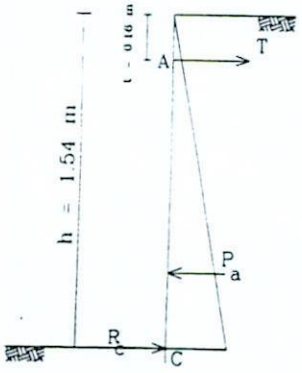

Figure A–1

Taking moments about and above the point of rotation C it is

Force (kN per m width of wall)	Lever arm (m)	Moment (kNm per m width of wall)
$P_a = \frac{1}{2}K_a\gamma z^2$ $= \frac{1}{2}\times 0.19\times 14.4\times 1.54^2$ $= 3.24$	$\frac{1}{3}z = \frac{1}{3}\times 1.54 = 0.51$	1.65
- T	z - t = 1.54 - 0.16 = 1.38	- 1.38T
$-R_c$	0	0

So,

$$\Sigma M_c = 0,$$

$$1.65 - 1.38T = 0,$$

$$T = \frac{1.65}{1.38},$$

$$\underline{T = 1.20 \text{ kN per m width of wall}}.$$

For width of wall b = 0.21 m, then $\underline{T = 252 \text{ N}}$.

Design of anchorage

The anchorage is continuous ($b_a = b$).

P_a is ignored being a considerably small parameter.

Ideally, the depth to bottom of anchorage, so as the anchor resistance would be equal to the tie–rod force, should be

$$A_p = T = \frac{1}{2}\gamma d_a^{\,2}\left(K_p - K_a\right),$$

$$d_a = \sqrt{\frac{2T}{\gamma\left(K_p - K_a\right)}},$$

$$= \sqrt{\frac{2 \times 1.20}{14.4 \times (5.29 - 0.19)}},$$

$$= 0.18 \text{ m}.$$

Thus, according to conventional design the height of the anchor should be $h_a \geq {}^{d_a}/_{2} = 0.09$ m.

But for $h_a = 0.12$ m and $d_a = 0.22$ m (parameters used in the model tests) and the case of non–intersection of active and passive soil zones the anchor resistance is

$$A_p = \frac{1}{2}\gamma d_a^{\,2}\left(K_p - K_a\right) = \frac{1}{2} \times 14.4 \times 0.22^2 (5.29 - 0.19),$$

$$\underline{A_p = 1.78 \text{ kN per m width of wall}}.$$

For width of wall $b = 0.21$ m, then $\underline{A_p = 373 \text{ N}}$.

Thus, $\underline{A_p > T}$ imposing stability of the system.

Structural design of wall

The bending moment at any point down the surface until the point of excavation is given by

$$M = \frac{K_a \gamma z^3}{6} - T(z - t),$$
$$= \frac{0.19 \times 14.4 \times z^3}{6} - 1.20(z - 0.16),$$
$$M = 0.46z^3 - 1.20z + 0.19.$$

The bending moment becomes maximum when $\frac{dM}{dz} = 0$. Hence,

$$0 = (0.46z^3)' - (1.20z)' + (0.19)',$$
$$0 = 0.46 \times 2z^2 - 1.20,$$
$$z = \sqrt{\frac{1.20}{0.92}},$$
$$z = 1.14 \text{ m}.$$

For z = 1.14 m,

$$M_{max} = 0.46 \times 1.14^3 - 1.20 \times 1.14 + 0.19,$$
$$\underline{M_{max} = -0.50 \text{ kNm per m width of wall}}.$$

For width of wall b = 0.21 m, then $\underline{M_{max} = -104 \text{ Nm}}$.

For the appropriate thickness of the cross–section of the wall it is $\sigma = \frac{M_{max}}{Z}$, where $Z = \frac{bt^2}{6}$ the section modulus of the cross–section of the pile.

Taking $\sigma_{allow} = 30 \times 10^6$ Pa the allowable stress for wood and for width of wall b = 0.21 m, and the thickness (t) of the model wall must be at least

$$30 \times 10^6 = \frac{104}{bt^2/6},$$

$$t = \sqrt{\frac{6 \times 104}{0.21 \times 30 \times 10^6}},$$

$$\underline{t = 9.95 \times 10^{-3}\ m = 10\ mm.}$$

For more rigidity the model wall was designed in 18 mm thickness.

– Description Of The Method Used For The Determination Of The Shear Strains In The Soil

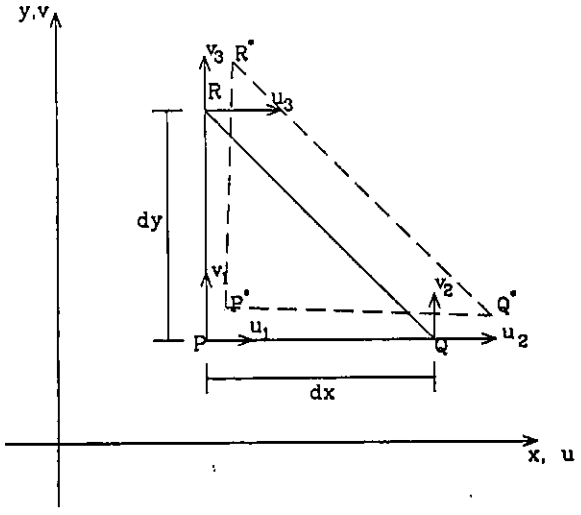

Figure A-2

Consider three adjacent markers P (x, y), Q (x + dx, y), and R (x, y + dy) which form a triangular element, as shown in Figure A–2. Under the action of the set of applied forces P moves to the point P* ($x + u_1$, $y + v_1$), Q moves to the point Q* ($x + dx + u_2$, $y + v_2$), and R moves to the point R* ($x + u_3$, $y + dy + v_3$).

On the determination of cumulative shear strain in the element the following assumptions have been made:

1. The deformation of the element is uniform
2. Plane strain condition occurs
3. The element is subject to a rigid rotation Ω_z about z axis

The incremental displacement components of marker P relative to the adjacent markers Q and R may be expressed as

$$du = \frac{\partial u}{\partial x}dx + \frac{\partial u}{\partial y}dy, \qquad \text{and} \qquad dv = \frac{\partial v}{\partial x}dx + \frac{\partial v}{\partial y}dy,$$

$$du = (u_2 - u_1) + (u_3 - u_1) \qquad dv = (v_2 - v_1) + (v_3 - v_1)$$

The rotation of the element about z axis is given by

$$\Omega_z = \frac{1}{2}\left(\frac{\partial v}{\partial x} - \frac{\partial u}{\partial y}\right),$$

$$\Omega_z = \frac{1}{2}\left[(v_2 - v_1) - (u_3 - u_1)\right].$$

The incremental relative displacements are due to both distortion an rotation of the triangular element. Thus, the shear strain can by given by the equations

$$\frac{\partial u}{\partial y} = \frac{1}{2}\gamma - \Omega_z \qquad \text{or} \qquad \frac{\partial v}{\partial x} = \frac{1}{2}\gamma + \Omega_z$$

Therefore, the shear strain can be determined as

$$\gamma = \frac{\partial u}{\partial y} + \frac{\partial v}{\partial x},$$

$$\gamma = (u_3 - u_1) + (v_2 - v_1).$$

APPENDIX B

- Calculations For The Design Of The Structural Elements In *FLAC* Analysis
- Programme Instructions For The Model With l_r = 1.54 m, d_a = 0.24 m, v = 2e-6
- Variation Of Anchor Resistance With Anchorage Displacement For Different l_r And d_a
- Vectors Of Soil Displacement At Failure For Various Models
- Earth Pressure Distributions Behind The Wall And Plate

– Calculations For The Design Of The Structural Elements In *FLAC* Analysis

The dimensions of each structural element were tried to be kept same as the ones used in the laboratory experiments, but with 1m width of wall. Thus, every dimension was readjusted to 1 m width of wall.

Model sheet pile wall

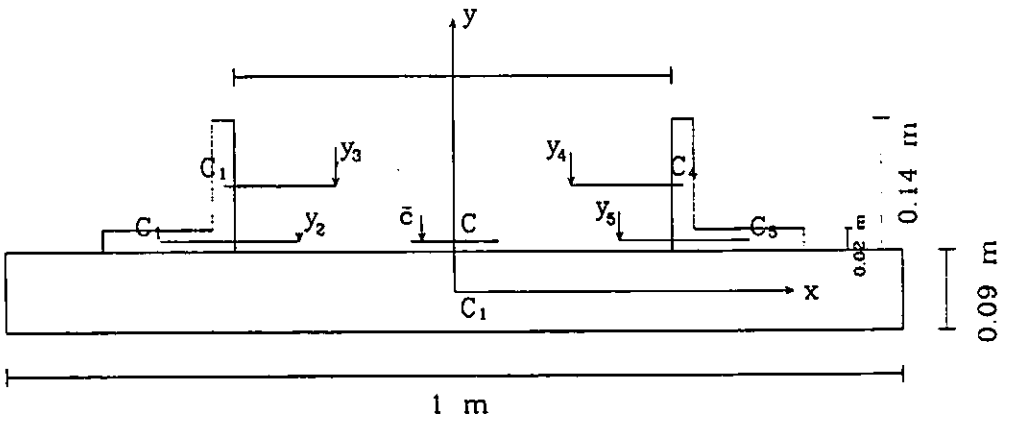

Figure B–1 Cross–section of model sheet pile wall

The knife–edges of the pile were ignored in the calculations.

The model pile has a composite cross–sectional area due to steel ribs. Therefore, it is divided into five parts, as represented in Figure B–1. Let the centroids of theses cross–sectional areas to be denoted as C_1, C_2, C_3, C_4, and C_5 respectively. Also the corresponding areas are

$$A_1 = 1 \times 0.09 = 0.09 \text{ m}^2$$
$$A_2 = A_5 = 0.12 \times 0.02 = 2.4 \times 10^{-3} \text{ m}^2$$
$$A_3 = A_4 = 0.02 \times 0.15 = 3.6 \times 10^{-3} \text{ m}^2$$

First the centroidal of the composite area must be located. If x and y axes are taken with origin at C_1, the centroidal distances from the five areas are

$$y_1 = 0$$
$$y_2 = y_5 = 0.05 \text{ m} \qquad y_3 = y_4 = 0.12 \text{ m}$$

The area A, and the first moment Q_x of the entire cross–section are

$$A = A_1 + A_2 + A_3 + A_4 + A_5 = 0.10 \text{ m}^2$$
$$Q_x = y_1A_1 + y_2A_2 + y_3A_3 + y_4A_4 + y_5A_5$$
$$= 0 + 2 \times 0.05 \times 2.4 \times 10^{-3} + 2 \times 0.12 \times 3.6 \times 10^{-3}$$
$$= 0.001 \text{ m}^3$$

The co-ordinate to the centroid C is obtained from the following equation:

$$\bar{y} = \frac{Q_x}{A} = \frac{0.001}{0.1} = 0.01 \text{ m}$$

So, the centroidal of the entire area is located at a distance $\bar{c} = 0.01$ m above x axis.

The moments of inertia of the five parts with respect to their own centroids are as follows:

$$I_1 = \frac{bt^3}{12} = \frac{1}{12} \times 1 \times 0.09^3 = 6.08 \times 10^{-5} \text{ m}^4$$
$$I_2 = I_5 = 8.00 \times 10^{-5} \text{ m}^4$$
$$I_3 = I_4 = 5.63 \times 10^{-6} \text{ m}^4$$

Using the parallel–axis theorem, the moments of inertia, about an axis through C, for the five cross–sectional areas can be calculated

$$I_{c_1} = I_1 + A_1\bar{c}^2 = 9.68 \times 10^{-5} \text{ m}^4$$
$$I_{c_2} = I_{c_5} = I_2 + A_2(y_2 - \bar{c})^2 = 4.88 \times 10^{-6} \text{ m}^4$$
$$I_{c_3} = I_{c_4} = I_3 + A_3(y_3 - \bar{c})^2 = 4.16 \times 10^{-5} \text{ m}^4$$

The sum of these moments of inertia is

$$I_c = I_{c_1} + I_{c_2} + I_{c_3} + I_{c_4} + I_{c_5} = 1.90 \times 10^{-4} \text{ m}^4$$

which is the centroidal moment of inertia of the entire cross–section.

Anchor

The moment of inertia of the cross–section of the anchor is

$$I_a = \frac{b_a t_a^{\,2}}{12} = \frac{1}{12} \times 1 \times 5.75 \times 10^{-3} = 1.58 \times 10^{-8} \text{ m}^4$$

and the area of the section is $A_a = b_a \times t_a = 5.75 \times 10^{-3}$ m^2

Tie–rod

The area of the tie–rod is

$$A_r = \frac{\pi d_r^{\,2}}{4} = 6.40 \times 10^{-4} \text{ m}^2$$

where $d_r = 2.85 \times 10^{-2}$ m the diameter of the rod.

The ultimate tensile and compressive yield strength of mild steel are given by British Steel Corporation as $\sigma_{tens} = 430 \times 10^6$ Pa and $\sigma_{comp} = 240 \times 10^6$ Pa respectively. Hence, for the particular diameter the tensile and compressive strength, in terms of forces, are

Ultimate tensile strength	$y = 2.75 \times 10^5$ N
Compressive yield strength	$y_c = 1.53 \times 10^5$ N

- **Programme Instructions For The Model With l_r = 1.54 m, d_a = 0.24 m, v = 2e-6**

; Model with tie–rod length l_r = 1.54 m, depth of anchorage d_a = 0.24 m, and applied horizontal velocity at the wall, uniformly distributed from zero at the bottom of excavation to 2×10^{-6} at the top. The wall fixed at the bottom of excavation. Height of retained soil h = 1.44 m. All the properties for 1 m width of wall.

```
se log k0.log
se log on

; Grid generation  17 x 28 with dimensions 2.38 m x 1.68 m
gr 17 28
gen 0,0 0,1.68 2.38,1.68 2.38,0

; Apply restrains on the boundary
fix x y i=1
fix x y i=18
fix y j=1

; Initial soil stress
m e
pro bu=40e6 d=1480 sh=15e6; Poisson's ratio v = 0.33
se g=9.81; apply gravitational force
se large
ste 1000; let the model to equilibrate

;Apply elastoplastic behaviour
m m
pro bu=40e6 d=1480 sh=15e6
pro c=0 f=43; no dilation

ini xd=0
ini yd=0

; Install sheet pile wall. Fixed at bottom of excavation. H = 1.56 m
str prop 1 e=200e9 i=1.90e-4 a=0.10
str beam beg gr=4,3 end gr=4,4 pr=1
```

```
str beam beg gr=4,4 end gr=4,5 pr=1
str beam beg gr=4,5 end gr=4,6 pr=1
str beam beg gr=4,6 end gr=4,7 pr=1
str beam beg gr=4,7 end gr=4,8 pr=1
str beam beg gr=4,8 end gr=4,9 pr=1
str beam beg gr=4,9 end gr=4,10 pr=1
str beam beg gr=4,10 end gr=4,11 pr=1
str beam beg gr=4,11 end gr=4,12 pr=1
str beam beg gr=4,12 end gr=4,13 pr=1
str beam beg gr=4,13 end gr=4,14 pr=1
str beam beg gr=4,14 end gr=4,15 pr=1
str beam beg gr=4,15 end gr=4,16 pr=1
str beam beg gr=4,16 end gr=4,17 pr=1
str beam beg gr=4,17 end gr=4,18 pr=1
str beam beg gr=4,18 end gr=4,19 pr=1
str beam beg gr=4,19 end gr=4,20 pr=1
str beam beg gr=4,20 end gr=4,21 pr=1
str beam beg gr=4,21 end gr=4,22 pr=1
str beam beg gr=4,22 end gr=4,23 pr=1
str beam beg gr=4,23 end gr=4,24 pr=1
str beam beg gr=4,24 end gr=4,25 pr=1
str beam beg gr=4,25 end gr=4,26 pr=1
str beam beg gr=4,26 end gr=4,27 pr=1
str beam beg gr=4,27 end gr=4,28 pr=1
str beam beg gr=4,28 end gr=4,29 pr=1
str node 3 fix x

; Install tie–rod. l_r = 1.54 m, t = 0.18 m
str prop 2 e=200e9 a=6.40e-4 y=2.75e5 yc=1.54e5 kb=0 sb=0
str cable beg gr=4,26 end gr=5,26 pr=2
str cable beg gr=5,26 end gr=6,26 pr=2
str cable beg gr=6,26 end gr=7,26 pr=2
str cable beg gr=7,26 end gr=8,26 pr=2
str cable beg gr=8,26 end gr=9,26 pr=2
str cable beg gr=9,26 end gr=10,26 pr=2
str cable beg gr=10,26 end gr=11,26 pr=2
str cable beg gr=11,26 end gr=12,26 pr=2
str cable beg gr=12,26 end gr=13,26 pr=2
str cable beg gr=13,26 end gr=14,26 pr=2
str cable beg gr=14,26 end gr=15,26 pr=2
```

;Install anchor. h_a = 0.12 m, d_a = 0.24 m

str prop 3 e=200e9 i=1.58e-8 a=5.75e-3

str beam beg gr=15,25 end gr=15,26 pr=3

str beam beg gr=15,26 end gr=15,27 pr=3

;Excavate the soil (h=1.44 m) and apply velocity

m n l=1,3 j=5,28

apply xv=0 var 0,-2e-6 l=4 j=5,29

ti

f=43deg. h=1.44m. lr=1.54m. da=0.24m. v=2e-6

ret

- **Variation Of Anchor Resistance With Anchorage Displacement For Different l_r And d_a**

The variation is represented in the following figures B–2, B–3, and B–4 in which the depth of anchorage is $d_a = 0.18$ m, $d_a = 0.24$ m, $d_a = 0.42$ m respectively.

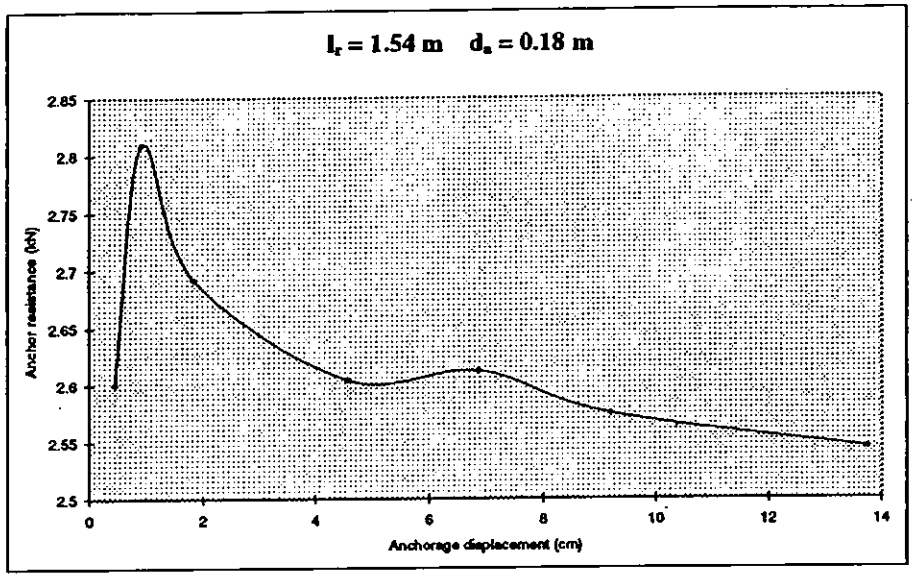
l_r = 1.54 m d_a = 0.18 m
Anchor resistance (kN)
2.85
2.8
2.75
2.7
2.65
2.6
2.55
2.5
0
2
4
6
8
10
12
14
Anchorage displacement (cm)

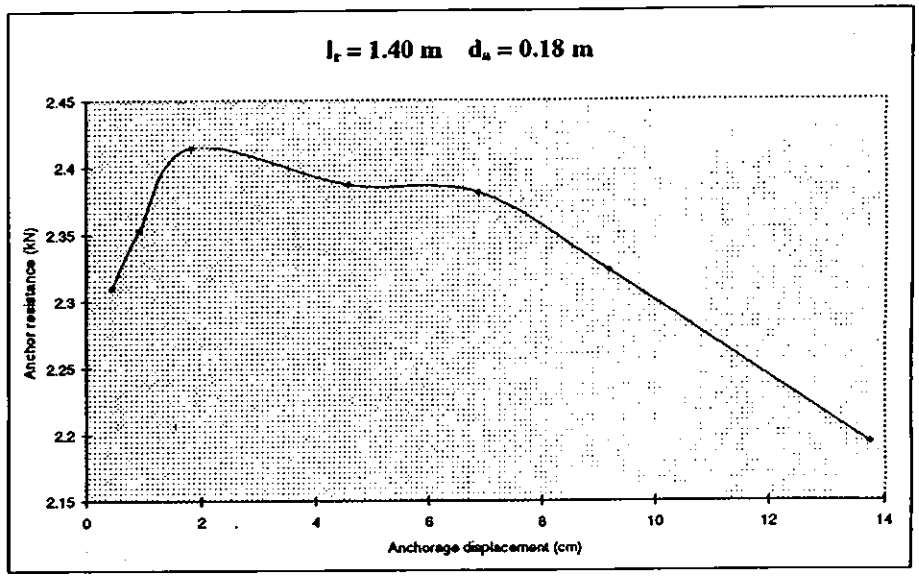
l_r = 1.40 m d_a = 0.18 m
Anchor resistance (kN)
2.45
2.4
2.35
2.3
2.25
2.2
2.15
0
2
4
6
8
10
12
14
Anchorage displacement (cm)

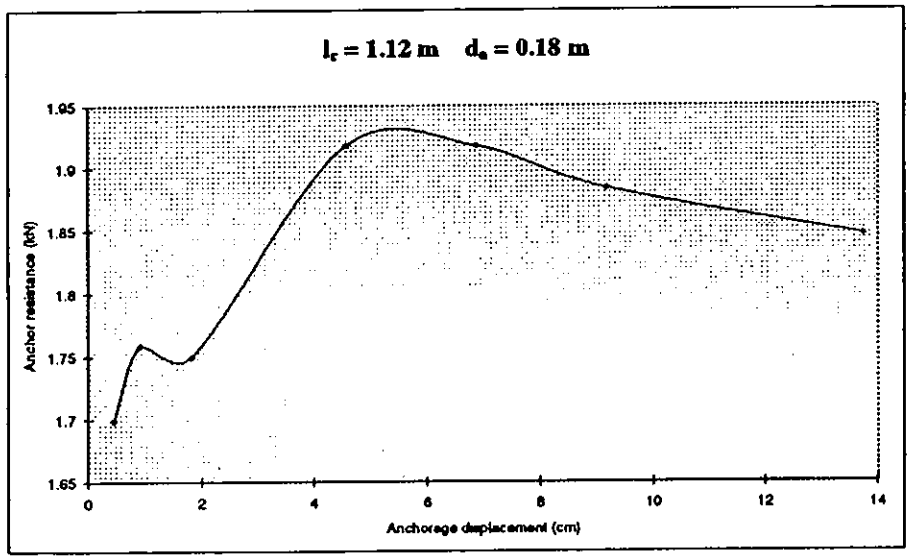
l_r = 1.12 m d_a = 0.18 m
Anchor resistance (kN)
1.95
1.9
1.85
1.8
1.75
1.7
1.65
0
2
4
6
8
10
12
14
Anchorage displacement (cm)

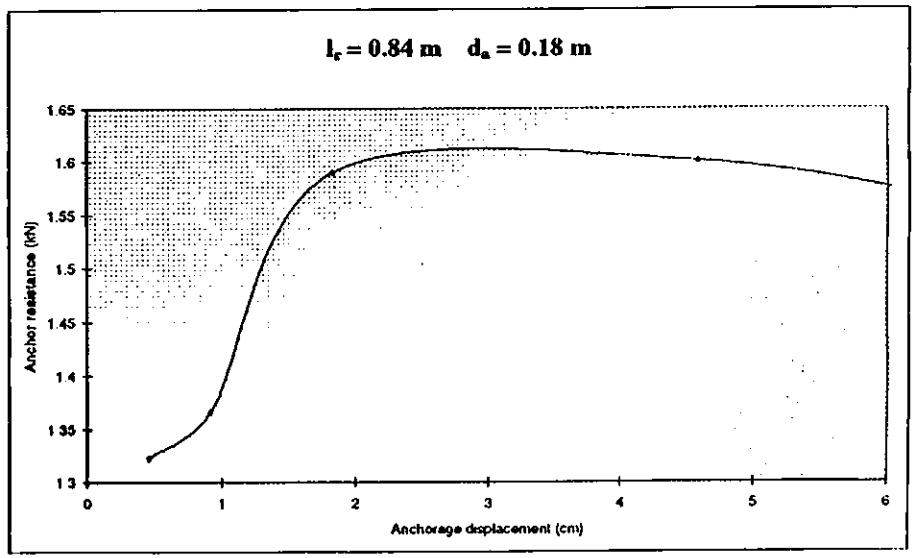
l_r = 0.84 m d_a = 0.18 m
Anchor resistance (kN)
1.65
1.6
1.55
1.5
1.45
1.4
1.35
1.3
0
1
2
3
4
5
6
Anchorage displacement (cm)

Figure B-2

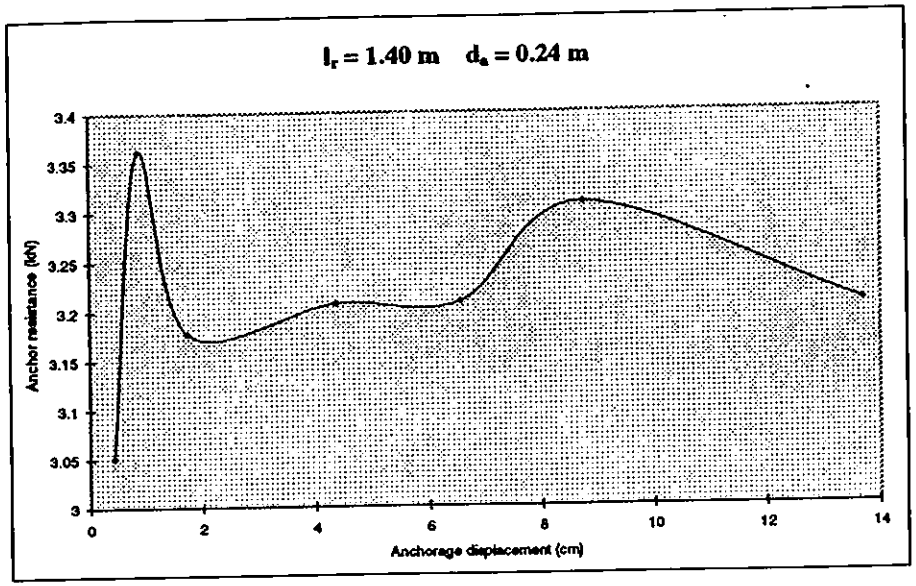
l_r = 1.40 m d_a = 0.24 m
Anchor resistance (kN)
Anchorage displacement (cm)

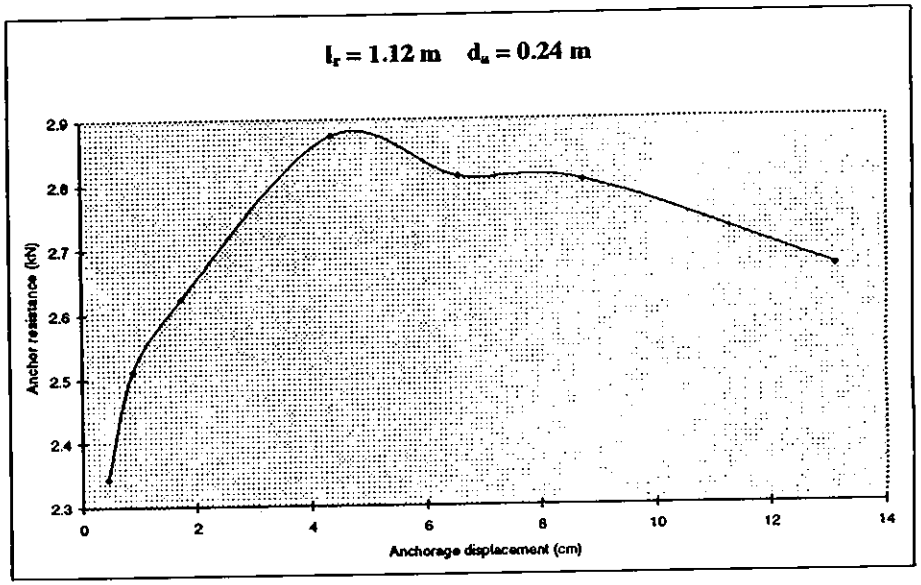
l_r = 1.12 m d_a = 0.24 m
Anchor resistance (kN)
Anchorage displacement (cm)

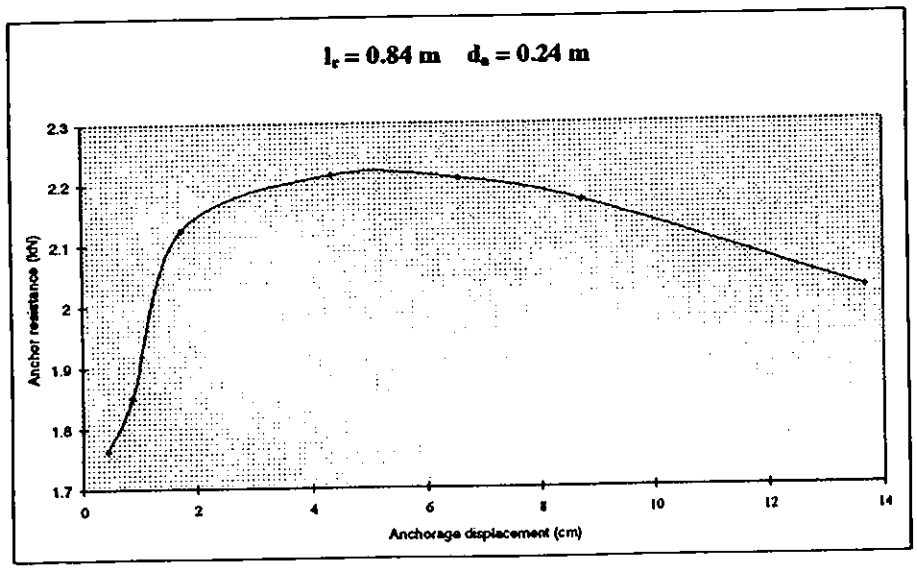
l_r = 0.84 m d_a = 0.24 m
Anchor resistance (kN)
Anchorage displacement (cm)

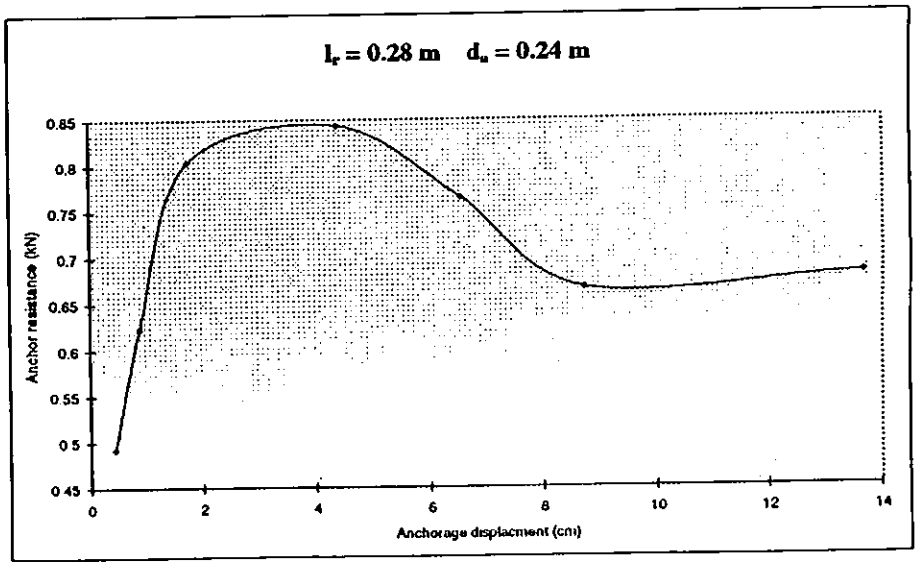
l_r = 0.28 m d_a = 0.24 m
Anchor resistance (kN)
Anchorage displacement (cm)

Figure B-3

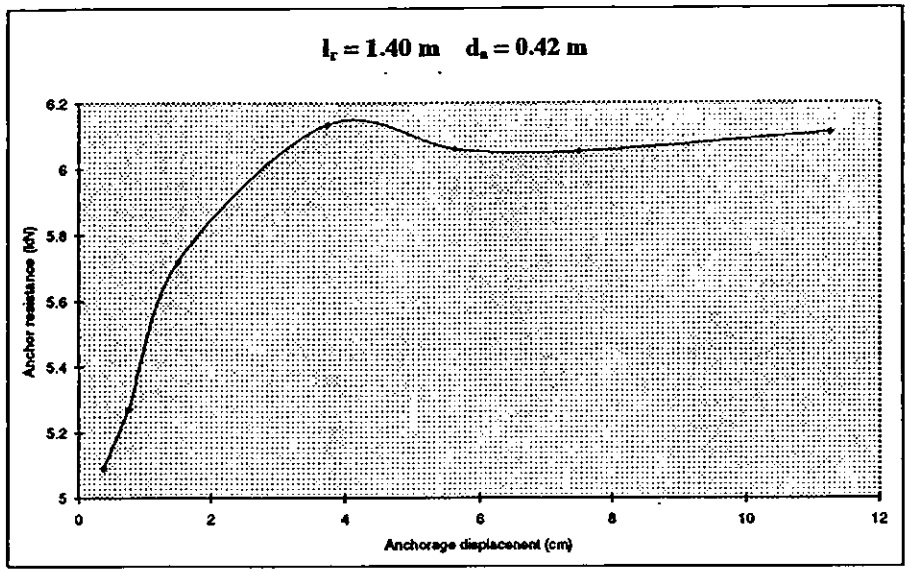
l_r = 1.40 m d_a = 0.42 m
Anchor resistance (kN)
6.2
6
5.8
5.6
5.4
5.2
5
0
2
4
6
8
10
12
Anchorage displacement (cm)

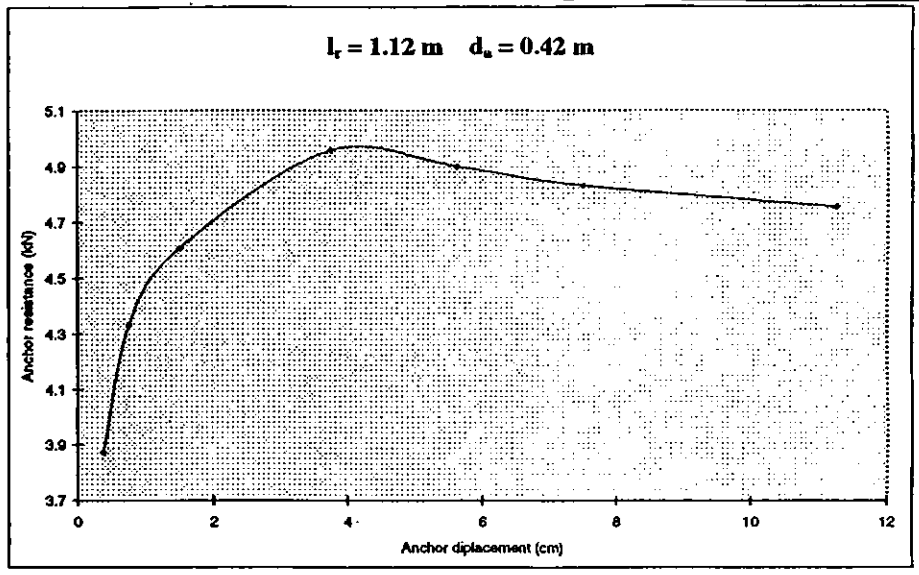
l_r = 1.12 m d_a = 0.42 m
Anchor resistance (kN)
5.1
4.9
4.7
4.5
4.3
4.1
3.9
3.7
0
2
4
6
8
10
12
Anchor diplacement (cm)

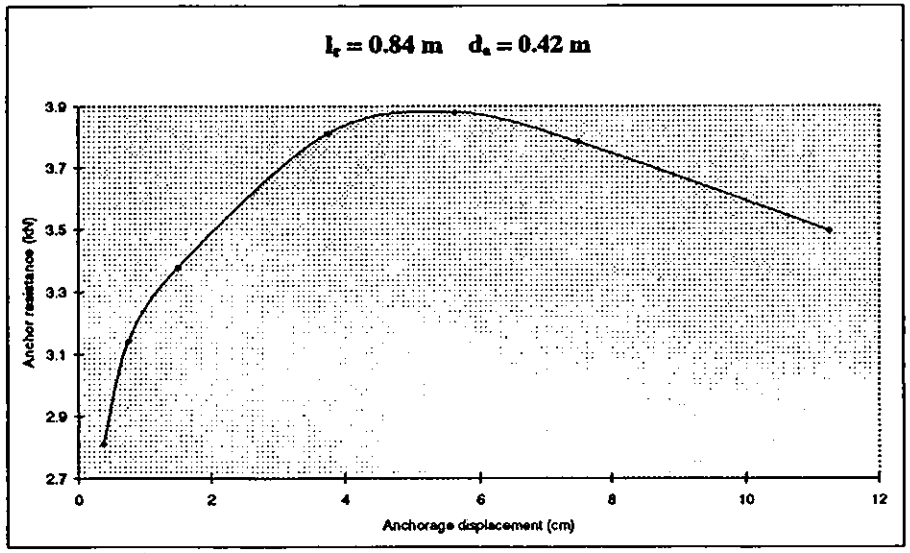
l_r = 0.84 m d_a = 0.42 m
Anchor resistance (kN)
3.9
3.7
3.5
3.3
3.1
2.9
2.7
0
2
4
6
8
10
12
Anchorage displacement (cm)

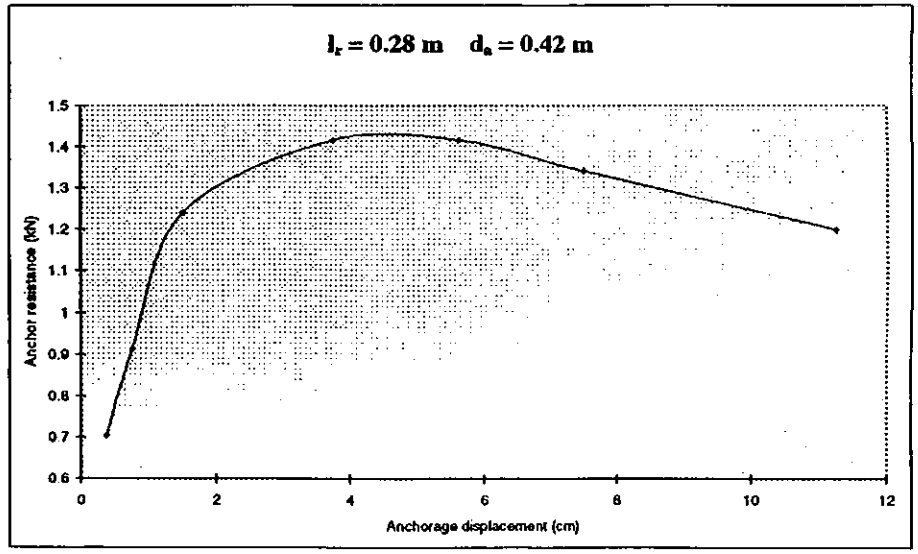
l_r = 0.28 m d_a = 0.42 m
Anchor resistance (kN)
1.5
1.4
1.3
1.2
1.1
1
0.9
0.8
0.7
0.6
0
2
4
6
8
10
12
Anchorage displacement (cm)

Figure B-4

– Vectors Of Soil Displacement At Failure For Various Models

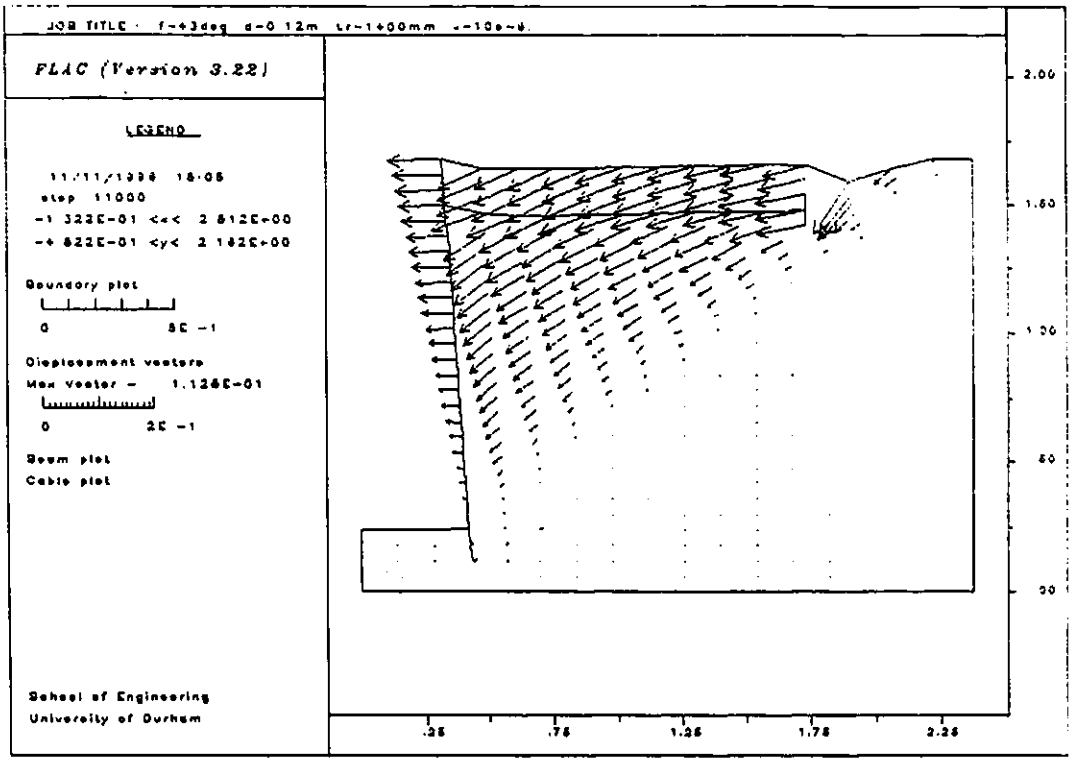

Figure B–5 $l_r = 1.40$ m, $d_a = 0.24$ m

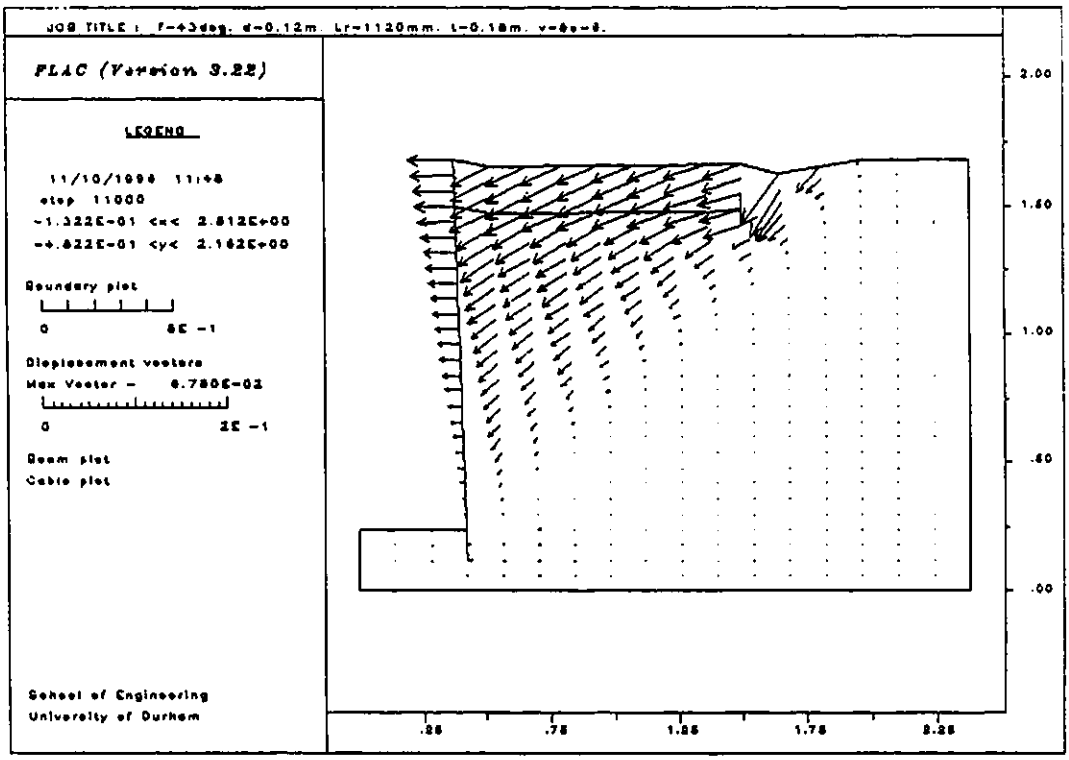

Figure B–6 $l_r = 1.12$ m, $d_a = 0.24$ m

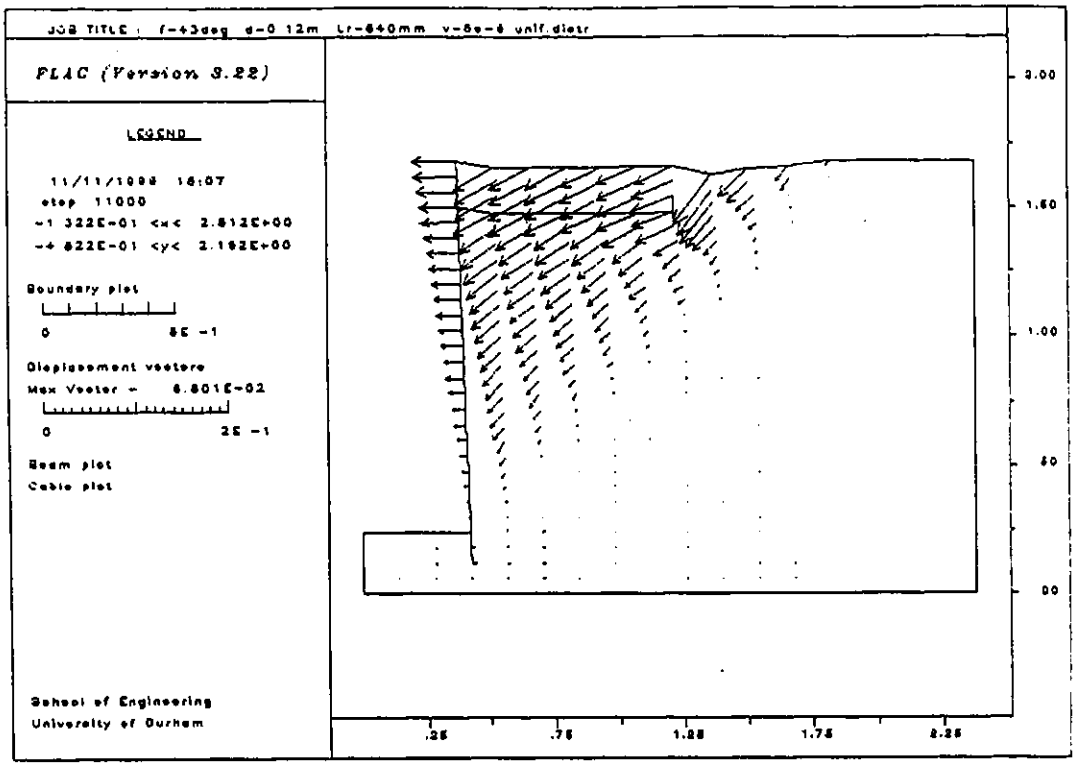

Figure B–7 $l_r = 0.84$ m, $d_a = 0.24$ m

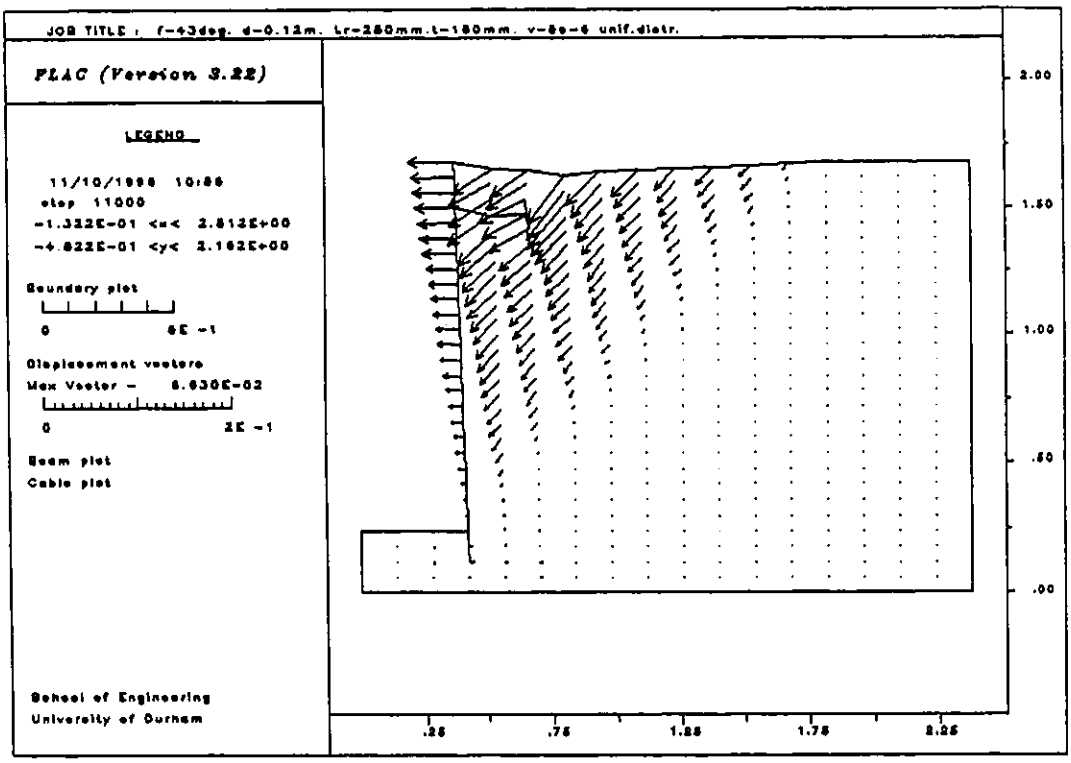

Figure B–8 $l_r = 0.28$ m, $d_a = 0.24$ m

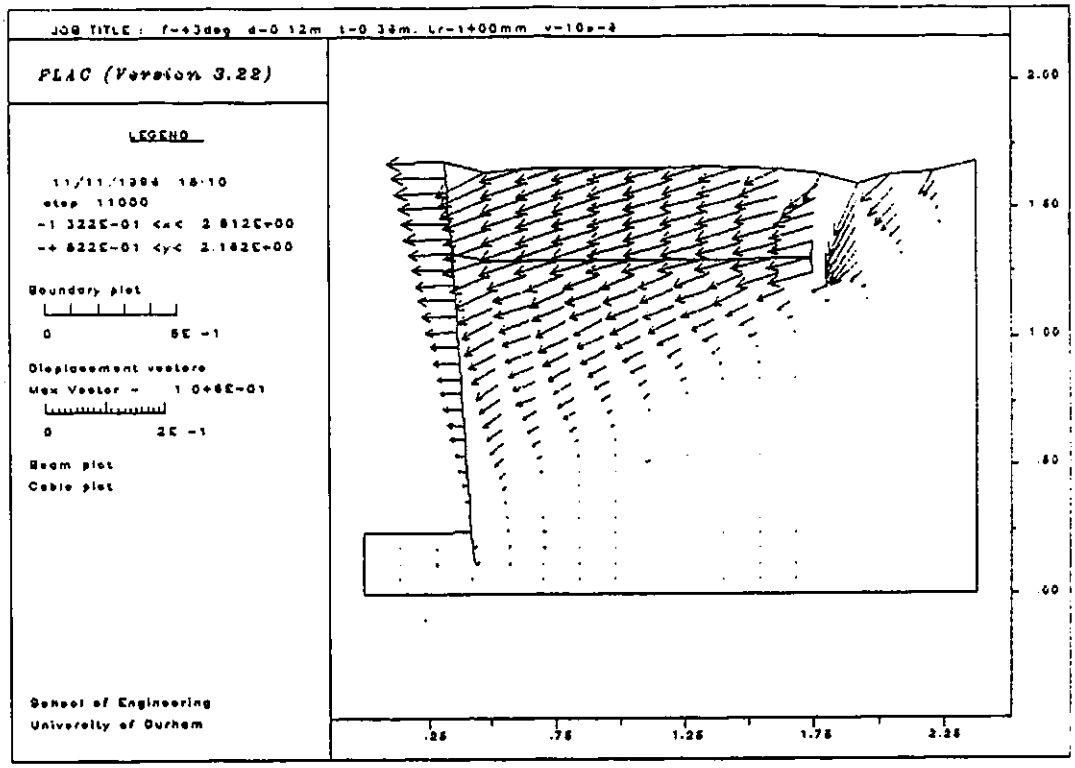

Figure B–9 $l_r = 1.40$ m, $d_a = 0.42$ m

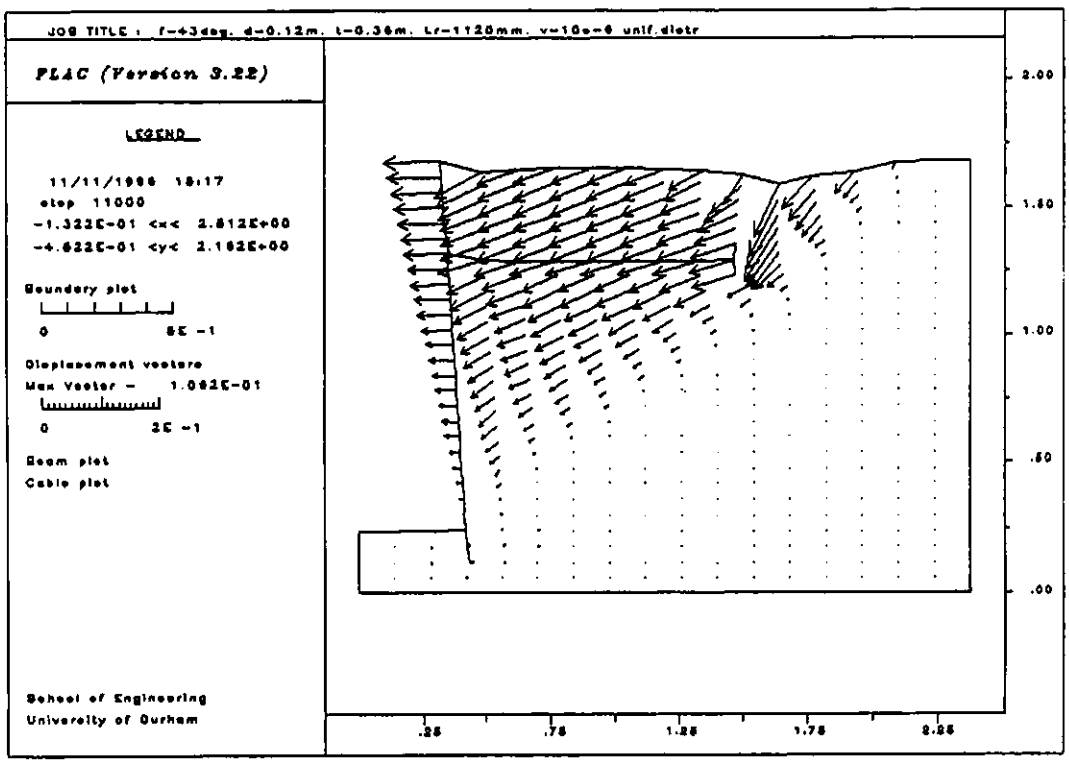

Figure B–10 $l_r = 1.12$ m, $d_a = 0.42$ m

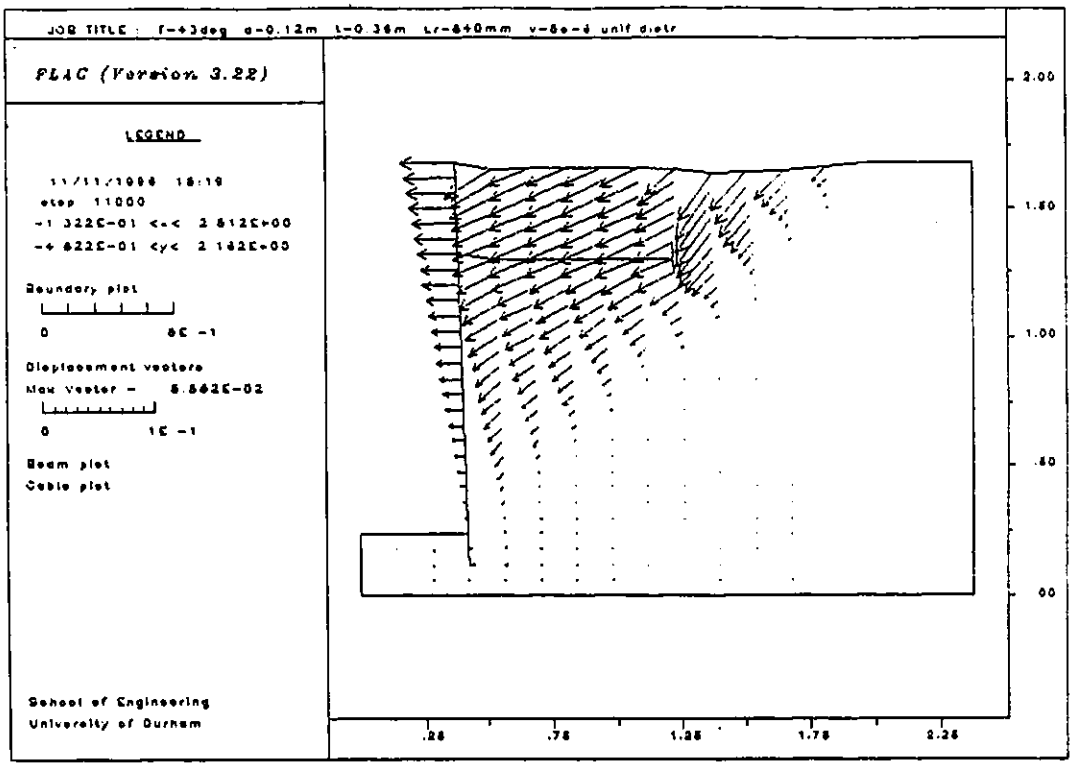

Figure B–11 $l_r = 0.84$ m, $d_a = 0.42$ m

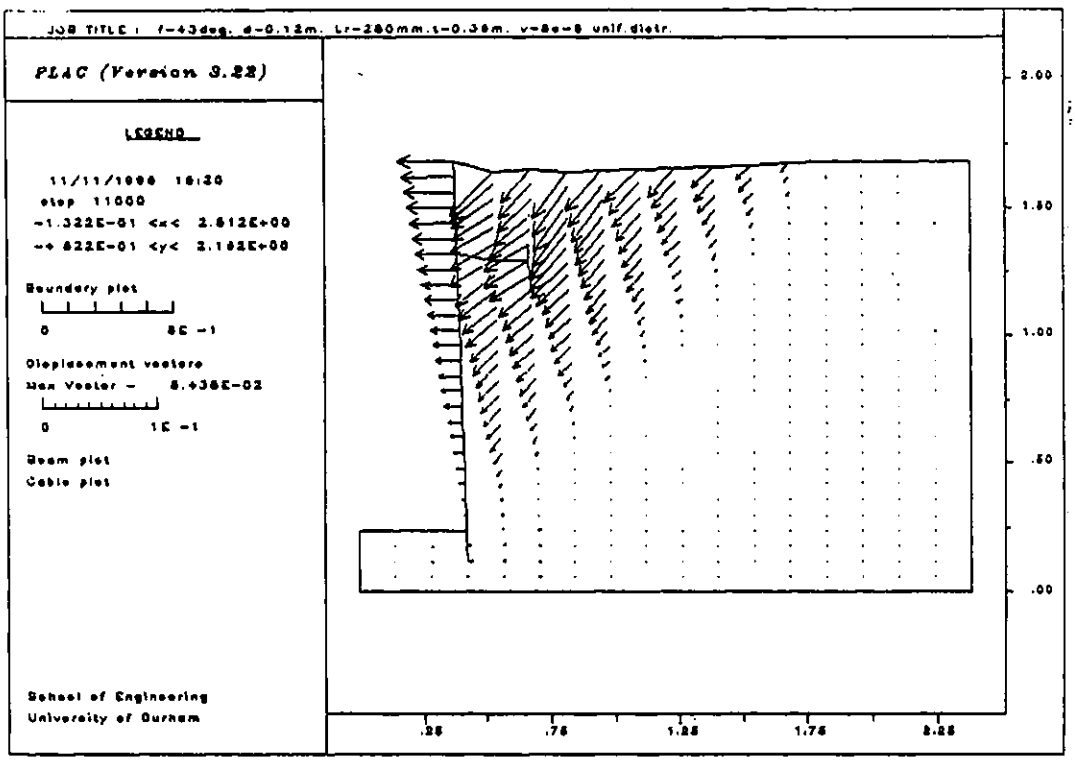

Figure B–12 $l_r = 0.28$ m, $d_a = 0.42$ m

– Earth Pressure Distributions Behind The Wall And Plate

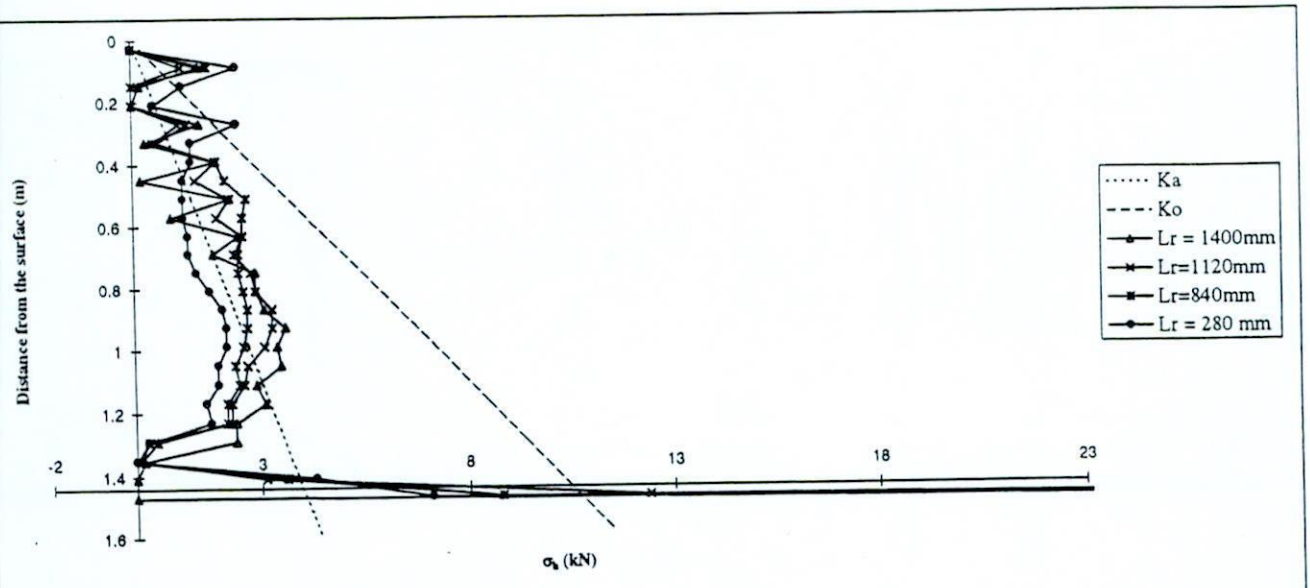

Figure B-13 Earth pressures behind the wall. Anchorage depth da = 0.18 m.

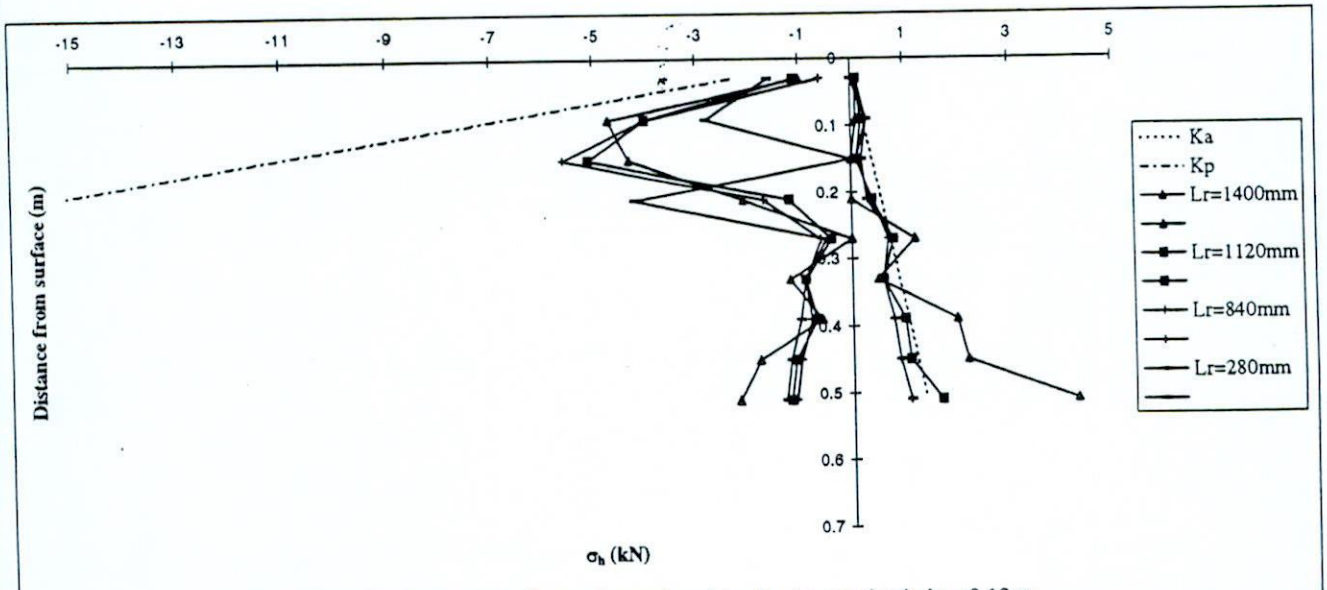

Figure B-14 Earth pressures adjacent the anchor plate. Anchorage depth da = 0.18 m.

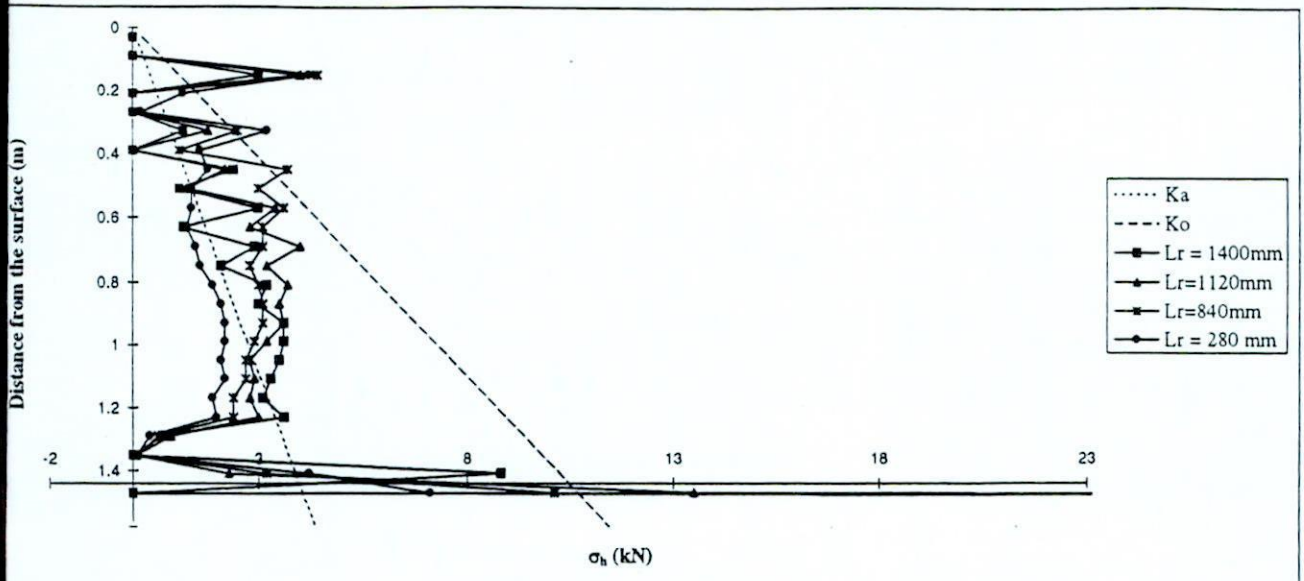

Figure B-15 Earth pressures beside the wall. Anchorage depth d_a = 0.24 m.

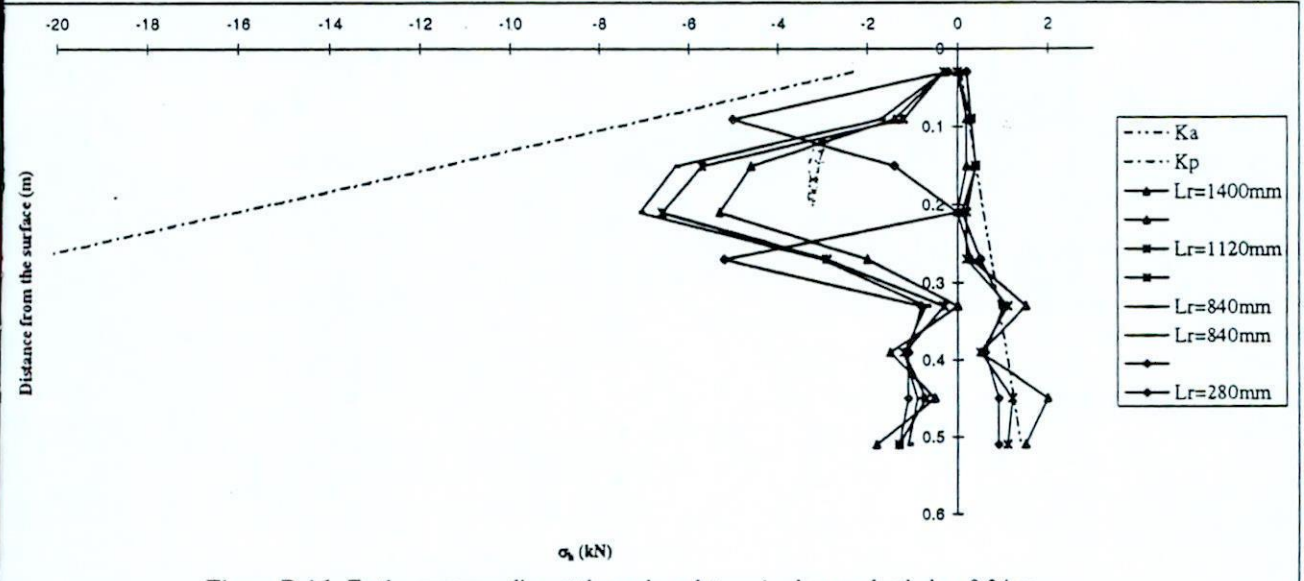

Figure B-16 Earth pressures adjacent the anchor plate. Anchorage depth d_a = 0.24 m.

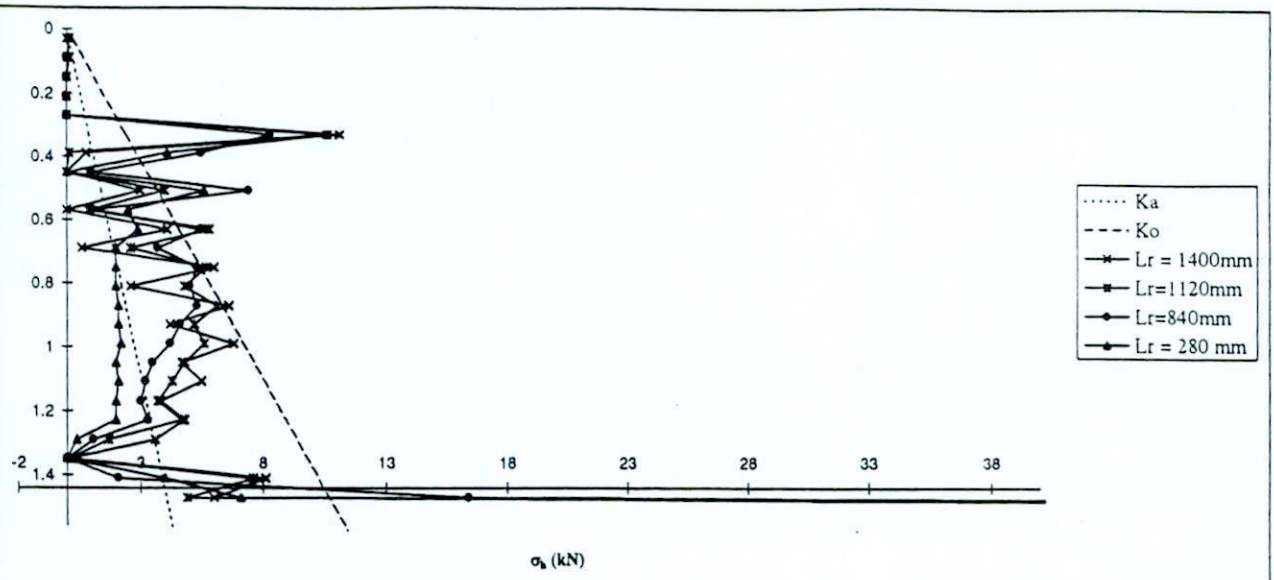

Figure B-17 Earth pressures beside wall. Anchorage depth d_a = 0.42 m.

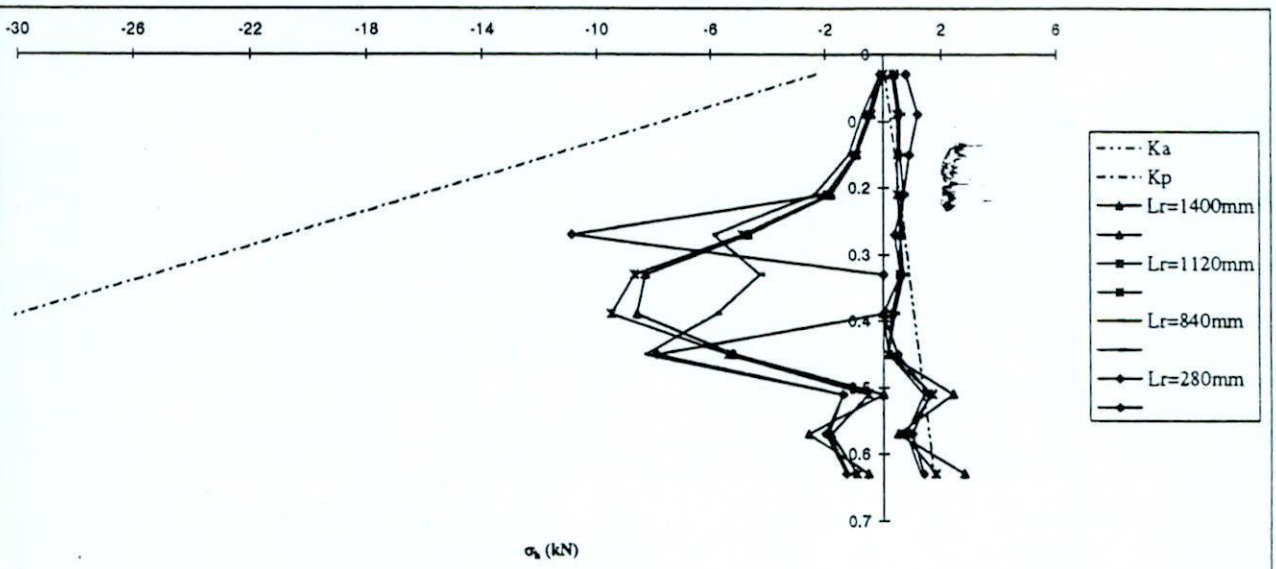

Figure B-18 Earth pressures adjacent to anchor plate. Anchorage depth da = 0.42 m.